

UNIVERSIDADE DE LISBOA
FACULDADE DE MEDICINA



Internal Limiting Membrane Peeling in Macular Hole

Mun Yueh de Faria

Tese orientada por: Professor Doutor Manuel Monteiro Grillo

Doutoramento em Medicina
Especialidade de Oftalmologia

2020

UNIVERSIDADE DE LISBOA
FACULDADE DE MEDICINA



Internal Limiting Membrane Peeling in Macular Hole

Mun Yueh de Faria

Tese orientada por: Professor Doutor Manuel Monteiro Grillo

Doutoramento em Medicina, especialidade de Oftalmologia

Júri:

Presidente: Doutor José Augusto Gamito Melo Cristino, Professor Catedrático e Presidente do Conselho Científico da Faculdade de Medicina da Universidade de Lisboa.

Vogais:

- Doutor João Pereira Figueira, Professor Auxiliar da Faculdade de Medicina da Universidade de Coimbra.
- Doutor Amândio António Rocha Dias de Sousa, Professor Associado Convidado com Agregação da Faculdade de Medicina da Universidade do Porto
- Doutor Manuel Eduardo Teixeira Monteiro Grillo, Professor Auxiliar Jubilado da Faculdade de Medicina da Universidade de Lisboa; (orientador)
- Doutor Alexandre Valério de Mendonça, Professor Catedrático Convidado da Faculdade de Medicina da Universidade de Lisboa
- Doutor Carlos Alberto Matinho Marques Neves, Professor Associado de Oftalmologia da Faculdade de Medicina da Universidade de Lisboa

2020

As opiniões expressas nesta publicação são da exclusiva responsabilidade do seu autor.

O trabalho descrito na presente tese foi desenvolvido no Serviço de Oftalmologia do Centro Hospitalar Universitário Lisboa Norte, Hospital Santa Maria e no âmbito do Programa Doutoral do CAML sob a orientação do Prof. Doutor Manuel Monteiro Grillo.

A impressão desta dissertação foi aprovada pelo Conselho Científico da Faculdade de Medicina de Lisboa em reunião de 11 de Fevereiro de 2020.

Agradecimentos

Durante a longa viagem deste PhD, algumas foram as pessoas que contribuíram para a elaboração desta tese.

Primeiramente, quero agradecer ao meu orientador, Professor Doutor Monteiro Grillo por me ter dado a oportunidade de desenvolver este trabalho e orientar a minha tese de Doutoramento. Obrigada, Professor, por me ter orientado quando me iniciei em Oftalmologia e me incentivou para a uma área tão nobre e tão completa como a Retina Cirúrgica.

De seguida, aos membros do meu Comité de Tese, Professor Doutor Domingos Henrique e Professor Doutor Rui Proença, pelas discussões científicas e conselhos sobre este trabalho.

À Faculdade de Medicina de Lisboa e ao Instituto de Medicina Molecular pelas excelentes condições e pela grande comunidade científica, tão importante para o desenvolvimento deste trabalho.

À Professora Doutora Constança Coelho que me apoiou e com êxito conseguiu decifrar as minhas ideias e ajudou-me a colocá-las em escrita.

A todos os meus colegas de oftalmologia, em especial, Sofia Mano, Nuno Ferreira, David Sousa, Eliana Neto, Helena Proença e Carlos Marques Neves, pela ajuda na recolha de dados clínicos para a construção da base de dados, sugestões e revisão de textos.

Aos técnicos de ortóptica e enfermagem, que me apoiaram nos inúmeros exames, muitas vezes fora do horário de trabalho. Telma, Pedro, Teresa, Armandina, Rita, Diana e Sofia, muito obrigada por todos os meus pedidos e solicitações.

Gostaria também de agradecer às minhas amigas e colegas, Avelina Moniz e Helena Carvalho, que me incentivaram e apoiaram sempre.

Finalmente, agradeço a todo o meu apoio familiar, Zé, Diogo e Sara. Foram indispensáveis para que se concretizasse este projecto.

“You can’t go back and change the beginning, but you can start where you are and change the ending.”

—*C. S. Lewis*

Table of Contents

List of figures.....	XII
Abstract.....	XV
Sumário.....	XIX
Abbreviations.....	XXV
Overview of the thesis.....	XXVII
CHAPTER 1.....	1
1. Introduction.....	1
2. Hypotheses and Aims.....	4
3. Background.....	6
4. Surgery.....	25
5. Materials and Methods.....	33
CHAPTER 2.....	37
CHAPTER 3.....	55
CHAPTER 4.....	67
CHAPTER 5.....	79
CHAPTER 6.....	91
1. Global Discussion.....	93
2. Concluding Remarks.....	101
References.....	105

List of figures

Figure 1- Horizontal spectral-domain optical coherence tomography scan of an asymptomatic 47-year-old man showing a large pre-macular liquefied pocket. Legend: Its posterior wall, the vitreous cortical layer overlying the macular area, is very thin, and shallow vitreous separation is beginning in the peripheral macula	2
Figure 2- Fundus photography of the Optic nerve head, Macula and Fovea.....	6
Figure 3 - A drawing of a section through the eye with a schematic enlargement of the retina.....	7
Figure 4- Diagram of organization of the retina.....	7
Figure 5- Retinal layers with outer plexiform layer in red.....	8
Figure 6- Retinal layers with Inner plexiform layer in red	9
Figure 7- Graphic scheme of the retinal structure highlighting its major structures.	10
Figure 8- ILM in TEM, magnification 1000 xs. Legend: Vitreous side is smooth and retinal side is convoluted.....	11
Figure 9- ILM in TEM, magnification 5000 xs. Legend: The upper smooth side is the vitreous side, the lower rough side is the retinal side.	11
Figure 10- Schematic representation of the normal human fovea centralis from Gass, based on the histological findings of Yamada and Hogan et al. Legend: The Müller cell cone (M) is shown with its base forming the internal limiting membrane (arrow) and its apex forming the external limiting membrane (arrowhead).....	12
Figure 11- Split in foveola and cyst seen in OCT of left eye of patient with macular hole on right side	13
Fig 12- A- Fundus photo of a normal human macula, optic nerve and blood vessels around fovea. (200µm) B- Optical Coherence tomography. Legend: Image of the same normal macula in the area boxed in light green and between 3.00 mm diameter limited by medial yellow circle, parafoveal area, centered on fovea. The foveal pit (arrow) and the sloping walls with displaced inner retina neurons (yellow and red cells) are clearly seen. Green cells are packed photoreceptors, primarily cones, above the foveal center.....	15
Figure 13 - The superimposed illustration is a representational drawing of the cell types found in a normal fovea. Legend: Cells not to scale. Drawing is color coded by cell type.....	16

Figure 14- SD-OCT with identification of retinal layers in colors and correspondence in cell type and interface layers.	17
Figure 15 - Complete PVD. Legend: The posterior face of the vitreous is completely separated from the retina.	17
Figure 16- The posterior face of the vitreous is pulling on the fovea, resulting in a peaked appearance of the photoreceptors.....	17
Figure 17- The posterior face of the vitreous is pulling on the fovea, resulting in a cyst.....	17
Figure 18 – SD OCT of 71 years old man, A-left eye in top and B-right eye in bottom with vitreomacular traction in both eyes and cystic lesions right eye.	18
Figure 19- The full-thickness macular hole in the OCT image has a partial roof and the traction from the posterior face of the vitreous is clearly visible, both in A and B	18
Figure. 20 Full-thickness macular hole. Legend: The hole goes all the way through the retina, exposing the RPE (shaded blue). The curling of the photoreceptor layers can most easily be identified by tracing the external limiting membrane (shaded yellow) between the photoreceptor nuclear layer and the photoreceptor inner segments. Several small intraretinal cysts (shaded orange) can be seen within the inner nuclear layer, between the outer plexiform layer (shaded green) and the inner plexiform layer (shaded red).	19
Figure 21- Evolution of a macular hole in one of our patients, 68 years old, fellow eye of eye with macular hole, visualized with optical coherence tomography (OCT). Legend: A - OCT- Image of macula with posterior vitreal adherence and foveal traction. B-cavitation and rupture of outer retina layers. C-Full thickness macular hole. D-fifteen days after macular hole surgery; hole is closed. Note the subtle area of increased reflectance in the center.....	20
Figure 22- Full-thickness macular hole showing a surrounding cuff of subretinal fluid.....	21
Figure 23 - Circular ILM peel. Brilliant Blue dye.	27
Figure 24- Peeled ILM over the hole.....	29
Figure 25- Inverted flap of ILM dyed with Brilliant Blue	30
Fig. 26- (A) preoperative macular hole; (B-D) postoperative temporal thinning of the retinal layers respectively after 20 days, 5 months and 2 years.	32

Abstract

Macular hole (MH) is a full-thickness defect in the fovea, the central part of the neurosensory retina. As the fovea is the site responsible for central vision, the main clinical manifestation of MH is central visual field defect and metamorphopsia.

Descriptions of MH in the medical literature are available since the 19th century. However, these only aroused renewed interest after Kelly and Wendel had shown that surgery of pars plana vitrectomy (PPV), combined with vitreous cortex detachment and fluid–gas exchange could close MH in a significant proportion of cases, although it was assumed that the retina would be unable to heal. With time, the success rate of MH surgery gradually increased and this surgery is now one of the most successful vitreoretinal surgeries.

A recent innovation was the introduction of internal limiting membrane (ILM) peeling, which leads to a reduction in tangential traction and a higher rate of closure, with less recurrence. In the last 10 years, ILM peeling during MH surgery has thus become a routine step and is nowadays performed by most retinal surgeons. With the advent of modern spectral-domain (SD) optic coherence tomography (OCT), however, one can now see abnormal structural changes to the inner retinal surface after surgery with ILM peeling, suggesting that the procedure can cause retinal damage, even though vision improves. Moreover, some clinical studies found adverse functional events that have given rise to concerns regarding the safety of ILM peeling.

The purpose of the present PhD thesis was to examine anatomical and functional effects of ILM peeling in MH surgery. We conducted a prospective study in 72 patients with MH, (stages 2, 3 and 4). MH surgery consisted in PPV, ILM peeling, intraocular gas and face down position. Morphologic and functional outcomes were assessed, 3, 6 and 12 months after surgery. The results reveal the presence of microstructural alterations in the different macular layers after MH surgery with ILM peeling, when compared to pre-operative

measurements. Thinning of the Ganglion Cell Layer (GCL) and Inner Plexiform Layer (IPL) on both sides of the fovea were the main structural alterations, in particular at the temporal region. In addition, nasal Internal Retinal Layer (IRL) thickening and shortening of papilo-macular distance could also be detected in cases of successful MH surgery with ILM peeling.

Multifocal electroretinography (mf ERG) is a noninvasive method that analyses multiple retinal locations around macular area, and was used in this work to provide a topographic map of electrophysiological activity in central retina.

Before surgery, mf ERG showed almost undetectable retinal response in foveal and parafoveal areas, in ring 1 and ring 2. After surgery, the improvement in the retinal response density of mf ERG in the same ring seems to be consequent to closure of the MH, with realignment of photoreceptor cells and glial cell activation. Resolution of the central scotoma could be attributed to anatomical repair and, in our study, we found a statistically significant increase in N1 and P1 in ring 1. This increase was dependent on the integrity of Outer Retina Layers (ORL), External Limiting Membrane (ELM) and Elipsoide Zone (EZ).

To study the contribution of the peeled ILM to the outcome of MH surgery, the final position of the ILM after surgery was assessed. This analysis reveals that when the ILM flap ended buried into the hole after surgery, no realignment of external layers could be observed. In contrast, when the ILM flap remained over the hole, ELM and EZ were realigned, and vision was improved. In this study, duration of MH and ORL integrity were studied and we concluded that duration of symptoms of MH seem to relate to integrity to these layers.

The ultrastructure and behavior of peeled ILM was studied by using light and transmission electron microscopy. We found that when both ILM vitreous sides are in apposition, there are signs of fibrotic activity, producing a basal membrane with collagen microfibrils between the two sides. This suggests that the two ILM surfaces may adhere, flanking the hole and establish a bridge that contributes to better hole closure after MH surgery.

Based on the above findings, we conclude that ILM peeling performed in cases of FTMH surgery allows hole closure and vision improvement, even though anatomical differences as seen in OCT, reveals thinning of inner retinal layers and nasal displacement of the closed

hole. Multifocal ERG revealed a functional alteration that is dependent on integrity of the ORL. Also, the position of ILM over the hole may have consequences on integrity of ORL and, consequently, BCVA.

Key words: Macular hole, Internal Limiting Membrane, Surgery, Optical Coherence Tomography.

A retina é um tecido neuronal transparente composto de várias camadas e que forra os dois terços posteriores do globo ocular. A mácula, responsável pela visão central, visão de cores e de alta resolução, está situada no chamado polo posterior, entre as arcadas vasculares da retina. Tem um diâmetro de cerca de 5,5mm estando o seu centro a 3,5 mm do bordo do disco óptico e 1mm abaixo do centro do disco, em olhos emétopes. A fóvea corresponde ao centro da mácula.

Na retina encontramos duas camadas básicas, a mais posterior, camada de epitélio pigmentar e a interna, camada neurosensorial. Esta retina neurosensorial é composta por 9 camadas, sendo do lado vítreo para o lado coróideu:

Membrana limitante interna (MLI)

Camada de células nervosas (CCN)

Camada de Células ganglionares (CCG)

Camada plexiforme interna (CPI)

Camada nuclear interna (CNI)

Camada plexiforme externa (CPE)

Camada nuclear externa (núcleo dos fotorreceptores)

Membrana limitante externa (MLE)

Camada de fotorreceptores (zona elipsoide, ZE)

Assim, a retina neurosensorial é composta de 3 camadas de corpos celulares neuronais e duas camadas de sinapses. A camada nuclear externa contém corpos celulares dos cones e bastonetes, a camada nuclear interna contém corpos celulares das células bipolares, horizontais e amácrinas. A camada de células nervosas é constituída por células ganglionares e algumas células amácrinas. Entre estas camadas de células neuronais, existem as camadas plexiformes em que ocorrem contactos sinápticos. Na camada plexiforme externa, ocorrem contactos entre cones, bastonetes e células bipolares e células horizontais. A camada plexiforme interna, permite a comunicação entre células

bipolares e células ganglionares, assim como informações das células amácrinas e horizontais sobre as células ganglionares.

A membrana limitante interna é camada mais interna da retina e faz fronteira com o humor vítreo pelo que forma uma barreira de difusão entre a retina neuronal e humor vítreo. É considerada a membrana basal das células de Müller, formada pelos podócitos destas células, colagénio e proteoglicanos, que permite a adesão da MLI à retina e adesão do vítreo cortical à MLI.

A membrana limitante externa forma a barreira para o espaço subretiniano, onde se projectam as porções internas e externas dos fotorreceptores para permitir associação com a camada de epitélio pigmentado atrás e a própria retina neuronal.

O Buraco Macular é um defeito retiniano na fóvea, zona central da retina neurosensorial. Sendo a fóvea responsável pela visão central, o buraco macular pode originar metamorfopsia e defeito central nos campos visuais.

O diagnóstico de Buraco Macular existe desde o século 19. No entanto, o seu interesse tem sido maior desde que Kelly e Wendell revelaram que era possível a resolução cirúrgica do buraco macular com vitrectomia via pars plana, descolamento posterior do vítreo e trocas fluido/ar. Apesar de se considerar que a retina não tivesse capacidade regenerativa, esta técnica permitia encerrar os Buracos Maculares em grande parte dos doentes. A taxa de sucesso no encerramento do Buraco Maculares foi gradualmente melhorando e, hoje em dia, é considerada a patologia vítreo-retiniana com maior sucesso cirúrgico.

Com a introdução de delaminação da MLI, reduziu-se a tracção tangencial o que permitiu uma maior taxa de encerramento do buraco e menos recidivas. Nos últimos 10 anos a delaminação da MLI na cirurgia de buraco macular tornou-se rotina e é praticada pela maioria de cirurgiões vítreo-retinianos. Com o advento da Tomografia de Coerência Óptica (OCT) de domínio espectral (SD), conseguem-se observar alterações estruturais da retina interna com a delaminação, sugerindo possível lesão retiniana, mesmo que se verifique que o buraco encerre e a visão melhore. Por outro lado, a maior ou menor integridade da MLE e ZE observados no OCT após encerramento do buraco, parecem ter relação com a

recuperação da função visual. No entanto, alguns estudos revelaram alterações adversas que originaram preocupação sobre a segurança desta manobra.

O objectivo da presente tese foi observar efeitos anatómicos e funcionais desta delaminação na cirurgia do buraco macular. Fizemos um estudo prospectivo em 72 doentes com buraco macular de estadio 2, 3 ou 4, submetidos a cirurgia de vitrectomia via pars plana, delaminação da membrana limitante interna, trocas fluído/ar, gaz e decúbito ventral. Os resultados pós-operatórios foram registados aos 3, 6 e 12 meses após a cirurgia.

Quanto a alterações anatómicas, os resultados revelaram alterações microestruturais nas diferentes camadas maculares após delaminação da MLI na cirurgia de buraco macular comparativamente aos dados pré-operatórios. Um estreitamento da camada de células ganglionares (CCG) e camada plexiforme interna (CPI), em ambos os lados, nasal e temporal da fóvea, parecem ser as maiores alterações. Mas a diferença de estreitamento das camadas, em cada um dos lados, nasal e temporal, são igualmente importantes, sendo a espessura total nasal maior que a espessura total temporal.

Encontrou-se, ainda, um aumento da espessura do sector interno das camadas internas da macula nasal, assim como um encurtamento da distância entre o disco óptico e a mácula, após cirurgia com pelagem da MLI e encerramento do buraco. Assim, o buraco macular encerra modificando a sua posição inicial, aproximando-se do disco óptico e aumentando a espessura nasal da mácula.

Utilizou-se o ERG multifocal para estudo de alterações funcionais da mácula antes e depois da pelagem da MLI na cirurgia do buraco macular. Trata-se de um método não invasivo que selecciona múltiplas zonas à volta da área macular, de modo a permitir um mapa topográfico de actividade eletrofisiológica na retina central. Após cirurgia eficaz, passa a haver um buraco encerrado, com ou sem integridade da membrana limitante externa, zona elipsoide e epitélio pigmentado. Neste estudo funcional, o ERG multifocal revelou, antes da cirurgia, uma resposta retiniana indetectável na área foveal e parafoveal nos anéis 1 e 2. Após encerramento do buraco, a melhoria da resposta retiniana nos dois anéis referidos parecem ser consequência do encerramento do buraco com realinhamento dos fotorreceptores. A resolução do escotoma central parece ser devida a reparação

anatômica do buraco. No nosso estudo houve um aumento das ondas N1 e P1 no anel 1. Este aumento foi dependente da integridade das camadas externas da mácula, MLE e EZ.

Em buracos maculares de dimensão elevada, superior a 400 micras, a MLI é delaminada até ao bordo do BM, reservando uma porção maior que é dobrada sobre si própria e colocada sobre o buraco, permitindo o seu encerramento. Comprovámos que o resultado funcional e a integridade dos fotorreceptores dependiam da posição final da porção de MLI sobre o BM. Neste estudo, verificámos que se um fragmento de MLI ficasse enterrada no buraco, havia encerramento do buraco, mas não realinhamento dos fotorreceptores. Se o fragmento de MLI se mantivesse sobre o BM, o BM encerrava e as camadas de fotorreceptores, traduzida pela membrana limitante externa e zona elipsoide, revelavam integridade em grande parte dos casos. Para esta integridade também tinha importância o tempo de evolução do BM. Quanto menor tempo de evolução do BM, melhor a taxa de realinhamento das camadas externas da mácula.

Sempre que possível, durante a cirurgia macular, depois da delaminação da MLI e de colocada uma porção evertida de MLI sobre o buraco, eram excisados dois outros pedaços de MLI e estes enviados para estudo. A ultra estrutura e o comportamento da membrana limitante interna excisada foram estudadas por microscopia óptica e electrónica.

Verificou-se que, em meio rico, e estando as duas faces vítreas da MLI em contacto, havia sinais de actividade fibrótica com produção de membrana basal, o que permitia a aderência destas duas faces de MLI. Sugerimos no nosso estudo que células epiretinianas na MLI pudessem ter capacidade proliferativa, com formação de microfibrilhas entre as duas faces adjacentes de MLI. Este facto poderia explicar a aderência observada entre o folheto de ILM e os bordos do buraco macular, depois da cirurgia, o que contribuiria para o encerramento do BM.

Baseados nos resultados encontrados, poderemos concluir que a delaminação de MLI em todos os casos de cirurgia de BM permite o encerramento do buraco e melhoria da visão, apesar de se verificar alterações importantes na anatomia, medidas pela tomografia de coerência óptica, antes e depois da cirurgia. As alterações anatómicas mais importantes são diminuição da espessura das camadas internas da mácula, nasal e temporal, um

aumento da espessura total da porção nasal da mácula e uma diminuição da espessura temporal. E, ainda, um desvio nasal do BM depois do seu encerramento.

O ERG multifocal revela alterações funcionais na mácula depois de cirurgia com pelagem da MLI e, esta alteração, depende da integridade das camadas externas da mácula.

A integridade das camadas externas, MLE, ZE e EP determinam a função visual final. Para ser possível esta integridade, a posição da porção de MLI sobre o BM é muito importante, dependendo se esta fica enterrada no meio do buraco ou se fica sobre o buraco. Por fim, na análise por microscopia electrónica da MLI excisada, encontrámos microfibrilhas de colagénio entre as duas faces vítreas da membrana, que poderão contribuir para o mecanismo de encerramento do Buraco macular.

Palavras chave - Buraco macular, membrana limitante interna, cirurgia, Tomografia de Coêrência Óptica.

Abbreviations

Anti-GFAP	- anti-Glial Fibrillary Acidic Protein
BCVA	- Best Corrected Visual Acuity
BM	- Bruch Membrane
CAML	- Centro Académico de Medicina de Lisboa
CCG	- Camada de Células Ganglionares
CCN	- Camada de Células Nervosas
CNI	- Camada nuclear interna
CPE	- Camada plexiforme externa
CPI	- Camada plexiforme interna
DONFL	- Dissociated Optic Nerve Fiber Layers
ELM	- External Limiting Membrane
ERL	- External Retinal Layers
EZ	- Elipsoide Zone
FTMH	- Full Thickness Macular Hole
GCL	- Ganglion Cell Layer
ICG	- Indocyanin Green
ILM	- Internal Limiting Membrane
INL	- Inner Nuclear Layer
IPL	- Internal Plexiform Layer
IRL	- Internal Retinal Layers
LMH	- Lamellar Macular Hole
mf ERG	- Multifocal Electroretinography
MLE	- Membrana limitante externa
MLI	- Membrana limitante interna
MH	- Macular Hole
OCT	- Optical Coherence Tomography
ORL	- Outer Retinal Layers
PPV	- Pars Plana Vitrectomy
PVD	- Posterior Vitreous Detachment

RCT	- Randomized Clinical Trial
RNFL	- Retinal Nerve Fiber Layer
RPE	- Retinal Pigment Epithelium
SD	- Domínio Espectral
SF6	- Sulfur hexafluoride
TA	- Triamcinolone Acetonide
VMA	- Vitreous Macular Adhesion
VMT	- Vitreous Macular Traction
ZE	- Zona Elipsoide

Overview of the thesis

Over the years preceding the execution of this work, compelling evidence had indicated an essential involvement of vitrectomy and ILM peeling in the treatment of MH. Given the concerns of ILM peeling, we proposed to study how ILM peeling could influence macular anatomy and macular function after surgery. In large macular holes, ILM was peeled around the hole, leaving one piece still attached and inverted over the hole. In this study, two other pieces of ILM were also collected elsewhere around the hole, prepared for transmission electronic analysis of peeled ILM and also allowing the study of behavior of ILM vitreal faces in contact. Closing the hole is not the only important result. Also, integrity of outer nuclear layers is fundamental for recovery of best corrected vision. Therefore, we studied the influence of ILM position over the hole and its relation to integrity of photoreceptor layer and pigment epithelium layer, after hole closure. The thesis is organized in five chapters. Chapter 1, a general introduction, hypothesis and aims, background that describes anatomy of macula, MH surgical treatment and complications, material and methods. Chapter 2, 3, 4 and 5 present the results obtained in the context of this thesis, published in peer review scientific journals.

In these chapters we also discuss the key findings obtained throughout this thesis and the putative relevance of ILM peeling in macular anatomy as seen in OCT, and macular function measured in electrophysiological studies. The ultrastructure study of peeled ILM was also evaluated and the relation of the position of ILM in MH surgery in outer nuclear layer integrity as well as best correct visual acuity. Chapter 6 includes discussion and conclusions.

1. Introduction

Idiopathic full thickness macular hole (MH) is a vitreomacular interface disorder, which can lead to severe visual impairment. (1) It is estimated that it is present in 33 of every 10,000 individuals older than 55 years, with a female-to-male ratio of 2 to 3:1 (2). As the fovea is the site responsible for central vision, this full-thickness defects in the neurosensory retina results in vision loss, metamorphopsia, and central visual field defects (1). If loss of vision is very severe and only peripheral vision is maintained, quality of vision and quality of life are seriously affected.

The role of the vitreous cortex in the pathogenesis of MH became better understood with the biomicroscopic observations of Donald Gass (3). The pathogenesis involves antero-posterior traction and/or tangential traction exerted by the posterior vitreous cortex at the fovea from an incomplete posterior vitreous detachment (PVD) as a result of aging (4)(5)(6). A MH may form when PVD occurs, but the vitreous still tenaciously adheres to the edges of the fovea (4)(7). This phenomenon is possible when the liquefaction of the vitreous is not accompanied by a simultaneous weakening of the adherence of the posterior hyaloid to the fovea and optic nerve.

OCT reveals, before the formation of MH, the presence of a partially detached ring of the vitreous extending from the fovea, where it remains attached to the papilla and to the vascular arcades on one side, and to the fovea in the center. A pocket of vitreous fluid is also visible immediately in front of the macula (4)(7). (Figure 1) Thus, passive movements of the vitreous fluid in the precortical vitreous pocket, along with the contraction of the posterior hyaloid adhering to the fovea, create antero-posterior traction.

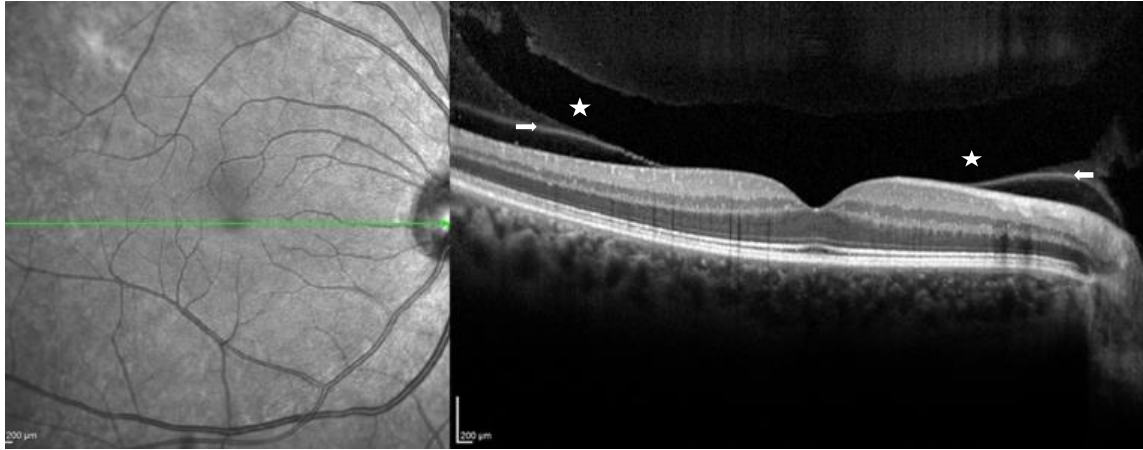


Figure 1-Horizontal spectral-domain optical coherence tomography scan of an asymptomatic 47-year-old man showing a large pre-macular liquefied pocket (black area with white stars). Its posterior wall, the vitreous cortical layer overlying the macular area, is very thin, and shallow vitreous separation is beginning in the peripheral macula. (white arrows)

The fovea consists mainly of photoreceptors and their axons covered by a cap of Müller cells. The ILM is rather thick at the macula but becomes thin over the fovea. (8) Generally, at sites where the ILM is thin, the vitreous fibers are more anchored to the retinal tissue and may exert greater tensile forces.

The ILM, the layer that defines the transition between the retina and the vitreous body, is composed of the internal expansions of Müller cells and by a basement membrane made primarily of collagen fibers, glycosaminoglycans, laminin, and fibronectin connected to peripheral fibers of the cortical vitreous. Under certain conditions, the focal traction of the vitreous adherent to the central ILM can break the retina at its thinnest point (9). Stiffening, distortion, and enlargement of the MH rim are consequences of epi-macular glial and Müller cell proliferation through the retinal hole and over the ILM surface. After the formation of a MH, enlargement is largely caused by tensile shear strain from shortening of the ILM edges causing tangential traction. Moreover, stiffening and thickening of the ILM are important contributory causes of other pathologic macular conditions such as epiretinal membranes, diabetic tractional maculopathy, vitreomacular traction (VMT), and myopic traction maculopathy (10).

Until the early 1990s, there was no treatment for established MH. MH surgery has evolved from the initial studies of Kelly and Wendel in 1991 (11), and became a treatable disease with PPV and elimination of the anteroposterior traction, allowing anatomical closure. The

rationale for surgical intervention originated in the identification of centrifugal traction as the cause of MH formation, rather than permanent loss of foveal tissue being responsible for the visual deterioration (12). Classic MH surgery by vitrectomy with posterior vitreous cortex separation, intraocular gas tamponade and face down position, has become the main treatment (13). The modification by addition of ILM peeling was first reported in 1997 by Eckardt et al (14). This intentional removal of the macular ILM resulted in a meaningful improvement in the anatomical success rate in the surgical treatment of an MH, and a cost-effective option for the treatment of this disorder (15)(16).

Nowadays, focus is on ILM peeling as adjuvant therapy for increasing closure rates, with a number of options to choose from. Surgery for MH is now one of the commonest vitreoretinal surgeries undertaken, accounting for approximately 10% of all vitrectomies (17). ILM peeling has gained widespread acceptance because it has been shown to improve closure rates and to prevent late postoperative reopening, one of the most common complications of successfully closed MH (14)(18).

Some authors like Kwok et al in 2005, described a number of changes in retinal structure and visual function after MH surgery, and suggest that ILM peeling may not be necessary in all cases (19). Nonetheless, several variations of the procedure have been described, depending on the hole dimension, including the extent of ILM peeled during surgery and various techniques of ILM peeling. Moreover, further developments of the technique have been proposed, including complete ILM peel and ILM peel associated to inverted ILM flap (20).

There is a general consensus that the rate of anatomical closure of MH improved significantly after ILM peeling (21)(22). However, regardless of its beneficial effects, ILM peeling has also been shown to lead to some structural and functional alterations. (23) Immediate effects are focal retinal hemorrhages, whitish nerve-fiber layer, and full thickness retinal defects caused by instrument trauma or iatrogenic eccentric holes (24)(25).

Swelling of the arcuate retinal nerve-fiber layer (RNFL) (26), on spectral domain optic coherence tomography (SD-OCT) seems to be the earliest short-term anatomical change in the macula after ILM peeling. A “Dissociated Optic Nerve-Fiber Layer” (DONFL)

appearance, first reported by Tadayoni et al, (27) after epiretinal membrane and ILM peeling, was described to occur a few months after ILM peeling in MH surgery and is believed to be related to loss of distal Müller cell processes resulting in dimpling of the nerve-fiber layer (27)(28).

A variety of other morphologic and functional changes in the retina have been noted after ILM peeling. Some authors have observed paracentral scotomas and reduced central retinal sensitivity after ILM peeling (23)(28). Terasaki et al found electrophysiologic changes with delay in the recovery of the b-waves of focal macular electroretinograms (29), and decrease in thickness of the macular retinal layers (30), whereas other authors have found no functional consequences possibly relating to the difficulty of testing (23).

In summary, in the last 10 years, ILM peeling during surgery for a MH has become a routine step and is performed by most surgeons. With the advent of modern spectral-domain SD-OCT, however, one can now see abnormal structural changes to the inner retinal surface with ILM peeling, suggesting possible progressive retinal damage. Moreover, some clinical studies found adverse functional events that have given rise to concerns regarding the safety of ILM peeling.

2. Hypotheses and Aims

In this study, we describe the current understanding regarding the pathogenesis of MHs. Surgical treatment with ILM peeling has allowed greater rate of MH closure, even for large MH. However, anatomic closure of MH is not always associated to the same functional outcomes. The purpose of the present thesis was to assess consequences in retina anatomy and function, after MH surgery with ILM peeling. More specifically, the questions addressed in this work were the following:

- 1- Does MH surgery with ILM peeling lead to changes in macula anatomy?
- 2- Does MH with ILM peeling affects retinal function as measured by Multifocal Electroretinography?
- 3- Does the surgical technique in ILM peel for large MH influences integrity of photoreceptor layer and visual acuity?

4- Is there a relation between duration of symptoms of MH and visual acuity after successful surgery?

5- What alterations in the ultrastructure and behavior of peeled ILM that may help to explain the mechanisms of hole closure?

3. Background

3.1 - Retina

The neural retina is a transparent tissue of multiple layers that lines the posterior 2/3 of the eye. The macula is in the so-called posterior pole, between vascular arcades, responsible for the central, high-resolution and color vision. The human macula is approximately 5.5 mm in diameter, its center is approximately 3.5 mm lateral to the edge of the optic disc and approximately 1 mm inferior to the center of the disc. The fovea is located at the center of the macula. (Figure 2)

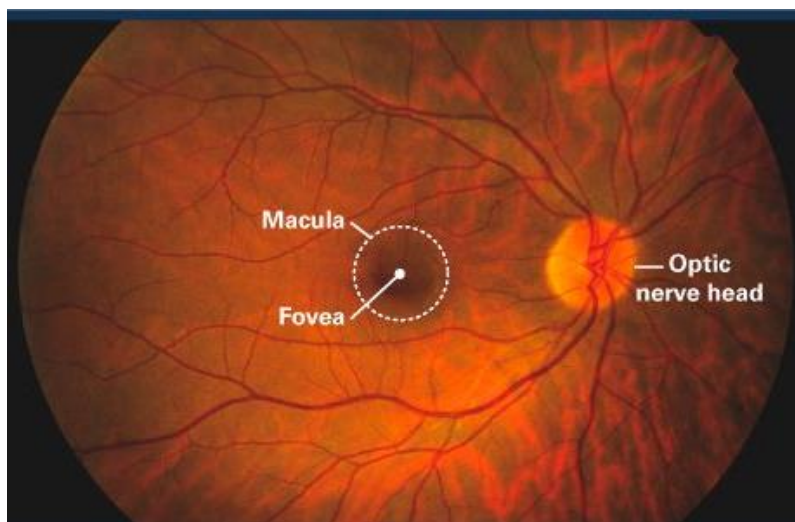


Figure 2- Fundus photography of the Optic nerve head, Macula and Fovea

3.1.1 - Macular layers

The retina is composed of two basic layers, the outer, more posterior retinal pigment epithelium layer (RPE) and the inner neurosensory layer. (Figures 3 and 4)

The neurosensory retina is composed of three layers of nerve cell bodies and two layers of synapses. The outer nuclear layer contains cell bodies of rods and cones, the INL contains cell bodies of the bipolar, horizontal and amacrine cells, and the ganglion cell layer contains cell bodies of ganglion cells and displaced amacrine cells. Between these nerve cell layers are two neuropils where synaptic contacts occur.

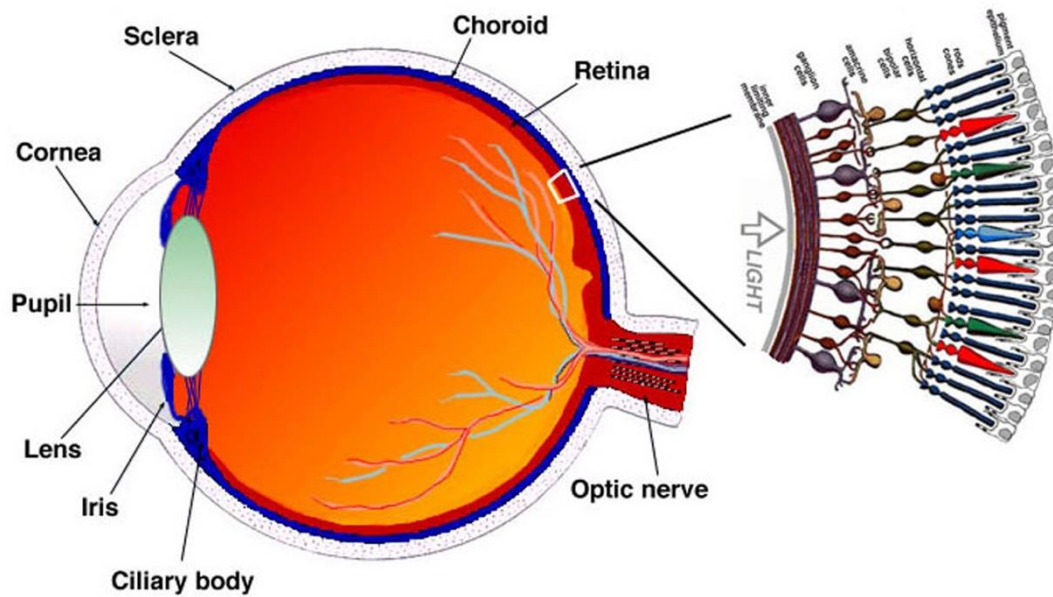


Figure 3 - A drawing of a section through the eye with a schematic enlargement of the retina. (From Simple Anatomy of the Retina by Helga Kolb)

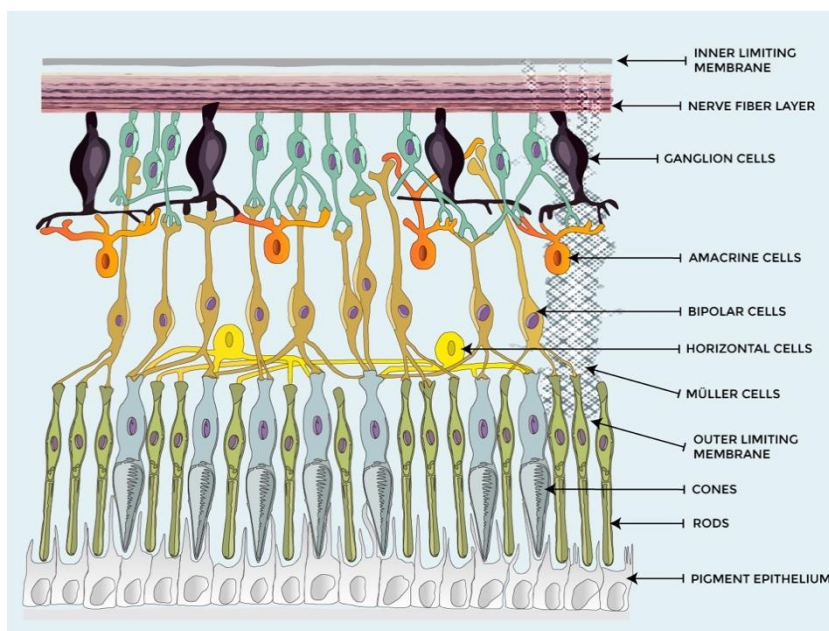


Figure 4- Diagram of organization of the retina

The first area of the synaptic layer is the OPL where connections between rod and cones, and vertically running bipolar cells and horizontally oriented horizontal cells occur. (Figure 5)

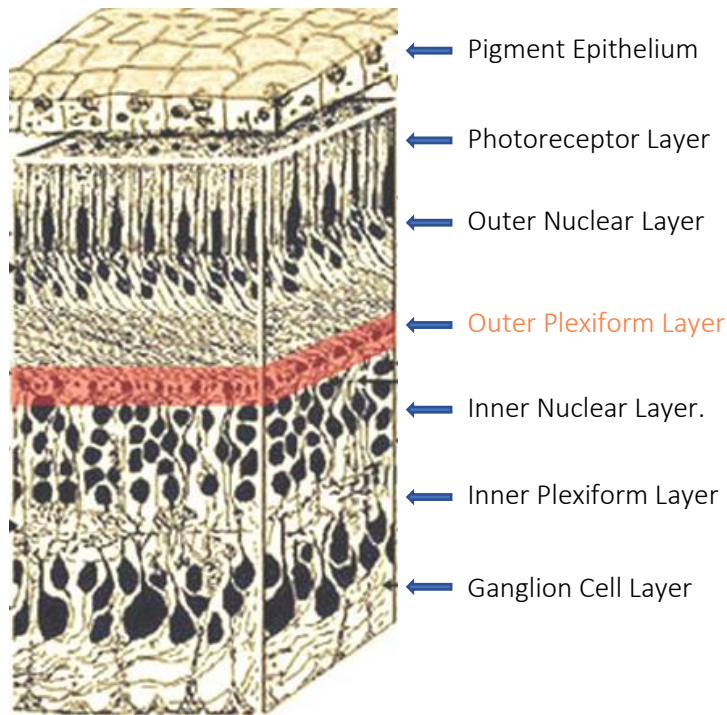


Figure 5- Retinal layers with outer plexiform layer in red (From *Simple Anatomy of the Retina* by Helga Kolb)

The second synaptic layer of the retina is the IPL, and it functions as a relay station for the vertical-information-carrying neurons, the bipolar cells, to connect to ganglion cells. In addition, different varieties of horizontally and vertically directed amacrine cells somehow interact in further networks to influence and integrate the ganglion cell signals. (Figure 6)

The central retina close to the fovea is considerable thicker than the peripheral retina due to the increased packing density of photoreceptors, particularly the cones, and their associated bipolar and ganglion cells in the central retina compared with the peripheral retina.

The fovea lies in the middle of the macula area of the retina to the temporal side of the optic nerve head. In this area, cone photoreceptors are concentrated at maximum density, with the exclusion of the rods, and arranged at their most efficient packing density which is in a hexagonal mosaic. No nerve fiber layers are found in the fovea, allowing direct access of light to photoreceptors.

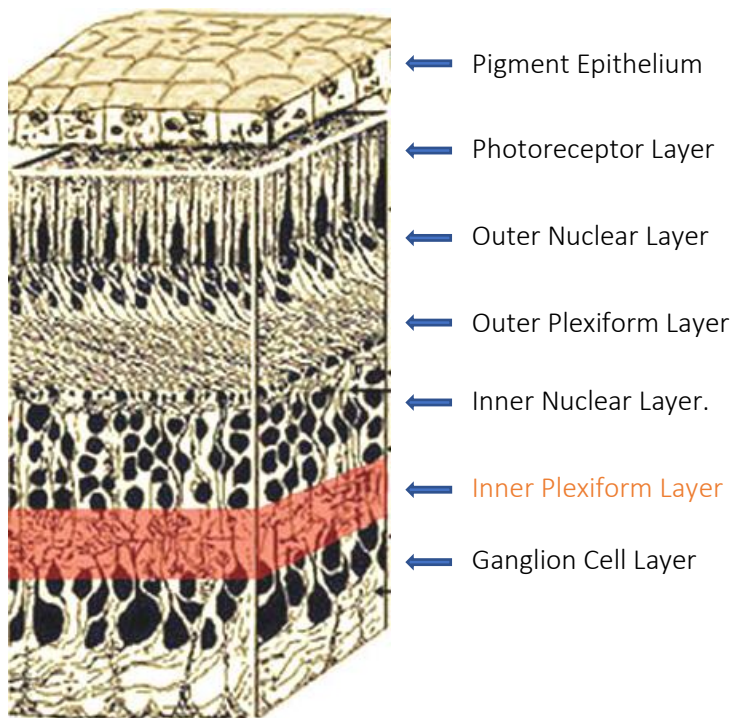


Figure 6- Retinal layers with Inner plexiform layer in red (From *Simple Anatomy of the Retina* by Helga Kolb)

The pigmented epithelial cells in the fovea are higher and contain more pigment than cells elsewhere in the retina, contributing to the darkness of this area.

Müller cells are the radial glial cells of the retina. The ELM of the retina is formed from adherens junctions between Müller cells and the inner segments of photoreceptors.

The ILM of the retina is likewise composed of laterally contacting Müller cells' end feet and associated basement membrane constituents. (Figure 7)

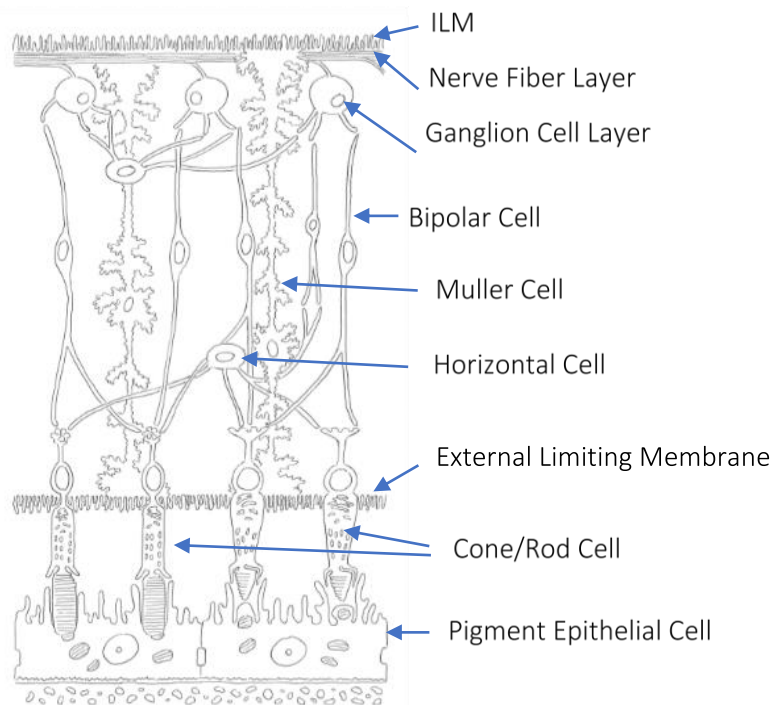


Figure 7- Graphic scheme of the retinal structure highlighting its major structures (Courtesy of S. Sciarini).

3.1.2 - Internal Limiting Membrane

The ILM sits at the inner surface of the retina bordering the vitreous humor and thereby forming a diffusion barrier between the neural retina and the vitreous humor. It is formed by the basement membrane of the Müller cells and it is composed of collagen and a wide variety of proteoglycans (31), many of which are involved in both the adhesion of the ILM to the retina and also the adhesion of the cortical vitreous to the ILM. The ILM thickens and becomes more rigid with age (32). Its vitreous side is smooth where it meets the condensed cortical vitreous but is deeply convoluted on the retinal side (33). (Figures 8 and 9)

Although thin, the ILM has a mechanical strength in the mega-pascal range, similar to articular cartilage and approximately 1,000-fold stronger than cell layers, contributing to at least 50% of the retinal rigidity (32)(34). Despite the ILM being only a few microns thick, it contributes very significantly to retinal rigidity, and its removal during MH surgery results in an increase in retinal compliance, aiding hole closure. Also, this alteration in retinal compliance facilitates movement of the temporal retina towards the optic disk (35), thereby contributing to MH closure.

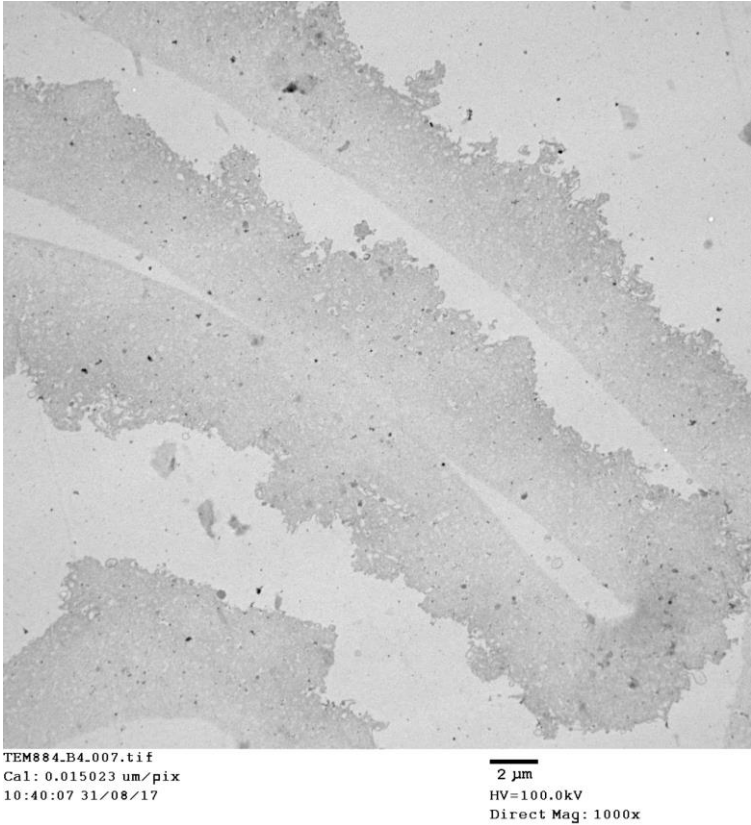


Figure 8- ILM in Transmission Electron Microscope (TEM), magnification 1000x s. Vitreous side is smooth and retinal side is convoluted.

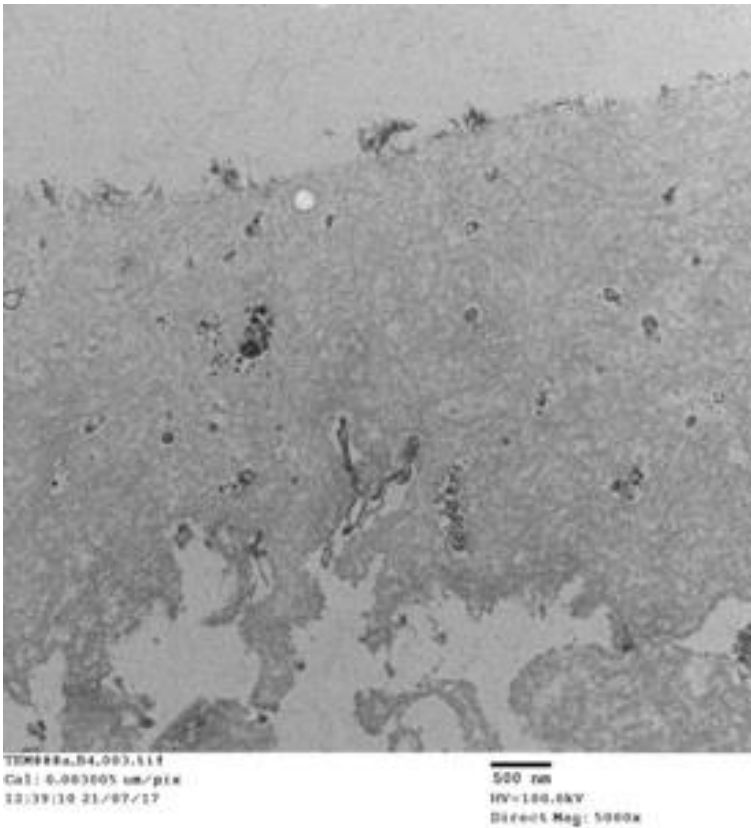


Figure 9- ILM in Transmission Electron Microscope, magnification 5000 x s. The upper smooth side is the vitreous side, the lower rough side is the retinal side.

Surgical peeling of ILM not only removes the remaining macular cortical vitreous, which could exert residual tangential traction, but also inhibits the formation of postoperative epiretinal membranes and secondary tangential traction(6)(36). Finally, ILM removal, and the consequent trauma to the Müller cell end feet, may lead to a retinal glial cell proliferation reaction, which could paradoxically enhance MH contraction and repair (6)(36).

3.1.3 - Müller Cells

Müller cells represent the major type of glial cells in the retina. In recent decades, Müller cells have been acknowledged to be far more influential on neuronal homeostasis in the retina than previously assumed (37). With their unique localization, spanning the entire retina and interposed between the vessels and neurons, Müller cells are responsible for the functional and metabolic support of the surrounding retinal neurons (38). Müller cells end feet are part of the ILM. In 1969, Yamada (39) reported the anatomy of the fovea centralis and described that the inner half of the foveola is composed of an inverted cone-shaped zone of Müller cells, the Müller cell cone. (Figure 10)

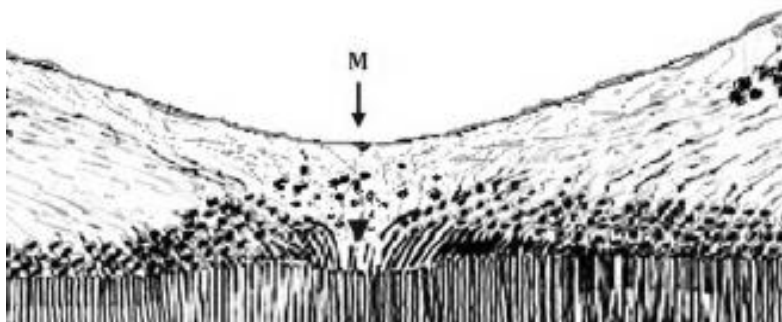


Figure 10- Schematic representation of the normal human fovea centralis from Gass, based on the histological findings of Yamada and Hogan et al. The Müller cell cone (M) is shown with its base forming the internal limiting membrane (arrow) and its apex forming the external limiting membrane (arrowhead).

The cell bodies of Müller cells are located in the inner nuclear layer (INL), and many cellular processes in Müller cells span the whole thickness of the neurosensory retina. Müller cells end feet are part of the ILM, and all types of cell bodies and the retinal neuronal processes are ensheathed in these cells. On the other hand, Müller cells proliferate and form the ELM at the photoreceptor layer level. The ELM is connected to the ILM at the fovea center due to thickening of the Müller cell layer, creating a cone-shaped appearance. This forms the Müller cap, which is a reservoir of xanthophylls, and it enables Müller cells to protect

to the retina. It has been proposed that the Müller cell cone serves as a plug to bind together the receptor cells in the foveola (40). Without this plug of glial cells, the retinal receptor cell layer with its thin layer of horizontally radiating nerve fibers would be highly susceptible to disruption and hole formation. There is indeed considerable evidence that MH formation begins with contraction of the pre-foveolar vitreous cortex that is tightly adherent to the ILM of the Müller cell cone. It is likely that Müller cell invasion and proliferation within the pre-foveolar vitreous cortex are important in causing contraction of the pre-foveolar vitreous cortex and the sequence of events of MH formation.

Recently, investigators using OCT and scanning electron microscopy to study patients with impending MH have demonstrated evidence of a split in the foveola with cyst formation in some patients (41)(42). (Figure 11)

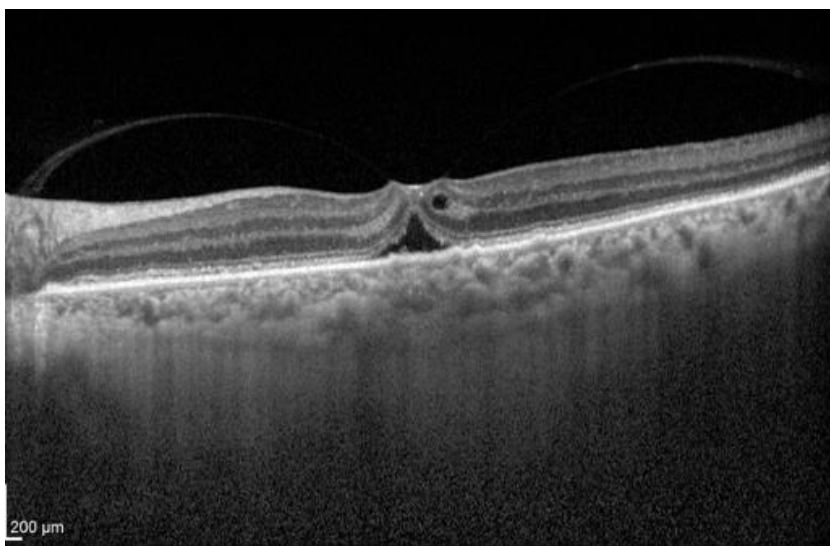


Figure 11- Split in foveola and cyst seen in OCT of left eye of patient with macular hole on right side

3.2 - Optical Coherence Tomography

OCT is a non-invasive diagnostic imaging modality that enables in-vivo cross-sectional or three-dimensional visualization of the retinal microstructure. It has a rapid and simple execution, repeatability and precise measurements. OCT imaging is analogous to ultrasound, except that it uses light instead of sound. Measurements are performed by directing a beam of light onto tissue and measuring the echo time delay and magnitude of reflected or backscattered light using low-coherence interferometry. In Ophthalmology,

OCT has enhanced the detection of many subtle vitreous, retinal, and choroidal changes, which are difficult or impossible to be visualized by ophthalmoscopy (43) (44).

OCT is currently the gold standard imaging technique for diagnosis and follow-up of retinal diseases including MH. (41) Our understanding and treatment for retinal diseases have been improved (45), especially the changes occurring in the vitreoretinal interface (46).

The preoperative assessment of MH by means of OCT is fundamental for the evaluation of several important features that have been recognized to contribute to the anatomical and functional outcomes after surgical repair. The noninvasive morphological investigation of these lesions has allowed for the pivotal distinction between FTMH, characterized by an interruption in the neuroretina involving all the sensory layers (47), and other types of MH, such as lamellar macular hole (LMH) and pseudo-holes (48).

Besides pre-operative OCT studies, the intra-operative and post-operative monitoring of the surgical outcomes has allowed for unattended insights on the response of the retinal tissue to the closing procedures (49)(50). In fact, ocular biomicroscopy is seldom able to evaluate the extent of retinal morphologic changes that take place after the surgery and is not able to establish any correlation between the anatomical and functional findings.

The standard field of view in the OCT systems is 30° and it is important to examine disease primarily affecting the macula (43). Its ability to non-invasively image detailed ocular structures and associated microvasculature *in vivo* with high resolution has improved quality of patient care. OCT technology is based on the principle of low-coherence interferometry, where a low-coherence light beam is directed on to the target tissue and a three-dimensional volume of structural and flow information can be compiled. Typically, spectral domain OCT instruments use an infrared light source centered at a wavelength of about 840 nm. For a given wavelength, the axial resolution is dictated by the band-width of the light source. The latest commercial instruments typically have an axial resolution of approximately 5 μm, while research instruments have been built with a resolution as high as approximately 2 μm (Figure 12). The lateral resolution is limited by the diffraction caused by the pupil and it is normally about 20 μm. For clinical purposes, the image acquisition time is limited by the patient's ability to avoid eye movements, the availability

of scanning techniques to adjust for movements, and the availability of tracking software that adjusts for eye movements.

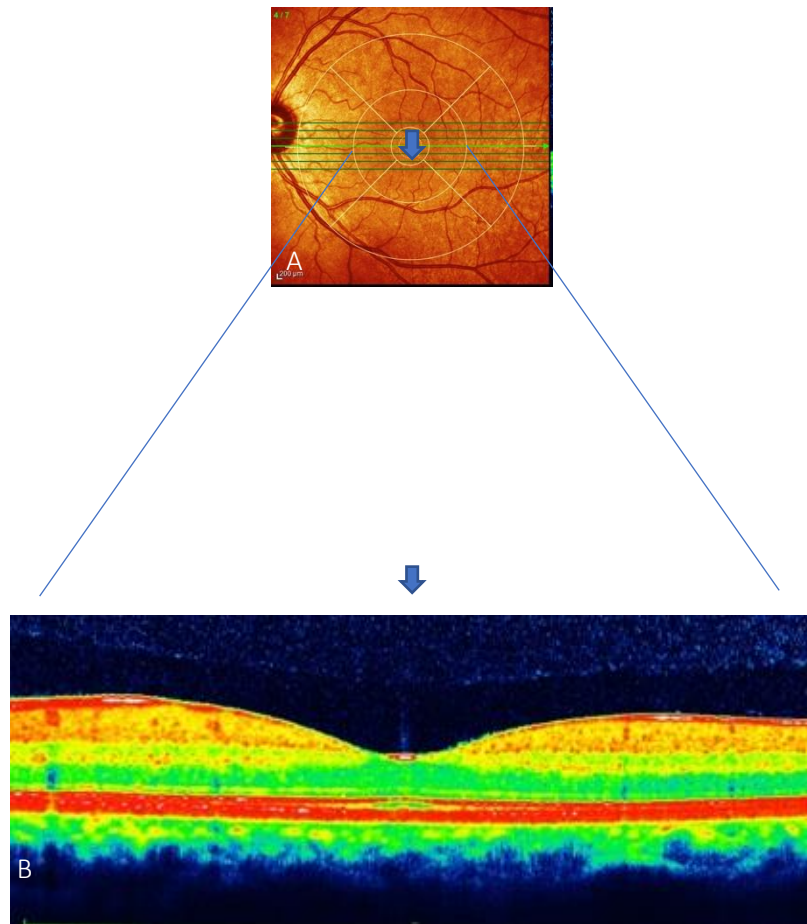


Fig 12- A- Fundus photo of a normal human macula, optic nerve and blood vessels around fovea. (200 μ m) B- Optical Coherence tomography (OCT) image of the same normal macula in the area boxed in light green and between 3.00 mm diameter limited by medial yellow circle, parafoveal area, centered on fovea. The foveal pit (arrow) and the sloping walls with displaced inner retina neurons (yellow and red cells) are clearly seen. Green cells are packed photoreceptors, primarily cones, above the foveal center.

The most commonly used quantitative parameter derived from OCT datasets is retinal thickness, obtained by segmenting the ILM and a boundary representing the RPE (Figures 13 to 21). This information can be used to generate surface maps of the ILM and the RPE as well as two-dimensional and three-dimensional retinal thickness maps. These maps can be very useful in identifying and describing deviations from the normal anatomy and changes over time. In addition to total retinal thickness, a number of other quantitative parameters have been proposed, such as the thickness of the GCL or the thickness of the photoreceptors' outer segments, as well as measurements of retinal lesions.

Spectral domain OCT has allowed researchers to assess the multilayer microstructure of the retinal fovea and demonstrate the importance of proper recovery of retinal lines in improving BCVA. Different retinal lines have been shown to influence visual improvement after closure of the MH. Wakabayashi and Bottoni (51)(52), emphasized ELM recovery as a sign of intact photoreceptor cell bodies and Müller cells.

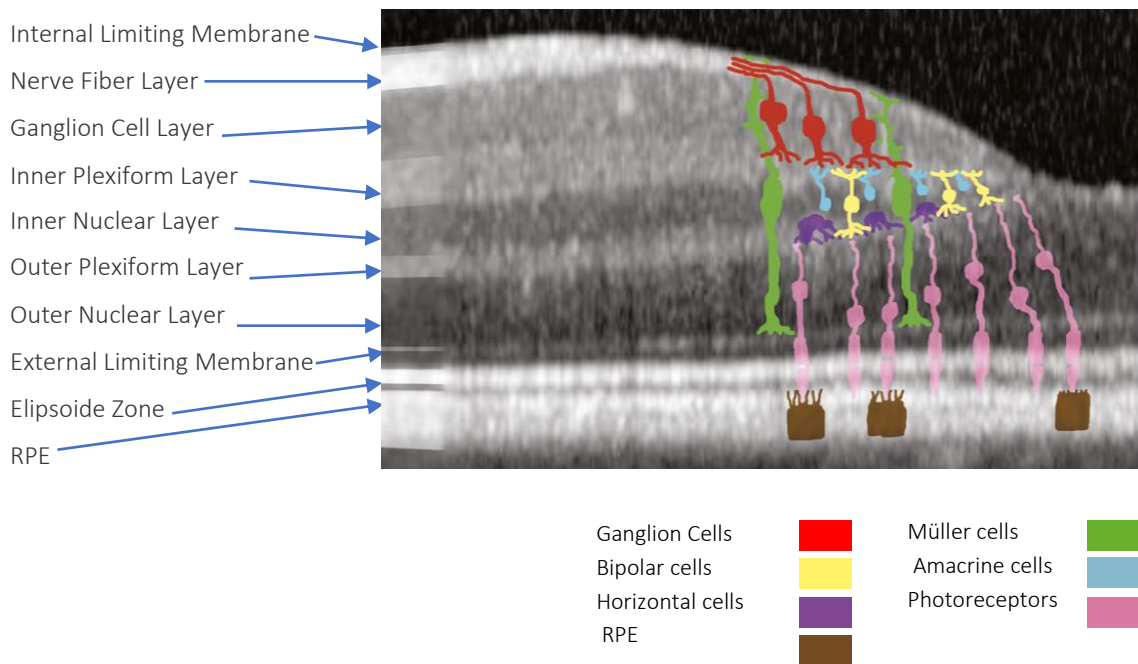


Figure 13 - The superimposed illustration is a representational drawing of the cell types found in a normal fovea (cells not to scale). Drawing is color coded by cell type. (From Atlas of OCT - Neal A. Adams, Heidelberg Engineering)

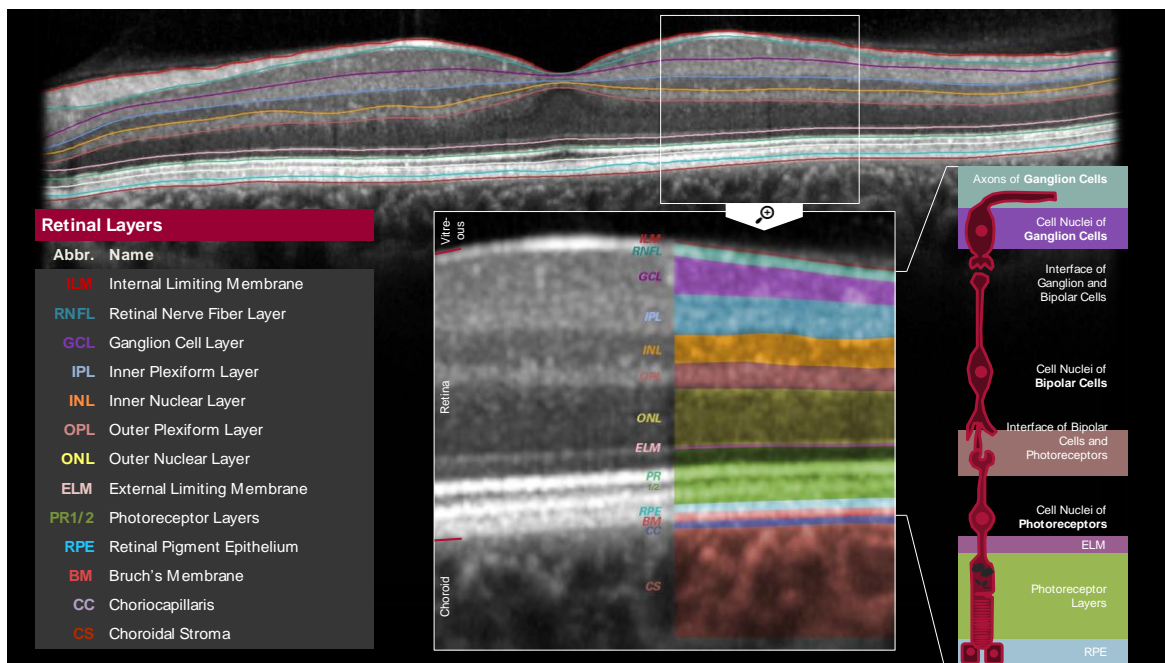


Figure 14- SD-OCT with identification of retinal layers in colors and correspondence in cell type and interface layers. (Courtesy of Heidelberg Engineering).

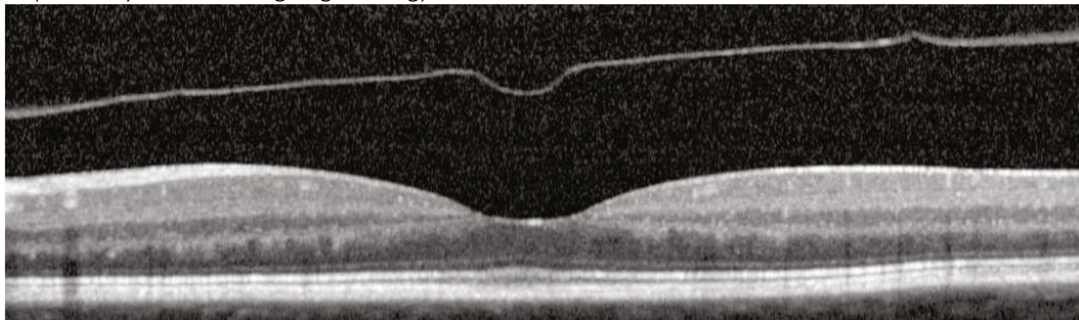


Figure 15 - Complete PVD. The posterior face of the vitreous is completely separated from the retina.

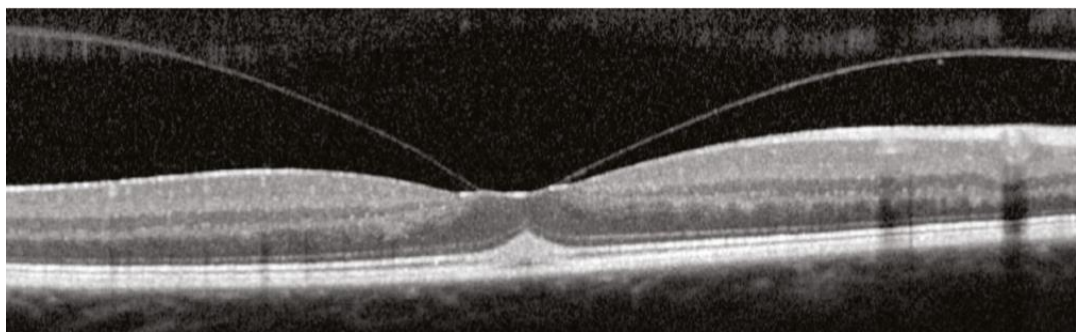


Figure 16- The posterior face of the vitreous is pulling on the fovea, resulting in a peaked appearance of the photoreceptors

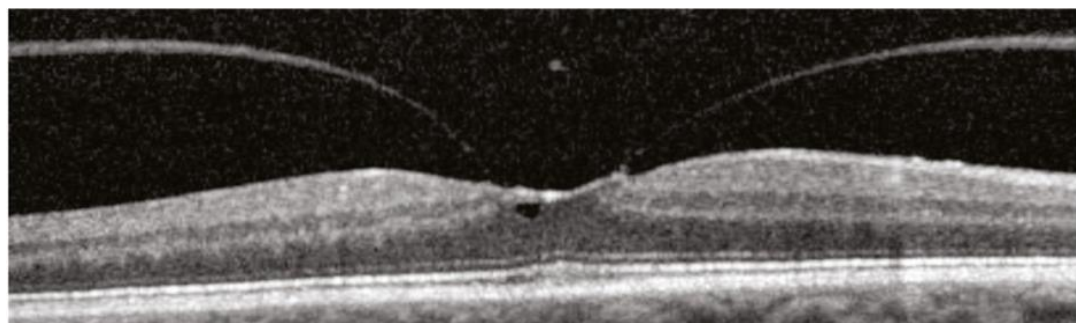


Figure 17- The posterior face of the vitreous is pulling on the fovea, resulting in a cyst.

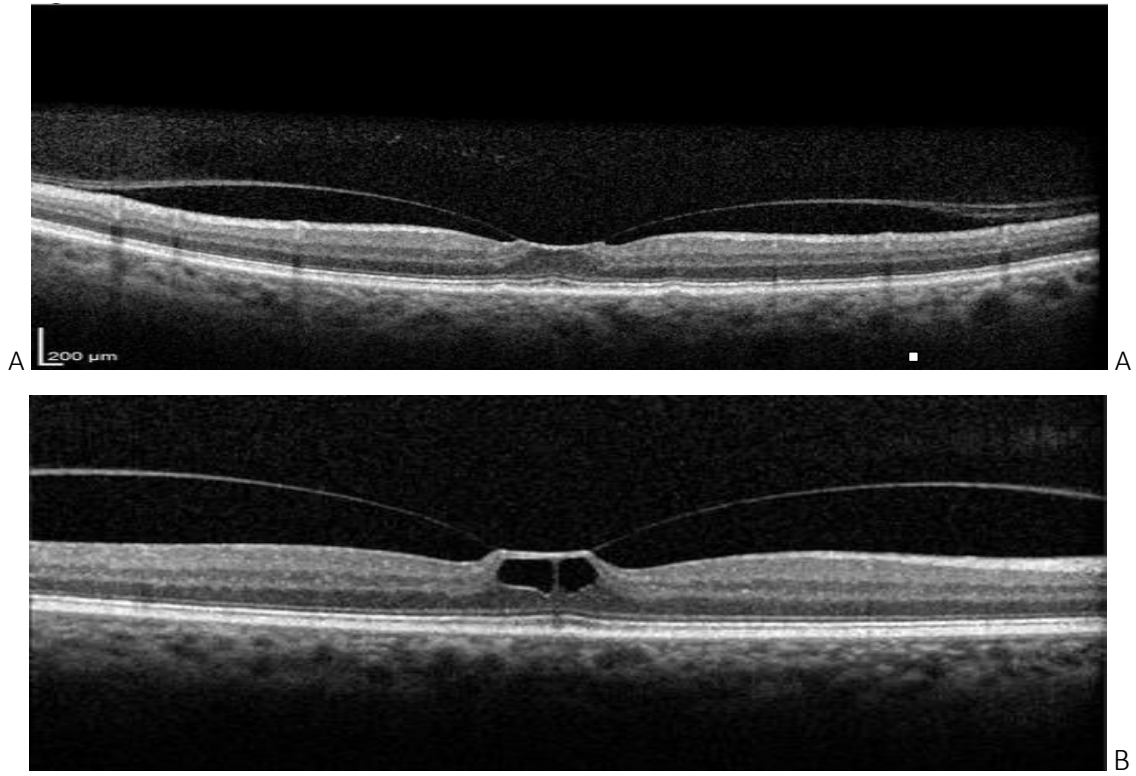


Figure 18 – SD OCT of 71 years old man, A-left eye in top and B-right eye in bottom with vitreomacular traction in both eyes and cystic lesions right eye.

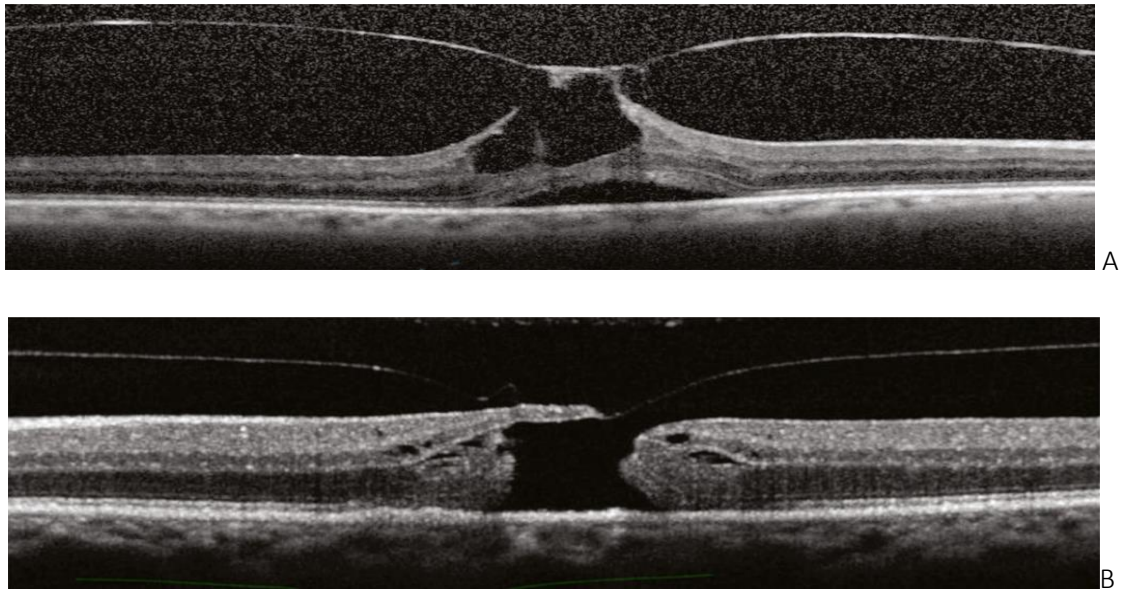


Figure 19- The full-thickness macular hole in the OCT image has a partial roof and the traction from the posterior face of the vitreous is clearly visible, both in A and B

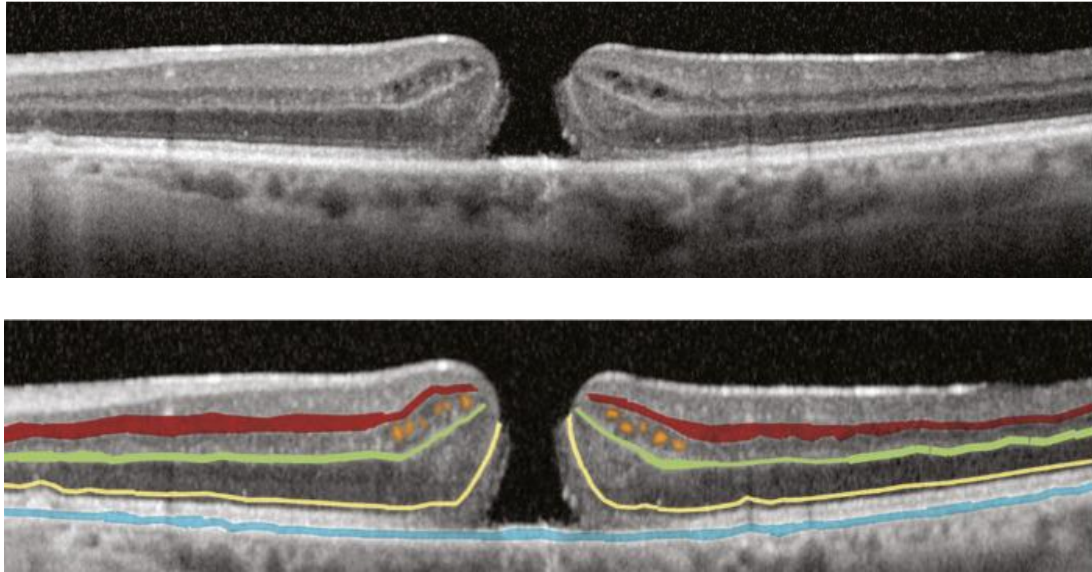


Figure. 20 Full-thickness macular hole. The hole goes all the way through the retina, exposing the RPE (shaded blue). The curling of the photoreceptor layers can most easily be identified by tracing the external limiting membrane (shaded yellow) between the photoreceptor nuclear layer and the photoreceptor inner segments. Several small intraretinal cysts (shaded orange) can be seen within the inner nuclear layer, between the outer plexiform layer (shaded green) and the inner plexiform layer (shaded red). (From Atlas of OCT - Neal A. Adams, Heidelberg Engineering)

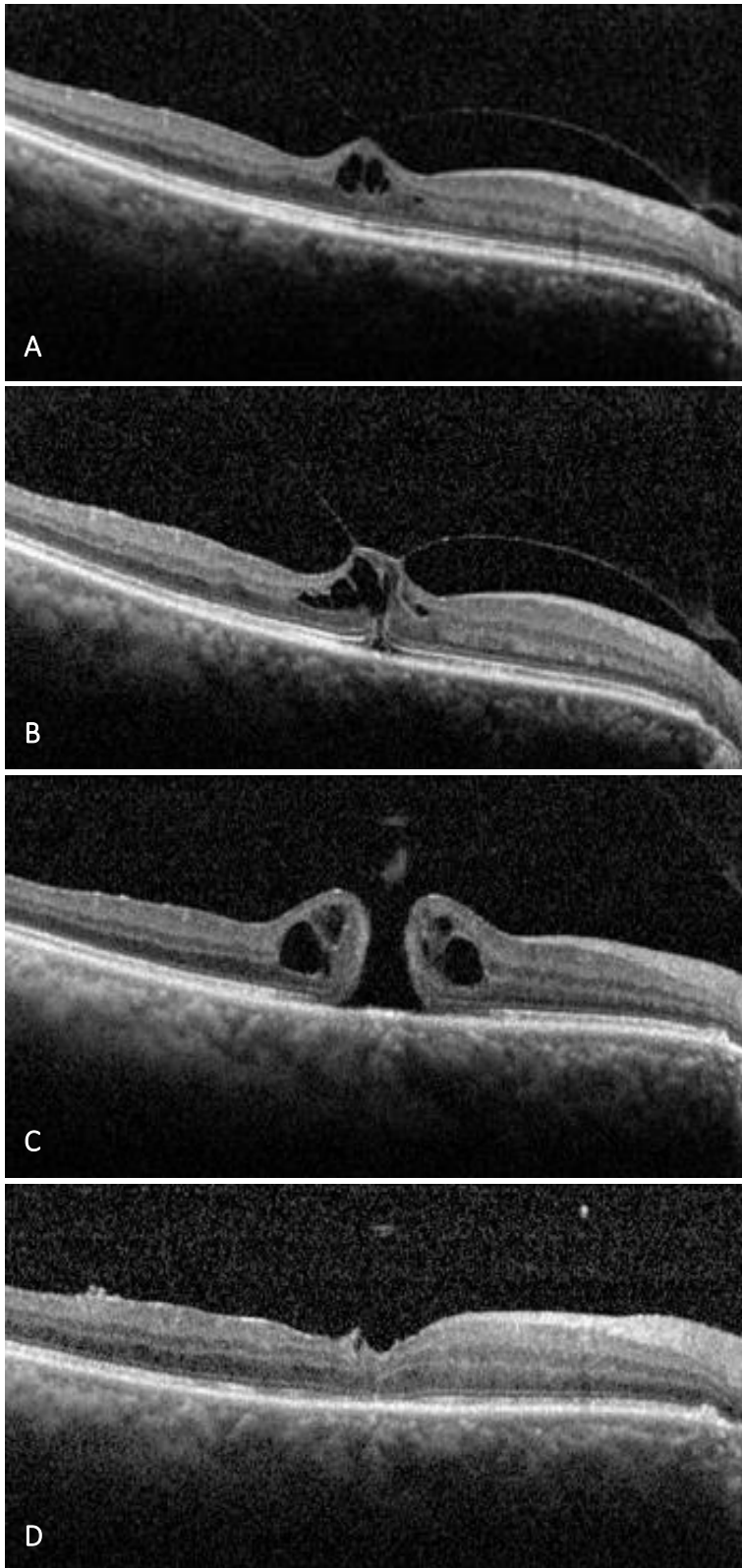


Figure 21- Evolution of a macular hole in one of our patients, 68 years old, fellow eye of eye with macular hole, visualized with optical coherence tomography (OCT). A - OCT- Image of macula with posterior vitreal adherence and foveal traction. B-cavitation and rupture of outer retina layers. C-Full thickness macular hole. D-fifteen days after macular hole surgery; hole is closed. Note the subtle area of increased reflectance in the center.

3.3 - Macular Hole

3.3.1 - Definition

MH are full-thickness retinal defects in the foveal neurosensory retina, (Figure 22) leading to loss of central vision, metamorphopsia and a central scotoma in the affected eye. The majority of MH are primarily idiopathic (85%) with a smaller proportion being as a result of trauma, inflammation or high myopia (53)(54).

The modern history of MH started with J.D. Gass who proposed a staging system ranging from impending to full-thickness MH, on the basis of biomicroscopic observation (3). Hee and Puliafito (41), were the first to describe the stages of MH on OCT scans, and Kelly and Wendel, (11) performed the first successful MH surgery.

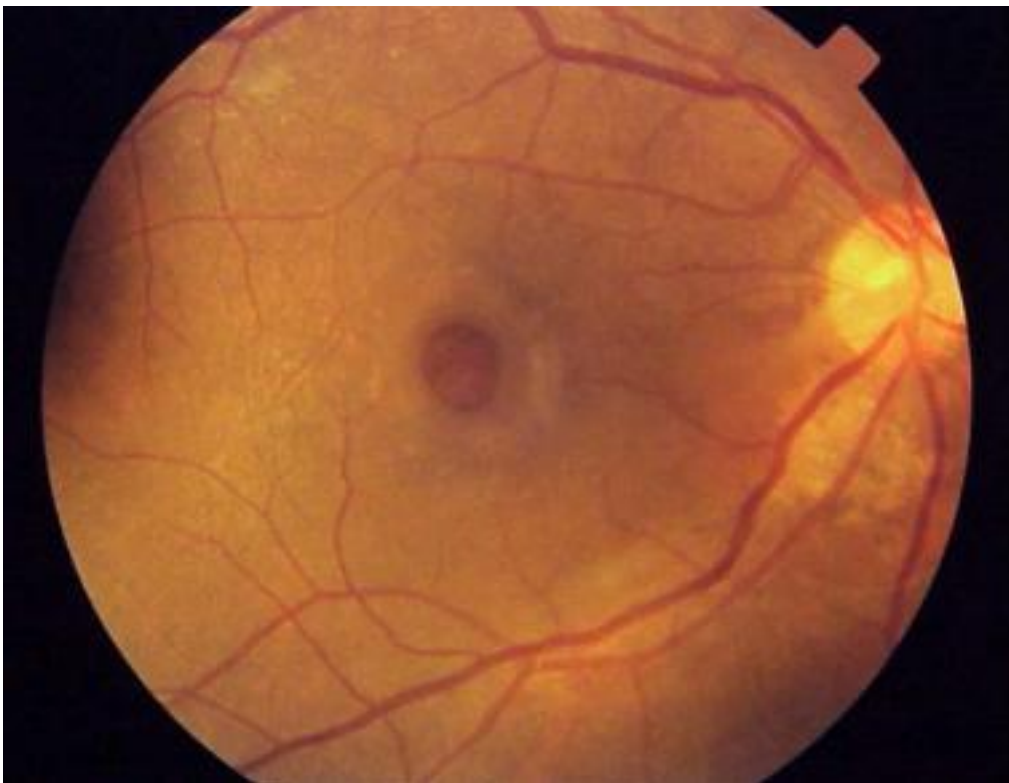


Figure 22- Full-thickness macular hole showing a surrounding cuff of subretinal fluid.

3.3.2 - Prevalence of Macular Hole and Risk Factor

The prevalence of MH reported in literature varies greatly, with a prevalence of 0.02 to 0,8 % in the general population (2) (55) (56). Bilateral MH varies considerably from 5% to 16%.

Age >65 is an important risk factor for the development of MH. Liquefaction of the vitreous and the development of PVD increases with older age. Given that PVDs are known to increase the predisposition for the development of MH, this finding likely explains some of the heightened risk of MH among older individuals. Females have a higher risk of developing MHs relative to males (57) (58). This finding is thought to be associated with the effects of decreased estrogen in the vitreous gel (59). Estrogen changes during perimenopausal years and plays a role in the cross-linking and loss of vitreous collagen and glycosaminoglycans that occurs with vitreous liquefaction, subsequent vitreomacular traction, and the onset of MH pathological findings (2). Over 70% of MHs occur in women and more than half in patients 65-74 years old(60).

3.3.3 - Physiopathology of Macular Holes.

In recent years, the role of the vitreous in ocular physiology (61), and the pathobiology of vitreo-retinal diseases have been increasingly appreciated (62). During youth, there is a strong adhesion between the posterior vitreous cortex and the ILM of the retina, primarily at the vitreous base and at the posterior pole. After the fourth decade of life there is a significant decrease in the gel volume and an increase in the liquid volume of the human vitreous (63). With age, there is a weakening of vitreo-retinal adhesion, most likely due to biochemical alterations at the vitreo-retinal interface (63).

When vitreous liquefaction occurs without concomitant vitreo-macular interface weakening, PVD can be pathologic and may develop into several kinds of vitreo-macular interface diseases (64)(65)(66)(67).

If there is insufficient dehiscence at the vitreoretinal interface, PVD can induce a split within the posterior vitreous cortex (vitreoschisis) (68). Clinical diagnosis of a suspected PVD is based on clinical story of flashes and floaters, (69) and usually results in innocuous separation of the vitreous from the retina. Anomalous PVD is the consequence of gel liquefaction without sufficient dehiscence at the vitreoretinal interface, causing a variety of untoward sequelae. Sebag unified this concept and coined it anomalous PVD. According to Sebag, for an uncomplicated PVD to occur, two processes must occur concurrently: weakening of vitreo-retinal adhesion and vitreous liquefaction (63). An anomalous PVD

occurs when the extent of vitreous liquefaction exceeds the degree of weakening of vitreo-retinal adhesion and leads to posterior vitreoschisis: when splitting of the posterior cortical vitreous occurs and forward displacement of the vitreous body leaves the outer layers of the posterior vitreous cortex still attached to the retina, potentially resulting in the formation of macular disease (68).

It is now widely accepted that antero-posterior and dynamic vitreous traction associated with peri-foveal PVD is the primary cause of MH formation (13). Johnson et al (65), suggested that dynamic tractional forces that are generated by posterior cortical vitreous movement during the rotations of the eye may play an important role in MH development. In 2012, Mori et al. published the results of wide-angle montaged images of SD-OCT in patients with MH and described the mobility of posterior cortical vitreous, using the OCT tracking system. The mass and movement of the vitreous represents the potential force to act on the retina. Therefore, they proposed that the contribution of dynamic forces to the development of idiopathic MH is greater than what has been thought previously (70). Work by Gass (3)(42) in 1988 and data provided from OCT of impending MH have indicated that the first changes in macular hole formation is an intra-retinal split in the macula evolving into an intra-retinal cyst (71). This may lead to disruption of the cone-shaped zone of Müller cells that makes out the primary structural support in the central and inner part of the fovea centralis (40).

3.3.4 - Classification of Macular Holes

Gass described the stages of MH formation based on biomicroscopic findings, and this traditional staging system is still widely used in the clinics and in the literature. In Stage I, a central yellow spot is observed at the foveal center, with loss of the foveal depression (Stage Ia), which can be followed by the formation of a ring-shaped yellow reflex (Stage Ib) without a full thickness defect. In Stage II, a small FTMH (<400 μm) is formed, usually with a visible operculum. In Stage III, the FTMH widens to more than 400 μm in diameter, but complete PVD has not yet occurred, whereas Stage IV is the same as Stage III after complete vitreous separation from the disk (3).

The international study group directed by Duker and colleagues proposed a new anatomic classification of vitreo-retinal interface anomalies based on the use of SD-OCT (72). This classification defines 3 main conditions: vitreo-macular adhesion (VMA), VMT and MH. Vitreo-macular adhesion is not a pathological condition because the fovea is not deformed by vitreous traction, and vision is usually not disturbed. Retinal specialists suggest that this aspect is the first stage of PVD and occurs commonly after the age of 40 years (73). In VMT, the vitreous adhesion causes distortion of the foveal contour with visual impairment. This can be sub-classified as focal or large, according to the size of the vitreous adhesion. A full-thickness MH is characterized by a macular lesion with interruption of all retinal layers extending from the ILM to the RPE. It is subclassified according to the size of the hole determined by OCT and by the presence or absence of VMT. In the first case, an MH can be classified as small (250 μm), medium (250 to 400 μm), or large (>400 μm). According to the state of the vitreous, an MH is classified as with or without VMT.

Besides of the leading criteria driving the therapeutic approach to MHs, OCT also identified important prognostic parameters, including the presence of an epiretinal membrane or a lamellar hole-associated epiretinal proliferation (74) and the status of the internal or external retinal layers (75).

According to Soon et al (76), there is little difference between 350 μm and 450 μm MH, and when planning surgery, 400 μm should not be considered large. According to this study, 650 μm is a much better marker to divide medium and large MH, based on their results with 90% success in standard FTMH vitrectomy, involving ILM peel and gas tamponade on medium MH between 250 and 650 μm . They noted in their study that standard surgery for large MH (>650 μm) is less successful, and such techniques as ILM flaps and retinal expansion for MH apposition should be considered for this matter (76).

4. Surgery

4.1 - Pars Plana Vitrectomy

PPV was developed by Robert Machemer in 1970 (77). Machemer created a first closed-system vitrectomy device with multifunctional 17-gauge cutter called the vitreous infusion suction cutter. PPV was a major advance, because for the first time it allowed for the removal of vitreous through a closed system, rather than through an open sky technique. In 1975, O'Malley and Heintz described the use of a 20-gauge 3 port PPV system (78) and this became the gold standard and remained so for at least 3 decades. Over the past several years, the development of small incision transconjunctival, sutureless PPV has led to a major shift in how many diseases are treated in the operating room.

The development of new instruments and surgical strategies through the 1970s and 1980s was spearheaded by surgeon/engineer Steve Charles (79). More recent advances have included smaller and more refined instruments for use in the eye, illumination techniques and wide-angle viewing systems that have increased the safety, the effectiveness and the repeatability of the surgical maneuvers.

4.2 - Macular hole Surgery

In a 1991 pilot study by Kelly and Wendel(11), who performed vitrectomy and removal of the posterior cortical vitreous to relieve traction over the macula in 52 patients, shedding light on PPV as a possible therapy in the treatment of MH. Prior to this, idiopathic MH were considered an untreatable condition(11). In 1993, Kelly and Wendel (80) suggested a strategy for treating MHs based on a 3-port PPV with removal of the posterior hyaloid and apposition of the MH edges, by flattening them with intraocular tamponade in additional 118 eyes. The goal of the surgery was to relieve all anteroposterior traction in the macular region.

We now know, from randomized clinical trials (RCT), that surgical treatment is indicated for FTMH (stages 2, 3 and 4) whereas stage 1 should be handled conservatively as many resolve spontaneously (8)(13)(81). At present, surgical management can achieve anatomic closure rates better than 90% when surgery is performed with adjuvant therapy such as

ILM peeling (Figure 23) (19)(82)(83). Functional outcomes are more difficult to predict, and despite the high anatomic closure rates, reading vision remains compromised in 30-40% of patients (8). A visual acuity gain of more than 2 lines however can be expected in 60-85% of patients (82)(83). The reason for this discrepancy between function and morphology is unclear, but studies of closed MH with OCT have reported changes in ORL (sub-foveal cysts, photoreceptor defects) as possible explanations of compromised function after anatomically successful MH surgery (84)(85). The outcome of MH surgery is thought to depend mainly on pre-operative MH size and duration of symptoms, but outcomes have also been reported to depend on the used surgical technique (ILM-peeling, Indocyanine Green staining) (86)(87). Post-operative visual field defects, which previously have been attributed to dehydration of the retina during fluid–air exchange, now seems to be a complication with low incidence (88). Small asymptomatic paracentral scotoma and macular RPE alterations seen postoperatively have been related to intraoperative retinal light toxicity and surgery with ILM peeling (89).

The primary goal of MH surgery is to induce hole closure which is an absolute requirement for visual acuity improvement. The rationale for surgical management as originally described by Kelly and Wendel (13) is mobilization of hole edges by removing tangential and anterior-posterior vitreous traction, activation of marginal glial cells by vitrectomy and epiretinal membrane peeling, and finally, immobilization and apposition of hole edges by intraocular gas tamponade and face-down positioning. Since the initial report by Kelly and Wendel numerous adjuvant surgical techniques focusing on any of these general surgical principles have been tried in an attempt to enhance closure rates, but at present no convincing evidence exists to support the supposition that any of these improvements will result in a better functional outcome.

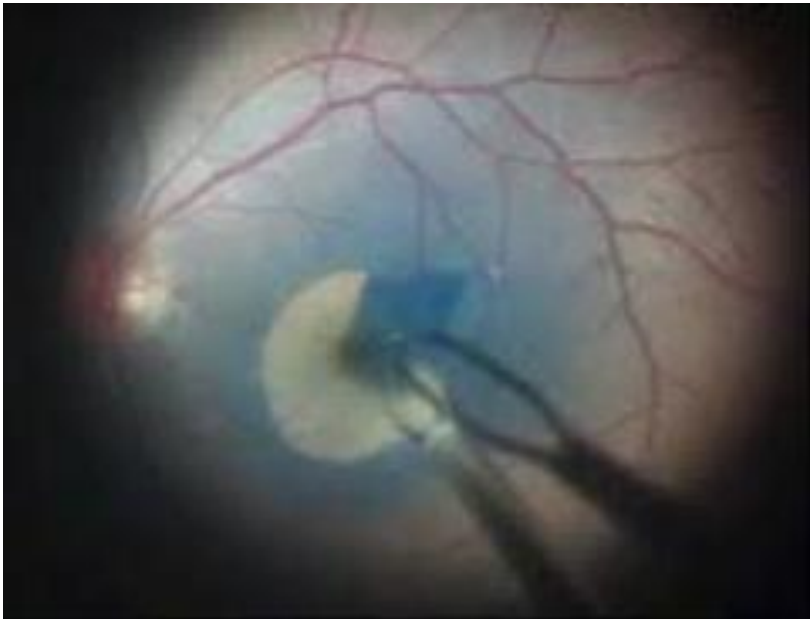


Figure 23 - Circular ILM peel. Brilliant Blue dye.

4.2.1 - ILM Peeling

The ILM represents the structural boundary between the retina and the vitreous. It is formed by the basal lamina of the Müller cells and also by projections from the Müller cells footplates. The ILM is translucent and 1.5 μm thick in the peripheral foveal area (39).

Surgical removal of the ILM in MH surgery was first performed in 1996 in an attempt to ensure complete removal of all tangential tractional components (glial cells, macrophages, fibrocytes, myofibroblasts) involved in MH formation (90). By removing the ILM, it was believed that the scaffold, where upon the cellular proliferation occurred, was removed.

Despite lack of scientific evidence for its beneficial effects on anatomical and functional outcomes, the procedure has been adopted by most vitreoretinal surgeons as a supplementary treatment in MH surgery. Eckardt et al in 1997 (14), were one of the first to describe ILM peeling, and it was reported to give good results and increase the rate of closure for MH. Several publications confirmed the efficacy of ILM peeling in MH surgery. According to Lois et al (22), at 1 month postoperatively in patients undergoing ILM peeling, closure was achieved in 84% of patients compared to 48% of patients who did not have ILM peeling. Park et al (91), also showed in 58 eyes that VPP with ILM peeling was superior than vitrectomy alone in closing MH. Schaal et al (92), Mester et al (93), and Brooks (94), based on case series, reported better primary anatomic closure rates with ILM peeling.

Christensen (8) in a randomized trial comparing outcomes with and without ILM peeling in 78 patients, concluded that surgery with ILM peeling, is associated to a significantly higher closure rate than surgery without ILM peeling (95% versus 45%) (Figures 24 and 25).

While ILM peeling may improve anatomic closure rates, its effect on functional outcomes after MH surgery is even more controversial with some case studies reporting loss of functional potential after surgery with ILM peeling, as referred by Navarro et al in 2003 (95) and Abdulla et al in 2004 (87), while others studies have reported visual outcomes to be better after ILM peeling. In a large prospective study focusing on the long-term outcomes of ILM peeling for MH after at least 12 months, Haritoglou et al described promising results (96). The authors reported anatomic closure in 87% of the cases after 1 year of surgery, closure in 96% of re-operated eyes, and a median best-corrected visual acuity improvement from a median of 20/100 pre-operatively to 20/40 postoperatively in 94% of the cases. As several sources have displayed favorable anatomic and functional outcomes with ILM peeling, this technique has become part of the standard of practice for vitreoretinal surgeons repairing FTMH.

4.2.2 - Technique

ILM peeling has become a more widely accepted procedure since the introduction of vital dyes. Because the ILM is poorly visible, its identification is challenging, and its removal difficult, even for an experienced vitreoretinal surgeon because of the difficulty in distinguishing with confidence, the ILM from the nerve fiber layer. Moreover, incomplete ILM removal may cause a failure in MH closure, whereas inadvertent injury to the nerve fiber layer may cause paracentral scotomata (96).

To achieve reproducible, complete, and less traumatic ILM peeling, intraocular vital dyes have been introduced to facilitate clear ILM identification. Available materials are usually classified as a staining material such as ICG, acid violet or as coating material such as triamcinolone acetonide (TA) and blood. However, most clinicians discontinued the use of ICG as an intraoperative vital stain because of concerns about toxicity (97). Other vital dyes were later introduced to replace ICG: trypan blue and brilliant blue G. This last dye has a good safety profile, provides significant anatomical and functional postoperative results,

(98) and has the peculiar characteristic of staining the ILM and not the rest of the retina as satisfactorily as ICG.

Following dye injection and wash out, the ILM is grasped directly with forceps and a flap of the ILM is created and peeled in a circular motion parallel to the retinal surface, and removed or placed over the hole.

The technique of ILM peel and inverted flap was described by Michalewska et al in 2010 (20), and was shown to provide superior anatomical and functional outcomes in cases of large MH. This involves preserving a flap of the ILM connected to the margin of the macular hole and then fulcruming this tissue upside-down from all sides to cover the macular defect. Another modification in practice is the use of an ILM hinge, which connects the ILM flap to the hole margin, and is then folded and placed into the MH (99). Rizzo et al (100), also found in a retrospective study on 620 eyes of 570 patients, that vitrectomy, ILM peel and inverted flap technique together are more effective than the standard ILM peeling technique, showing better results in large MH and myopic MH.

According to recent RCT, the inverted ILM flap technique demonstrated higher anatomical success rates with a better functional outcome; however, statistically significance difference was not achieved (101). Soon et al reported application of ILM peeling for the management of large MH (76), and they claim 90% success with standard MH vitrectomy involving ILM peel and gas tamponade in medium MH between 250 and 650 μm . Free flap ILM is used in patients with persistent MH hole after previous surgery, where a free patch of peripheral peeled ILM is placed over or in the MH (102).

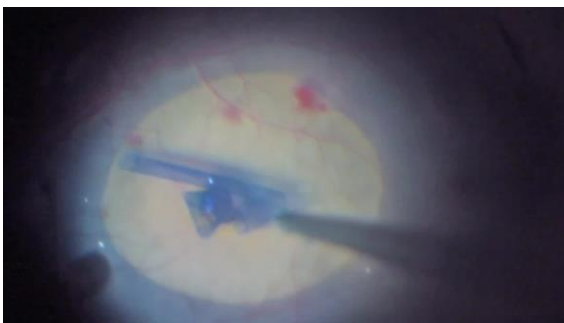


Figure 24- Peeled ILM over the hole.



Figure 25- Inverted flap of ILM dyed with Brilliant Blue

Intraocular tamponade with gas or silicone oil is performed to facilitate apposition of hole edges by providing buoyant forces that push the retina against the underlying RPE. The forces are greatest at the apex of the arc of contact, and by sustaining an accurate face-down position, the maximum vector forces can be directed against the MH. Favorable closure rates have been achieved with the use of short-acting gases, such as sulfur hexafluoride (SF₆) (103)(104)(105), and 2–4 days of prone positioning.

4.2.3 - Retinal Damage

ILM peeling is now a widely recognized technique used routinely for traction maculopathies, but what are the possible complications of this intervention? It is a technique that requires additional intraoperative agents, dyes, instruments, and surgical time. Few reports to date have shown adverse visual outcomes in patient status after an ILM peel, but there has yet to be a large enough randomized control trial assessing side effects of ILM removal, and therefore the question remains: Does the ILM have a function vital to the integrity of the retina that would render it damage upon ILM removal? If so, what type of retinal damage can this surgical technique induce?

Soon after peeling, the macula assumes a whitish color, frequently with small hemorrhages in the area of the denuded macula. This appearance is probably from swelling resulting from interruption in the axonal transport of ganglion fibers that run under the ILM. Swelling of the arcuate RNFL (106), is followed by a DONFL appearance, which is

sometimes visible on fundus examination with blue light a few weeks or months after surgery (27).

On OCT, a notch or dimples in the inner retinal layers may be detectable. These dimples probably form in areas where there are Müller cell attachment plaques that are thicker and more adherent to the ILM (107). In En face OCT frames, the dimples appear as concentric dark spots in the area of the macula, denuded from the ILM (108).

After ILM peeling and MH closure, the distance between the fovea and the optic disk is shortened and the foveal contour appears asymmetrical (109). The displacement of the fovea towards the disk thickens the retina on the nasal side and thins the retina on the temporal side (110). Thinning on the temporal side is increasingly evident months after surgery. (Figure 26)

RNFL thinning may result from an injury with the subsequent degeneration and apoptosis of Müller or ganglion cells. Despite these anatomical changes, the effects on vision are uncertain. Some authors have documented the occurrence of paracentral micro-scotoma measured with microperimetry in retinas denuded from the ILM (106)(27). This scotoma may be deep or multiple, may coexist with good visual acuity, and are usually asymptomatic; however, they sometimes may worsen the quality of vision, such as reductions in reading speed or contrast sensitivity. The cause of this micro-scotoma may be direct trauma to retinal cells induced by forceps and the mechanical stretching of the ILM, or they may be caused by secondary degenerative phenomena. ILM peeling could induce the degeneration of some arcuate fibers directed toward the optic nerve or apoptosis of some Müller cells that lie beneath the area of the peeled retina. Haritoglou and co-workers demonstrated that fragments of Müller cell end feet might remain attached to the ILM after peeling. This maneuver probably damages a certain percentage of these cells (111).

Furthermore, in most patients who underwent ILM peeling, Tadayoni found absolute micro-scotoma, which were not present in patients who did not undergo peeling (23).

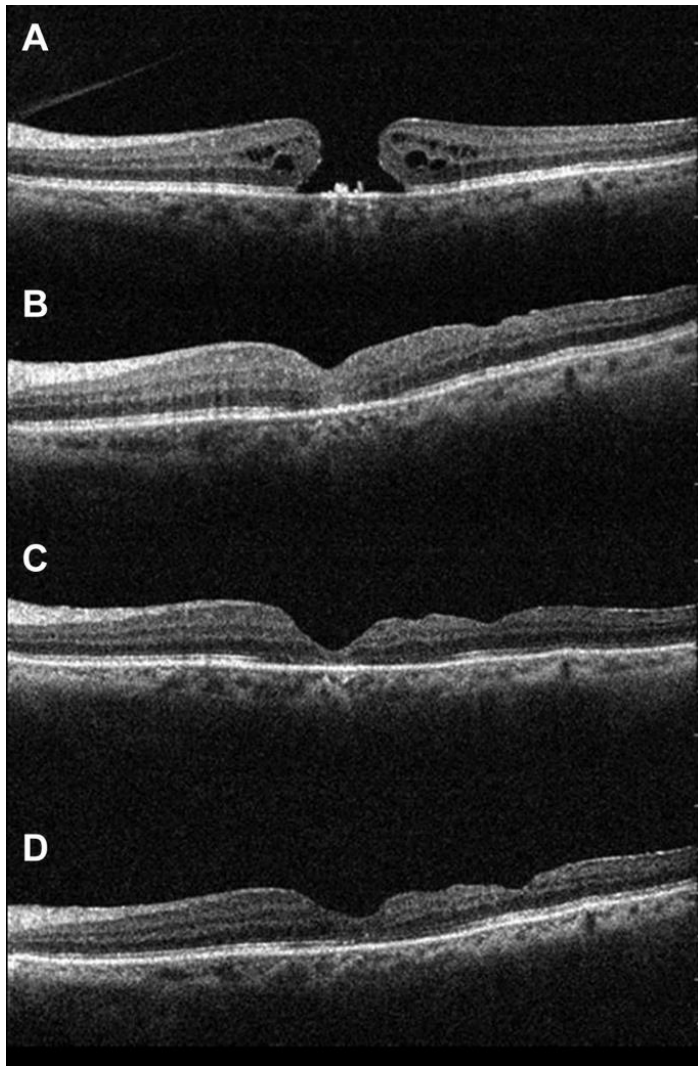


Fig. 26- (A) preoperative macular hole; (B-D) postoperative temporal thinning of the retinal layers respectively after 20 days, 5 months and 2 years.

In conclusion, there are several papers that present results comparing surgery of MH with ILM peeling and surgery with no ILM peeling, concluding that peeling was related to higher closure rates and less reopening. Focus has been on hole closure, a difficult achievement so far. After MH closure, central scotoma disappears and some patients regain visual acuity whilst others do not. With recent SD OCT, we can now measure anatomical consequences in each macular layer, before and after surgery, and integrity of each external cellular layer after hole closure. These variations of integrity may be the cause of functional limitations and visual acuity gain. Also, mf ERG measured before and after surgery may give results on visual function. In this thesis, we try to relate all these results with surgical technique, duration of symptoms before surgery and final visual acuity.

5. Materials and Methods

5.1 - Population

Enrollment was conducted between January 2015 and December 2017. During this period, 72 patients were referred to the Department of Ophthalmology of Hospital Santa Maria. Patients were examined to confirm the diagnosis of FTMH and, after inclusion and exclusion criteria were verified, were scheduled for MH surgery.

5.1.1 - Inclusion criteria

1. MH stage 2 or higher
2. Male or female aged 18 years or older
3. Visual symptoms due to MH
4. Intraocular pressure <21 mmHg
5. Signed informed consent form

5.1.2 - Exclusion criteria:

1. Epiretinal fibrosis
2. Systemic disease affecting retinal function
3. Axial length greater than 26.0 mm
4. Ocular disorders in the studied eye that may confound interpretation of study results (glaucoma, retinal detachment, optic nerve disease)

The tenets of the Declaration of Helsinki were followed. All patients provided written informed consent to the surgical and study procedures. Approval was obtained from the Ethics Committee of Hospital Santa Maria.

The study was registered in the clinicaltrials.gov database (NCT03799575: Internal Limiting Membrane and Macular Hole).

5.2 - Interventions

All patients were treated equally, by a retina surgeon of the ophthalmic department of CHLN-Hospital Santa Maria, following same surgical protocol: 23 or 25 G PPV, separation of posterior vitreous cortex with triamcinolone acetonide, brilliant blue assisted ILM peeling, 15% SF₆ gas tamponade and face down position.

A careful examination of the retinal periphery was then performed with indentation, and any iatrogenic retinal breaks found were treated by laser.

Preoperative examinations were performed the day before MH surgery, and follow-up was scheduled at 3, 6, and 12 months after MH surgery. All patient contacts included a standard ophthalmologic evaluation of anterior segment, applanation tonometry and fundus observation.

Functional outcomes assessment was through BCVA and mf ERG. BCVA was performed using Snellen Chart and converted to log Mar for statistical analysis, before and after surgery at 3, 6 and 12 months. Hand motion was considered as logMAR 3.0 and counting fingers as logMAR 2.0. Metamorphosia, other visual symptoms and patient quality of life were also recorded.

Subjects were stratified by, age, sex, MH staging, lens status, surgical details (ILM dissection technique if present, total excision, inverted flap, fovea sparing)

Multifocal ERG was recorded pre-operatively and at 12 months after surgery. RETIsan Multifocal ERG (Version 6.12.5.12; Roland Consult) was used for mf ERG recording. In the present study, we focused on amplitude and latency of N1 and P1, before and after surgery

Morphological outcomes were assessed by OCT, before and after surgery. All MH were staged based on the recent OCT based classification, and only full-thickness MH of grade 2–4 were considered for the study. The minimum diameter of the MH was assessed in all cases. Retinal sectional images were acquired using Spectralis SD-OCT (Heidelberg Engineering, Heidelberg, Germany), using eye-tracking software for posterior pole images centered on the fovea (61 acquisitions, 120- μ m intervals). Evaluations were performed at baseline, and 1, 3, and 6 months after surgery. The presumed foveal center was identified

as mid-distance of the nearest MH borders. The edge of RPE or the sclera in eyes with peripapillary atrophy was the disk margin. The papillo-foveal distance was manually measured with software calipers as the distance from the foveal center to the disc margin.

All thickness measurements were made automatically by SD-OCT auto-segmentation software before and after surgery. Reference data ensured that each measurement was at the same segmentation location irrespective of the layer analyzed. In cases of automatic layer misalignment, manual alignment was possible by SD-OCT software before automatic measurements. In order to limit measurement bias associated with MH-associated retinal derangement, we used nasal and temporal grids of retinal areas $\leq 1.750 \mu\text{m}$ away from the fovea for calculations and comparisons. Also, integrity of ORL, ELM and EZ were evaluated in OCT and compared with ILM position over the hole during surgery.

ILM Peeling were performed in every MH surgery and inverted flap was performed in large MH. Whenever possible, two samples of ILM per patient were collected and harvested for laboratory analysis. One of the samples was immediately fixed and submitted to Optic Microscopy (OM) and Transmission Electron Microscopy (TEM) analysis, and another sample was kept in enriched medium 199 (Gibco) for 20 minutes at room temperature, after which it was also fixed and submitted to OM and TEM analysis.

Both samples from same patient followed the protocol:

[dx.doi.org/10.17504/protocols.io.qjiduke](https://doi.org/10.17504/protocols.io.qjiduke)

Regions of interest in both conditions, immediately fixed and kept in enriched medium 199 (Gibco) for 20 minutes, were screened in a Hitachi H-7650 transmission electron microscope at 100kV acceleration.

All the results found in this study are in next Chapters.

CHAPTER 2

Tomographic Structural Changes of Retinal Layers After Internal Limiting Membrane Peeling for Macular Hole Surgery

Mun Faria, Nuno Ferreira, Diana Cristóvão, Sofia Mano, David Sousa, Manuel Monteiro-
Grillo

Ophthalmic Research, 2018, DOI: 10.1159/000480243

Internal Retinal Layer Thickness and Macular Migration After Internal Limiting Membrane Peeling in Macular Hole Surgery

Mun Faria, Nuno Ferreira, Sofia Mano, Diana Cristóvão, David Sousa, Manuel Monteiro-
Grillo

Eur J Ophthalmol 2018; 00 (00): 000-000 DOI: 10.5301/ejo.5001066

In this chapter we studied OCT data of MH before and after surgery to determine alterations in anatomy.

Aim: To determine tomographic structural changes of retinal layers after ILM in MH surgery.

Methods:

36 eyes of 32 patients, were subjected to 23 or 25 G pars plana vitrectomy and 3,5 mm diameter ILM peeling for MH.

Retinal cross-sectional images were acquired using spectral-domain OCT, using the eye-tracking feature with software posterior pole images centered on the fovea, before and after surgery at 1, 3, 6 and 12 months. Thickness of IRL and ORL were assessed, at 1750 μm from fovea, roughly the diameter of ILM peel at MH surgery. Each macular layer was also evaluated before and after surgery and distance from papilla to fovea before and after closed MH were measured.

Mun Faria contributed to Research Design, Data Interpretation, Manuscript Preparation, Conceptualization and Investigation. Nuno Ferreira was involved in Validation and Review, Diana Cristóvão contributed to Data Interpretation, Sofia Mano contributed in Resources, David Sousa was involved in Methodology, Review, and Editing. Manuel Monteiro Grillo contributed to Manuscript Preparation, Review and Editing. All authors read and approved the final manuscript.

The results of this study allowed the following peer reviewed publication:

Paper 1- Tomographic Structural Changes of Retinal Layers After Internal Limiting Membrane Peeling for Macular Hole Surgery Ophthalmic Research, October 2017, DOI: 10.1159/000480243.

Tomographic Structural Changes of Retinal Layers after Internal Limiting Membrane Peeling for Macular Hole Surgery

Mun Yueh Faria^{a, b} Nuno P. Ferreira^{a, b} Diana M. Cristóvão^c Sofia Mano^{a, b}
David Cordeiro Sousa^{a, b} Manuel Monteiro-Grillo^{a, b}

^aVision Sciences Study Center, CECV, Faculdade de Medicina, Universidade de Lisboa, ^bDepartment of Ophthalmology, Hospital Santa Maria, and ^cInstituto de Oftalmologia Dr Gama Pinto, Lisbon, Portugal

Keywords

Macular hole · Internal limiting membrane peeling · Optical coherence tomography · Macular structural changes

Abstract

Purpose: To highlight tomographic structural changes of retinal layers after internal limiting membrane (ILM) peeling in macular hole surgery. **Methods:** Nonrandomized prospective, interventional study in 38 eyes (34 patients) subjected to pars plana vitrectomy and ILM peeling for idiopathic macular hole. Retinal layers were assessed in nasal and temporal regions before and 6 months after surgery using spectral domain optical coherence tomography. **Results:** Total retinal thickness increased in the nasal region and decreased in the temporal region. The retinal nerve fiber layer (RNFL), ganglion cell layer (GCL), and inner plexiform layer (IPL) showed thinning on both nasal and temporal sides of the fovea. The thickness of the outer plexiform layer (OPL) increased. The outer nuclear layer (ONL) and outer retinal layers (ORL) increased in thickness after surgery in both nasal and temporal regions. **Conclusion:** ILM peeling is associated with important alterations in the inner retinal layer architecture, with thinning of the RNFL-GCL-IPL com-

plex and thickening of OPL, ONL, and ORL. These structural alterations can help explain functional outcome and could give indications regarding the extent of ILM peeling, even though peeling seems important for higher rate of hole closure.

© 2017 S. Karger AG, Basel

Introduction

Pars plana vitrectomy with peeling of the internal limiting membrane (ILM), intraocular gas tamponade, and face-down positioning is the current standard procedure to manage an idiopathic macular hole (IMH) [1, 2].

Because the ILM is the basement membrane of Müller cells, the inner barrier of the neural retina, and anatomically adjacent to retinal nerve fiber layer (RNFL) and ganglion cell layer (GCL), ILM removal may alter the architecture of the inner retinal layer (IRL) [3, 4]. Nerve fibers are joined and fixed at the lamina cribrosa, and after ILM peeling a dissociated optic nerve layer was reported by Tadayoni et al. [5, 6]. Also, contraction of this neural layer and ganglion cell axons allows underlying macular tissue to react to stretching and inflammation with altera-

KARGER

© 2017 S. Karger AG, Basel

E-Mail karger@karger.com
www.karger.com/ore

Mun Yueh Faria
Hospital Santa Maria
Rua Professor Egas Moniz
PT-1649-035 Lisbon (Portugal)
E-Mail munfaria1@gmail.com

tions in the cytoarchitecture of external retinal layers. Macular hole closing causes centripetal contraction. In addition, the contraction force of the RNFL displaces the retina nasally. Therefore, after ILM peeling, the integrity of each retinal layer may vary depending on its topographic location around the fovea, and all these anatomical and structural alterations may have consequences on postoperative visual outcome.

The present study tries to investigate the anatomical effects of ILM peeling on the different retinal layers and to assess structural changes using spectral domain optical coherence tomography (SD-OCT).

Patients and Methods

In a nonrandomized prospective study, 38 eyes (34 patients) with IMH underwent successful surgical hole closure as first intervention between January 2015 and June 2016 at the Department of Ophthalmology, Santa Maria Hospital, Lisbon. The tenets of the Declaration of Helsinki were followed. All subjects gave written informed consent to the surgical and study procedures. Approval was obtained from the Ethics Committee of the Santa Maria Hospital.

Exclusion criteria were maculopathy other than IMH, surgery for recurrent IMH, other retinal diseases, or an axial length >26.0 mm. Mean follow-up was at least 6 months after surgery. Preoperative data included age, gender, duration of symptoms, and a complete ophthalmic examination, including refraction and best-corrected visual acuity (BCVA), intraocular pressure by applanation tonometry, slit-lamp biomicroscopy, fundus examination, and OCT. All macular holes were staged based on a recent OCT-based classification [7], and only full-thickness IMH of grade 2–4 were considered for the study. The minimum diameter of the macular hole was assessed in all cases. Retinal sectional images were acquired using Spectralis SD-OCT (Heidelberg Engineering, Heidelberg, Germany), using eye-tracking software for posterior pole images centered on the fovea (61 acquisitions, 120- μ m intervals). Evaluations were performed at baseline, and 1, 3, and 6 months after surgery. The presumed foveal center was identified as mid-distance of the nearest IMH borders. The edge of retinal pigment epithelium or the sclera in eyes with peripapillary atrophy was the disk margin. The papillofoveal distance was manually measured with software calipers as the distance from the foveal center to the disk margin. OCT distance reading involved 3 observers (M.Y.F., S.M., and N.P.F.; M.Y.F. also acted as an adjudicator in case differences were >20%). The optic nerve head was also accessed for posterior vitreous traction.

All thickness measurements were made automatically by SD-OCT autosegmentation software before and after surgery. Reference data ensured that each measurement was at the same segmentation location irrespective of the layer analyzed. In cases of automatic layer misalignment, manual alignment was possible by SD-OCT software before automatic measurements.

In order to limit measurement bias associated with macular hole-associated retinal derangement, we used nasal and temporal grids of retinal areas $\leq 1,750 \mu\text{m}$ away from the fovea for calculations and comparisons, as detailed in Figure 1.

OCT delineates every macular layer, and we measured the thickness of individual retinal layers, e.g., IRL and the outer retinal layer (ORL). IRL is composed by the retinal nerve fiber layer (RNFL), ganglion cell layer (GCL), inner plexiform layer (IPL), inner nuclear layer (INL), and outer plexiform layer (OPL). ORL includes the external limiting membrane (ELM), ellipsoid zone, and retinal pigment epithelium. Baseline and 6-month follow-up ultra-high-resolution horizontal scans were used for analyses.

Surgical Technique

All surgeries were performed by the same surgeon (M.Y.F.). A standard surgical procedure consisted of 23- or 25-gauge, 3-port pars plana vitrectomy, including the induction of posterior vitreous detachment if needed, assisted with triamcinolone acetonide. Most of the patients underwent combined cataract surgery, except for 3 pseudophakic and 1 cataract-sparing surgery. Standard small-incision phacoemulsification and implantation of a standard foldable intraocular lens was combined with vitrectomy. Balanced salt solution (Alcon, Fort Worth, TX, USA) was used as an irrigation solution. A single-use macular contact lens (Grieshaber[®]; Alcon, TX, USA) was used in every ILM peeling. In every eye, Brilliant Peel[®] Dual (Fluoron, Geuder, Germany) assisted ILM peeling was performed, using end grip intraocular forceps to create a flap; peeling was done in a circular fashion up to the border of the macula, sparing the macular area. Balanced salt solution was exchanged with 15% SF₆ (sulfur hexafluoride) gas. The patients were instructed to maintain a face-down position for at least 5 days.

Postoperative observations were performed 1 day, 1 week, and 1, 3 and 6 months after surgery, and then, every 6 months or whenever needed. At each visit, intraocular pressure was always assessed. Whenever possible, BCVA, OCT, and fundus revision were performed. At the 6-month follow-up, parameters assessed were hole status, nasal and temporal total retinal thickness, ORL, IRL, RNFL, GCL, IPL, INL, and OPL layer thickness $\leq 1,750 \mu\text{m}$ away from the fovea. BCVA was accessed using a decimal visual acuity chart, and decimal visual acuity was converted to the logarithm of the minimum angle of resolution (logMAR) units for analysis.

The results are expressed as means \pm SD. Wilcoxon signed-rank test and STATA software were employed for statistical analysis. $p < 0.05$ was considered significant.

Results

Thirty-eight eyes of 34 patients treated with IMH surgery in the Santa Maria Hospital were included in this study. All macular holes were closed after one surgery. Two eyes with a flat open macular hole were excluded, so only 36 eyes were included in the analyses. Mean age of the patients was 69 ± 8.9 years; there were 9 males (36%) and 23 females (64%), and 17 right eyes (47%) and 19 left eyes (53%). Thirteen had grade 2 (36%), 12 grade 3 (33%), and 11 grade 4 (31%) in SD-OCT-based staging of macular holes.

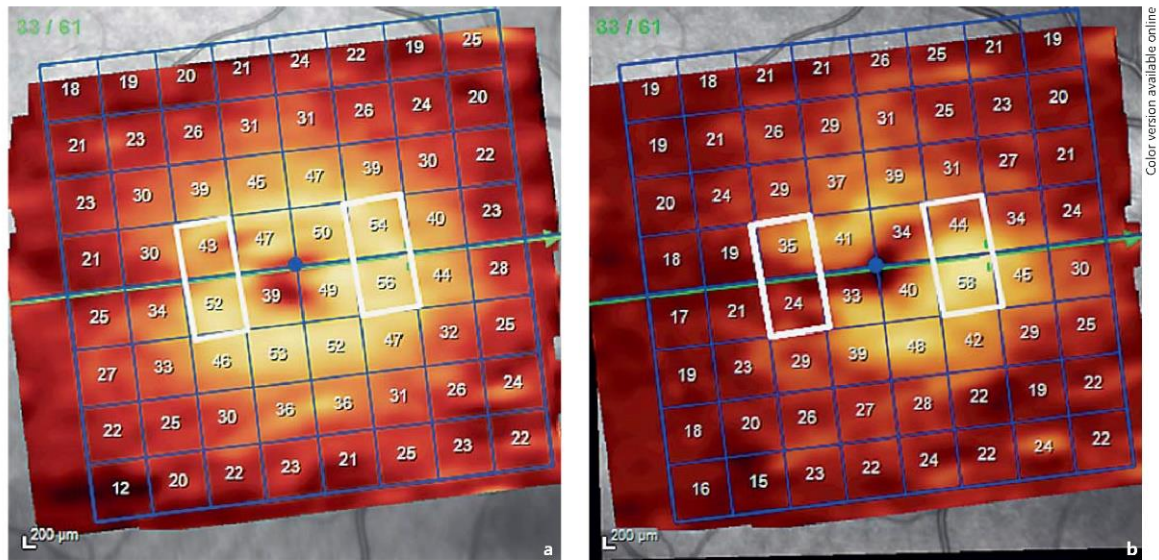


Fig. 1. Ganglion cell layer thickness before (a) and after surgery (b) in square grids. The mathematical average of 2 nasal and 2 temporal squares was considered for the study. Each square is $875 \times 875 \mu\text{m}$.

Mean macular hole evolution time was 24.5 ± 16.7 months and mean macular hole size $493 \pm 227 \mu\text{m}$ (Table 1). Preoperative mean BCVA was $1.29 \pm 0.5 \log\text{MAR}$, and, 6 months postoperatively, mean BCVA was $0.90 \pm 1.0 \log\text{MAR}$. However, because of concomitant standard small-incision phacoemulsification cataract surgery in almost every patient, improvement in vision owing to cataract surgery has to be taken into consideration.

Automatic segmentation and thickness analyses were performed $\leq 1,750 \mu\text{m}$ away from the fovea for nasal and temporal regions at baseline and 6 months (Fig. 1; Table 2). Median macular thickness after closure was $187 \mu\text{m}$. The postoperative distance of the optic disk border to the newly formed fovea was $190 \mu\text{m}$ shorter ($p < 0.0001$). At 6 months, total nasal retinal thickness had increased from 337 ± 37 to $346.3 \pm 43 \mu\text{m}$ ($p < 0.001$), RNFL had significantly decreased in thickness from 33.7 ± 13 to $31 \pm 12.2 \mu\text{m}$ ($p = 0.05$), as well as GCL (from 45.5 ± 10 to $39.0 \pm 13 \mu\text{m}$; $p < 0.01$) and IPL (from 37.1 ± 11 to $33.5 \pm 11 \mu\text{m}$; $p = 0.05$).

INL thickness did not change but varied from 44.3 ± 14 to $43.3 \pm 99 \mu\text{m}$ ($p = 0.76$); OPL thickness increased from 33 ± 7.4 to $37.0 \pm 15 \mu\text{m}$ ($p = 0.16$), and ONL thickness increased from 63.6 ± 17 to $66.6 \pm 15 \mu\text{m}$ ($p = 0.07$,

Table 1. Age and gender of the patients, and grade, size, and evolution time of the macular hole

Age (mean \pm SD), years	69 ± 8.9
Females, <i>n</i> (%)	23 (64)
Left eyes, <i>n</i> (%)	19 (53)
Macular hole grading, <i>n</i> of eyes (%)	
Grade 2	13 (36)
Grade 3	12 (33)
Grade 4	11 (31)
Macular hole parameters (means \pm SD)	
Postoperative mean central thickness, μm	187.4 ± 12
Evolution time, months	24.5 ± 16.7
Size, μm	493 ± 227

all nonsignificant, whereas ORL showed a significant increase from 77.9 ± 17.5 to $79.3 \pm 3.6 \mu\text{m}$ ($p < 0.05$). Completely different results were found in the temporal sub-field, with a total retinal thickness decrease from 312 ± 35 to $281 \pm 37 \mu\text{m}$ ($p < 0.001$) at month 6. RNFL thickness decreased from 19.1 ± 6.5 to $17.4 \pm 5.6 \mu\text{m}$ ($p = 0.22$), as well as GCL and IPL: from 41.0 ± 10.8 to $25.7 \pm 10.9 \mu\text{m}$ ($p < 0.001$) and from $39.7 \pm 9.9 \mu\text{m}$ to $27.1 \pm 8.7 \mu\text{m}$ ($p < 0.0001$), respectively.

Table 2. Results of visual acuity and OCT data of each retinal layer thickness before and after surgery (means \pm SD)

	Before surgery	At 6 months	<i>p</i> value
Visual acuity, logMAR	1.29 \pm 0.5	0.91 \pm 1.0	<0.01
Distance optic disc \rightarrow macular hole, μ m	3,651 \pm 323	3,461 \pm 279	<0.0001
Total nasal retinal thickness, μ m	337 \pm 37	346 \pm 43	<0.001
Total temporal retinal thickness, μ m	312 \pm 35	281 \pm 37	<0.0001
Nasal outer retinal layer, μ m	77.9 \pm 2.7	79.3 \pm 3.6	<0.05
Temporal outer retinal layer, μ m	77.1 \pm 2.5	79.6 \pm 4.6	<0.01
Nasal retinal pigment epithelium, μ m	13.5 \pm 2.1	13.5 \pm 2.7	0.74
Temporal retinal pigment epithelium, μ m	15.1 \pm 10.9	15.9 \pm 13.0	0.08
Nasal outer nuclear layer, μ m	63.6 \pm 17.5	66.6 \pm 15.7	0.07
Temporal outer nuclear layer, μ m	60.3 \pm 17.5	65.0 \pm 17.8	<0.01
Nasal outer plexiform layer, μ m	33.0 \pm 7.4	37.9 \pm 15.9	0.16
Temporal outer plexiform layer, μ m	33.1 \pm 11.1	31.7 \pm 8.2	0.49
Nasal inner nuclear layer, μ m	44.3 \pm 14.2	43.3 \pm 9.9	0.76
Temporal inner nuclear layer, μ m	39.5 \pm 13.1	33.8 \pm 9.4	<0.05
Nasal inner plexiform layer, μ m	37.1 \pm 11.6	33.5 \pm 11.1	<0.05
Temporal inner plexiform layer, μ m	39.7 \pm 9.9	27.1 \pm 8.7	<0.0001
Nasal ganglion cell layer, μ m	45.5 \pm 10.6	39.0 \pm 13.1	<0.01
Temporal ganglion cell layer, μ m	41.0 \pm 10.8	25.7 \pm 10.9	<0.0001
Nasal retinal nerve fiber layer, μ m	33.7 \pm 13.0	31.0 \pm 12.2	0.05
Temporal retinal nerve fiber layer, μ m	19.1 \pm 6.5	17.4 \pm 5.6	0.22

Wilcoxon signed-rank test.

INL thickness also decreased from 39.5 \pm 13 to 33.8 \pm 9.4 μ m (p < 0.005) and OPL from 33.1 \pm 11 μ m to 31.7 \pm 8.2 μ m (p = 0.49). ONL thickness increased from 60.3 \pm 17.5 to 65 \pm 17.8 μ m (p < 0.01) and ORL from 77.1 \pm 2.5 to 79.6 \pm 4.6 μ m (p < 0.01).

In summary, 6 months after ILM peeling, INL decreased (RNFL, GCL, and IPL), both in nasal (12.8 μ m) and in temporal regions (29.6 μ m). Analysis of nasal macular layers revealed a 9- μ m increase in total nasal retinal thickness and a marked decrease in total temporal retinal thickness of 31 μ m.

The OPL contributed most to the nasal increase in IRL thickness (on average 4.9 μ m) followed by the ONL (on average 3 μ m). ORL thickness was increased in both nasal and temporal regions 6 months after surgery.

We analyzed anatomic structural alterations and tried to find correlations with macular hole size, but no correlations between hole size and structural alterations were detected.

Discussion

A standard approach to IMH surgery is to relieve anterior-posterior traction by pars plana vitrectomy and tangential traction by ILM peeling [1, 2]. ILM peeling increases the success of macular hole surgery [2], but due to its close relationship with underlying retinal structures, ILM peeling may alter the normal architecture of the macula [3, 4].

Postoperative RNFL and GCL thinning has been described by Sabater et al. [8] after presumptive mechanical damage of ILM peeling to the GCL or Müller cells in the GCL.

The ganglion cell complex consists of 3 layers, RNFL, made of axons of ganglion cells, GCL, the bodies of ganglion cells, and IPL, made of dendrites of ganglion cells. The thickness of these 3 layers has been found to be decreased in this study, both nasal and temporal to the fovea, which seems to be an indicator of ganglion cell damage, as ganglion cells are concentrated in the macula and most sensitive to ischemic changes [9, 10].

In the present study, we also found increased nasal thickness that was dependent on the medial IRL part. This includes the deeper region of the IPL, INL, OPL,

and the inner segments of photoreceptors. In all these layers, layer thickness was altered after ILM peeling in the present study. INLs are mainly composed of bipolar, horizontal, and glial cells, and they seem to be the cells most altered. After ILM peeling, these cells are probably prone to inflammation and affected by stretching effects. OPL is the area in which photoreceptors communicate with horizontal and bipolar cells, and OPL thickness has markedly increased, which may have major effects on the development of glial proliferation, ELM centripetal bridging, and the recovery of disrupted photoreceptors.

Temporal macula thinning was also reported by several authors. The RNFL is thinner at the temporal than nasal area, and exposure to Brilliant Blue dye may be a factor worth consideration or traumatic temporal grasping. Nukada et al. [11] and Ohta et al. [12] also reported that deeper retinal structural damage was more frequent in the temporal macula, resulting in marked atrophy in macular hole surgery.

On nasal and temporal sides of the fovea, the outer retina is comprised of ELM, ellipsoid zone, and retinal pigment epithelium. ELM is the first membrane to restore continuity after macular hole closure [13]. Only afterwards begins reapproachment and restoration of the outer portion of photoreceptors with determination of continuity in the ellipsoid zone [14], which seems to explain the ORL thickening we found in this study [15]. This ORL thickening may be one explanation for ELM realignment and photoreceptor restoration as part of macular hole closure and vision restoration.

However, the study has several limitations. There is no control group, the follow-up time is short, and the number of patients is limited.

Conclusions

In summary, although ILM peeling improves closure rate in macular hole surgery, there are several reports, including this study, on microstructural alterations in the different macular layers after ILM peeling in macular hole surgery. Thinning of the GCL and IPL complex on both sides of the fovea seems to be the major damage, but changes in the thickness of layers on the nasal and temporal sides of the macula are also significant, with an increase in thickness in the nasal region and a decrease in the temporal region. Minimizing these anatomic structural alterations would eventually improve visual outcome in patients treated with macular hole surgery.

Disclosure Statement

No conflicting relationship exists for any author.

Funding Sources

This research did not receive any specific grant from funding agencies in the public, commercial, or not-for-profit sectors.

Author Contributions

Mun Y. Faria and Manuel Monteiro-Grillo were responsible for the conception and design of the study, Sofia Mano and Diana M. Cristóvão revised the content and drafted the article. Nuno P. Ferreira and David C. Sousa were responsible for analyses and interpretation of data. All authors approved the final version to be submitted.

References

- 1 Brooks HL: Macular hole surgery with and without internal limiting membrane peeling. *Ophthalmology* 2000;107:1939–1948; discussion 1948–1949.
- 2 Spiteri Cornish K, Lois N, Scott NW, Burr J, Cook J, Boachie C, et al: Vitrectomy with internal limiting membrane peeling versus no peeling for idiopathic full-thickness macular hole. *Ophthalmology* 2014;121:649–655.
- 3 Ooka E, Mitamura Y, Baba T, Kitahashi M, Oshitari T, Yamamoto S: Foveal microstructure on spectral-domain optical coherence tomographic images and visual function after macular hole surgery. *Am J Ophthalmol* 2011; 152:283–290.e1.
- 4 Bottoni F, De Angelis S, Luccarelli S, Cigada M, Staurenghi G: The dynamic healing process of idiopathic macular holes after surgical repair: a spectral-domain optical coherence tomography study. *Invest Ophthalmol Vis Sci* 2011;52:4439–4446.
- 5 Tadayoni R, Paques M, Massin P, Mouki-Benani S, Mikol J, Gaudric A: Dissociated optic nerve fiber layer appearance of the fundus after idiopathic epiretinal membrane removal. *Ophthalmology* 2001;108:2279–2283.
- 6 Tadayoni R, Svorenova I, Erginay A, Gaudric A, Massin P: Decreased retinal sensitivity after internal limiting membrane peeling for macular hole surgery. *Br J Ophthalmol* 2012; 96:1513–1516.
- 7 Duker JS, Kaiser PK, Binder S, de Smet MD, Gaudric A, Reichel E, et al: The International Vitreomacular Traction Study Group classification of vitreomacular adhesion, traction, and macular hole. *Ophthalmology* 2013;120: 2611–2619.

- 8 Sabater AL, Velázquez-Villoria Á, Zapata MA, Figueroa MS, Suárez-Leoz M, Arrevola L, et al: Evaluation of macular retinal ganglion cell-inner plexiform layer thickness after vitrectomy with internal limiting membrane peeling for idiopathic macular holes. *Biomed Res Int* 2014;2014:458631.
- 9 Quigley HA, Dunkelberger GR, Green WR: Retinal ganglion cell atrophy correlated with automated perimetry in human eyes with glaucoma. *Am J Ophthalmol* 1989;107:453-464.
- 10 Sellés-Navarro I, Villegas-Pérez MP, Salvador-Silva M, Ruiz-Gómez JM, Vidal-Sanz M: Retinal ganglion cell death after different transient periods of pressure-induced ischemia and survival intervals. A quantitative in vivo study. *Invest Ophthalmol Vis Sci* 1996; 37:2002-2014.
- 11 Nukada K, Hangai M, Ooto S, Yoshikawa M, Yoshimura N: Tomographic features of macula after successful macular hole surgery. *Invest Ophthalmol Vis Sci* 2013;54:2417-2428.
- 12 Ohta K, Sato A, Fukui E: Asymmetrical thickness of parafoveal retina around surgically closed macular hole. *Br J Ophthalmol* 2010; 94:1545-1546.
- 13 Inoue M, Watanabe Y, Arakawa A, Sato S, Kobayashi S, Kadonosono K: Spectral-domain optical coherence tomography images of inner/outer segment junctions and macular hole surgery outcomes. *Graefes Arch Clin Exp Ophthalmol* 2009;247:325-330.
- 14 Wakabayashi T, Fujiwara M, Sakaguchi H, Kusaka S, Oshima Y: Foveal microstructure and visual acuity in surgically closed macular holes: spectral-domain optical coherence tomographic analysis. *Ophthalmology* 2010; 117:1815-1824.
- 15 Hashimoto Y, Saito W, Fujiya A, Yoshizawa C, Hirooka K, Mori S, et al: Changes in inner and outer retinal layer thicknesses after vitrectomy for idiopathic macular hole: implications for visual prognosis. *PLoS One* 2015; 10:e0135925.

Paper 2- Internal retinal layer thickness and macular migration after internal limiting membrane peeling in macular hole surgery. Eur J Ophthalmol 2017; 00 (00): 000-000 DOI: 10.5301/ejo.5001066.

Internal retinal layer thickness and macular migration after internal limiting membrane peeling in macular hole surgery

Mun Y. Faria^{1,3}, Nuno P. Ferreira^{1,3}, Sofia Mano^{1,3}, Diana M. Cristóvão⁴, David C. Sousa^{1,3}, Manuel E. Monteiro-Grillo^{1,3}

¹ Hospital Santa Maria, Centro de Estudos das Ciências da Visão, Faculdade de Medicina, Universidade de Lisboa, Lisbon - Portugal

² Ophthalmology Department, Hospital Santa Maria, Lisbon - Portugal

³ University Ophthalmology Clinic, Faculty of Medicine, University of Lisbon, Lisbon - Portugal

⁴ Ophthalmology Department, Instituto de Oftalmologia Dr Gama Pinto, Lisbon - Portugal

ABSTRACT

Purpose: To provide a spectral-domain optical coherence tomography (SD-OCT)-based analysis of retinal layers thickness and nasal displacement of closed macular hole after internal limiting membrane peeling in macular hole surgery.

Methods: In this nonrandomized prospective interventional study, 36 eyes of 32 patients were subjected to pars plana vitrectomy and 3.5 mm diameter internal limiting membrane (ILM) peeling for idiopathic macular hole (IMH). Nasal and temporal internal retinal layer thickness were assessed with SD-OCT. Each scan included optic disc border so that distance between optic disc border and fovea were measured.

Results: Thirty-six eyes had a successful surgery with macular hole closure. Total nasal retinal thickening ($p < 0.001$) and total temporal retinal thinning ($p < 0.0001$) were observed. Outer retinal layers increased thickness after surgery (nasal $p < 0.05$ and temporal $p < 0.01$). Middle part of inner retinal layers (mIRL) had nasal thickening ($p < 0.001$) and temporal thinning ($p < 0.05$). The mIRL was obtained by deducting ganglion cell layer (GCL) and retinal nerve fiber layer (RNFL) thickness from overall thickness of the inner retinal layer. Papillofoveal distance was shorter after ILM peeling in macular hole surgery ($3,651 \pm 323 \mu\text{m}$ preoperatively and $3,361 \pm 279 \mu\text{m}$ at 6 months; $p < 0.0001$).

Conclusions: Internal limiting membrane peel is associated with important alteration in inner retinal layer architecture, with thickening of mIRL and shortening of papillofoveal distance. These factors may contribute to recovery of disrupted foveal photoreceptor and vision improvement after IMH closure.

Keywords: Internal limiting membrane, Macular hole, Macular thickness, Optical coherence tomography

Introduction

Surgical treatment of idiopathic full-thickness macular hole (IMH) was first described by Kelly and Wendel in 1991 (1). Since then, the surgical technique has been refined (2). Pars plana vitrectomy with peeling of the internal limiting membrane (ILM) and intraocular gas tamponade is the current standard procedure (3, 4).

Optical coherence tomography (OCT) is a powerful imaging technique that allows visualization of transparent retinal cell layers and monitoring of hole closure. After macular hole

closure, external limiting membrane (ELM) begins to recover its structure and integrity and this allows the start of photoreceptor microstructure recovery (5-7).

Internal limiting membrane is the basement membrane where the footplates of the Müller cells are attached and is anatomically adjacent to retinal nerve fiber layer (RNFL) and ganglion cell layer (GCL). Surgical peeling is an aggressive surgical maneuver that may alter the architecture of inner retinal layers (8-13) depending on specific location around peeled fovea. Also, there are topographic changes of the macula after hole closure, with nasal displacement being reported in the literature (9, 10).

The current study investigated the anatomic implications of ILM peel in retinal layers and its relation to reported shortening of the papillofoveal distance in the process of macular hole healing.

Methods

In a nonrandomized prospective study, 36 eyes of 32 patients with IMH underwent surgery with successful hole closure

Accepted: October 1, 2017

Published online: October 16, 2017

Corresponding author:

Mun Y. Faria
Rua Professor Egas Moniz
1649-035 Lisboa, Portugal
munfaria1@gmail.com

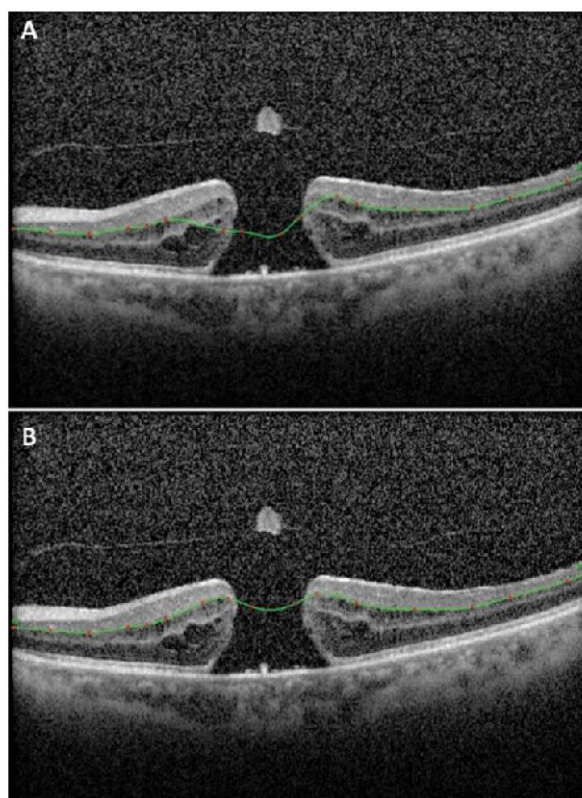


Fig. 1 - (A) Autosegmentation of inner plexiform layer in green line with red dots. **(B)** Manual correction of inner plexiform layer segmentation through relocation of red dots.

after first surgery between January 2015 and January 2017 at the Department of Ophthalmology of Santa Maria Hospital, Lisbon. The tenets of the Declaration of Helsinki were followed. All subjects gave written informed consent to the surgical and the study procedures. Approval was obtained from the ethics committee.

Exclusion criteria were glaucoma or other optic nerve diseases, any macular disease other than IMH, previous retinal surgeries, or an axial length greater than 26.0 mm. Mean follow-up after surgery was at least 6 months. Preoperative data included age, sex, duration of symptoms, and complete ophthalmic examination, including refraction and best-corrected visual acuity (BCVA), intraocular pressure (IOP) by applanation tonometry, slit-lamp biomicroscopy, fundus examination, and OCT. All macular holes were staged based on recent OCT-based classification (11), and only IMH grade 2 to 4 were considered for study. Macular hole size measurement in minimum hole diameter was performed in all cases. Retinal cross-sectional images were acquired using spectral-domain OCT (SD-OCT) (Heidelberg Engineering), using the eye-tracking feature with software posterior pole images centered on the fovea (61 acquisitions, 120 μm interval). Evaluations were performed at baseline, 1 month, 3 months, and every 6 months after surgery. We first identified the presumed foveal

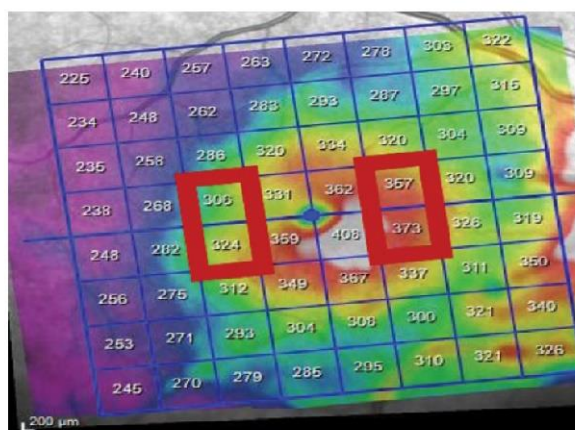


Fig. 2 - Total retinal layer thickness in square grids. The mathematical average of 2 nasal and 2 temporal squares was considered for study. Each square is 875 \times 875 μm (source: Heidelberg Engineering autosegmentation software).

center. We then identified the disc margin as the edge of the retinal pigment epithelium (RPE) or edge of the sclera in eyes with peripapillary atrophy. Papillofoveal distance was measured manually with software caliper from the disc margin to the foveal center before and after surgery. Optical coherence tomography distance reading involved 3 observers (S.M. and N.P.F.; M.Y.F. acted as an adjudicator in case the difference was more than 20%). Optic nerve head was also assessed for posterior vitreous traction.

All thickness measurements were made automatically by Spectralis SD-OCT, with Heidelberg Engineering autosegmentation software, before and after surgery. Reference data ensured that each measurement was at the same segmentation location whatever the analyzed layer. In cases of automatic misalignment of any layer, manual alignment was possible by SD-OCT software before automatic measurement, as seen in Figure 1, and that was done in every layer.

In order to limit measurement bias associated with macular hole-associated retinal derangement, we used for calculations and comparisons nasal and temporal grids of retinal areas 1,750 μm away from the fovea, corresponding to 3,500 μm diameter of ILM peel, centered on fovea, as detailed in Figures 2-4.

Optical coherence tomography delineates every macular layer and at the same time assesses thickness of individual retinal layers. We also measured inner retinal layer (IRL) and outer retinal layer (ORL).

Inner retinal layer comprises RNFL, GCL, inner plexiform layer (IPL), inner nuclear layer (INL), and outer plexiform layer (OPL).

Outer retinal layer includes ELM, ellipsoid zone, and RPE.

A middle section of IRL (mIRL) from posterior limit of IPL and anterior limit of ELM, clearly visible in Figure 5, A and B, was obtained by deducting GCL and RNFL thickness from automatic thickness of IRL.

Baseline and 6-month follow-up ultra-high-resolution horizontal scans were used for analysis.

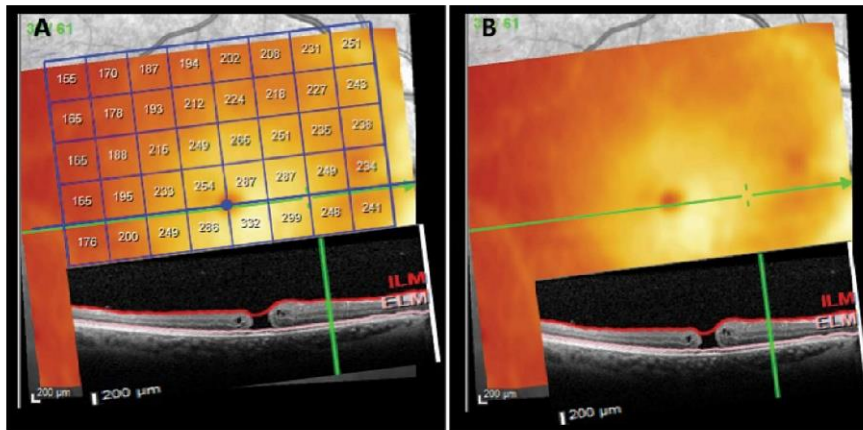


Fig. 3 - (A, B) Optical coherence tomography (OCT) image of macular hole with and without 8 × 8 posterior pole grid of inner retinal thickness by spectral-domain OCT Heidelberg automatic segmentation. Bottom: Optical coherence tomography image at same corresponding nasal distance. ELM = external limiting membrane; ILM = internal limiting membrane.

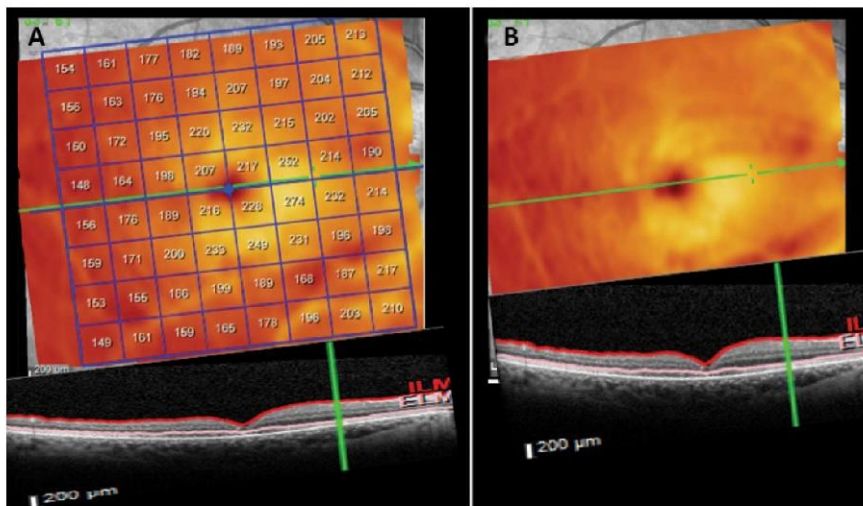


Fig. 4 - (A, B) Optical coherence tomography (OCT) image of closed macular hole with and without 8 × 8 posterior pole grid of inner retinal thickness by OCT Spectralis Heidelberg automatic segmentation. Bottom: Optical coherence tomography image at the same corresponding nasal distance.

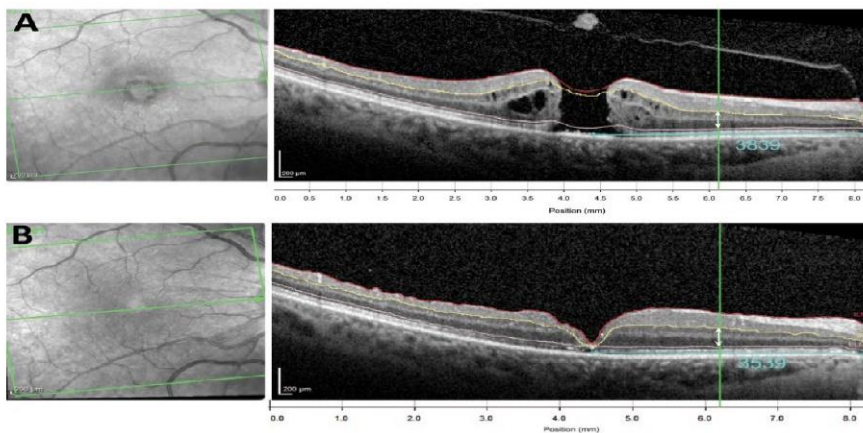


Fig. 5 - (A) 3,839 = Papillofoveal distance in μm , before surgery, in blue. White arrow = Distance of middle part of inner retinal layer (mRIL) from inner plexiform layer (IPL) (yellow line) to ELM external limiting membrane (pink line) at 1,750 μm from fovea, before surgery. **(B)** 3,539 = Papillofoveal distance in μm at 6 months postoperatively. White arrow = mRIL distance from IPL (yellow line) to ELM (pink line) at 1,750 μm from fovea, before and after surgery.

Surgical technique

All surgeries were performed by the same surgeon (M.Y.F.). A standard surgical procedure consisted of 23-G or 25-G 3-port pars plana vitrectomy (PPV) including the induction of a posterior vitreous detachment if needed, assisted with triamcinolone acetonide. Every patient underwent combined cataract surgery, except for 3 pseudophakic patients and 1 with cataract-sparing surgery. Standard small-incision phacoemulsification and implantation of a standard foldable intraocular lens was associated with vitrectomy. Balanced salt solution (Alcon) was used as an irrigation solution. A single-use macular contact lens (Grieshaber; Alcon) was used in every ILM peeling. In every eye, Brilliant Peel® Dual (Fluoron; Geuder)-assisted ILM peeling was performed, engaged with end grip intraocular forceps to create a flap, and then peeled in a circular fashion until the border of macula, sparing the macular area. Balanced salt solution was exchanged with 15% SF₆ gas. The patients were instructed to maintain a face-down position for at least 5 days.

Postoperative observations were performed at day 1, 1 week, 1 month, 3 months, 6 months, and subsequent 6 months or whenever needed. At each visit, IOP was always measured. Best-corrected visual acuity, OCT and fundus revision were performed. Parameters at 6-month follow-up were used for analysis: hole status and distance from optic disc border, nasal and temporal total retinal thickness, ORL, IRL, GCL, and RNFL layer thickness 1,750 µm away from fovea.

Best-corrected visual acuity was assessed using a decimal visual acuity chart, and the decimal visual acuity was converted to logarithm of the minimum angle of resolution (logMAR) units for analysis.

The results are expressed as mean ± SD. Wilcoxon signed-rank test was used and STATA software was used for statistical analysis. $p < 0.05$ Was considered significant.

Results

A total of 36 eyes of 32 patients who underwent macular hole surgery in Santa Maria Hospital were included in this study. Mean age was 69 ± 8.9 years, 9 male (36%) and 23 female (64%), 17 right eyes (47%) and 19 left eyes (53%). There were 13 grade 2 (36%), 12 grade 3 (33%), and 11 grade 4 (31%) with OCT-based staging of macular holes.

Medium macular hole evolution time was 25 ± 16.7 months, medium macular hole size 493 ± 227 µm, as seen in supplementary Table I, available online as supplementary material at www.eur-j-ophthalmol.com.

Preoperative mean BCVA was 1.29 ± 0.5 logMAR, and 6 months postoperatively, mean BCVA was 0.91 ± 1.0 logMAR. However, because of concomitant standard small-incision phacoemulsification cataract surgery in almost every patient, improvement of vision owing to cataract surgery has to be taken into consideration.

All macular holes were closed after 1 surgery. Two eyes had a flat open macular hole and were not considered in this study.

In the current study, we measured the papillofoveal distance on OCT images in all 36 eyes and found that the distance was significantly shorter at 6 months after PPV ($3,608$ µm vs $3,436$ µm) ($p < 0.001$) (Fig. 5, A and B).

Automatic segmentation and thickness analysis were performed at 1,750 µm nasal and temporal to fovea at baseline and 6 months (Figs. 1-3 and supplementary Tab. II, available online as supplementary material at www.eur-j-ophthalmol.com).

In the nasal subfield, total nasal retinal thickness increased from 337 ± 37 µm to 346.3 ± 43 µm ($p < 0.001$); mIRL from IPL to ELM increased from 189 ± 35 µm to 212 ± 39 µm ($p < 0.001$).

Ganglion cell layer and RNFL had decreased in thickness from 45.5 ± 10.6 µm to 39.0 ± 13.1 µm ($p < 0.01$) and 33.7 ± 13 µm to 31 ± 12.2 µm ($p = 0.05$), respectively.

Outer retinal layer increased in thickness, from 63.6 ± 17.5 µm to 66.6 ± 15.7 µm ($p < 0.05$).

The temporal subfield had a total retinal thickness decreased at month 6, from 312 ± 35 µm to 281 ± 37 µm ($p < 0.001$).

The GCL and RNFL showed a decrease in thickness from 41.0 ± 10.8 µm to 25.7 ± 10.9 µm ($p < 0.001$) and 19.1 ± 6.5 µm to 17.4 ± 5.6 µm ($p 0.22$), respectively.

The mIRL decreased from 188 ± 35 µm to 173 ± 33 µm ($p < 0.05$).

The outer retinal layers showed some increase in thickness, from 60.3 ± 17.5 µm to 65 ± 17.8 µm ($p < 0.01$).

We then investigated the relationship between macular location changes and the mIRL thickness, trying to relate shortening of the papillofoveal distance with increased mIRL thickness. The results were not statistically significant (Fig. 5, A and B).

In summary, at 6 months post ILM peel, analysis of nasal macular layers showed an increase in mIRL, the major contribution from INL and external plexiform layer. On the temporal side, a significant reduction in all retinal layers was noted. Outer retinal layers increased in every closed macular hole. Statistically significant nasal macular migration was also noted.

Discussion

A standard procedure of choice in idiopathic macular hole (IMH) surgery is to relieve anterior-posterior and tangential traction by vitrectomy and ILM peeling (3, 4).

Internal limiting membrane peeling releases the tangential traction of the residual prefoveal vitreous after the posterior vitreous detachment and the traction of the epiretinal cellular constituents adjacent to the macular hole. These 2 factors should alter the mobility of the macular hole edge (12).

Internal limiting membrane peeling is a major trauma that tears the footplates and parts of Müller cells. This trauma incites the contraction of glial cells that proliferated following the macular hole surgery with ILM peeling, leading to a centripetal movement of the photoreceptors and realignment of ELM (13).

Internal limiting membrane peeling increases the success of macular hole surgery (4), but due to its close relationship with inner retina, ILM peeling may alter the normal architecture of the macula (14, 15).

Postoperative thinning of RNFL and GCL has been described by Sabater et al (8), after presumptive mechanical damage of ILM peel over GCL or to Müller cells contained in the GCL.

In our study, we found asymmetric parafoveal retinal thickness in eyes with closed macular holes.

Nukada et al (16) and Ohta et al (17) described temporal retina thinning in ILM peeling in IMH surgery.

It seems that after removal of rigid preoperative ILM, there are biomechanical retinal forces that displace the fovea, resulting in stretching and thinning of retinal parenchyma in the temporal subfield (9, 17) and thickening of the nasal macula.

In the present study, we found that increased nasal thickness was dependent on mIRL. This layer includes deeper region of IPL, INL, OPL, and inner segments of photoreceptors. Although Modi et al (18) only refer to increased thickness of INL after ILM peel in macular hole surgery, in our study, all the layers seem to be thickened after ILM peeling. Inner nuclear layers are mainly horizontal, bipolar, and glial cells, which seem to be the most altered and thickened because of stretching and inflammation. The OPL is the area in which photoreceptors communicate with the horizontal cells and bipolar cells and we speculate it has major importance in inciting recovery of disrupted photoreceptors.

In other vitreomacular traction syndromes, like epiretinal membrane (19, 20), the middle part of the inner retinal layer structure is important for visual recovery and metamorphopsia improvement and we speculate that in ILM peeling in macular hole surgery, the thickening of mIRL should be important in macular closure, eventually inducing glial proliferation and anatomical restructuring of photoreceptor outer segment.

Our study aimed to study thickening of mIRL after closure of IMH and associated displacement of fovea.

In cases of spontaneous closure of macular hole there is no foveal displacement (21), so we can infer that ILM peeling is the cause of macular displacement. Internal limiting membrane is attached to optic disc and after peeling there is traction force rebalance and nasal shift of closed macular hole. The reason for displacement of the denuded and elastic retinal tissue after the removal of rigid preoperative ILM is yet to be established. Ishida et al (9) suggested neural contraction excited by ILM peeling. Thickening of nasal mIRL, especially IRL and OPL, may be a cause or consequence of this nasal shift.

Our results revealed nasal IRL thickening and shortening of papillomacular distance after surgery in cases of successful macular hole surgery with ILM peeling.

The study has several limitations. The area of ILM removal was estimated to be 1,750 μm and not measured on operative video, even though the surgeon was the same. Also, there were no data on relation of metamorphopsia and postoperative displacement.

However, this study could help clarify the importance of INL and OPL in triggering restructuring of ELM, which begins the reorganization of photoreceptor outer segment in the process of macular hole closure after vitrectomy and ILM peel.

Disclosures

Financial support: No financial support was received for this submission.

Conflict of interest: None of the authors has conflict of interest with this submission.

References

- Kelly NE, Wendel RT. Vitreous surgery for idiopathic macular holes. Results of a pilot study. *Arch Ophthalmol*. 1991;109(5):654-659.
- Wendel RT, Patel AC, Kelly NE, Salzano TC, Wells JW, Novack GD. Vitreous surgery for macular holes. *Ophthalmology*. 1993;100(11):1671-1676. A.
- Brooks HL. Macular hole surgery with and without internal limiting membrane peeling. *Ophthalmology* 2000;107(10): 1939-48; discussion 1948-9.
- Spiteri Cornish K, Lois N, Scott NW, et al. Vitrectomy with internal limiting membrane peeling versus no peeling for idiopathic full-thickness macular hole. *Ophthalmology*. 2014;121(3): 649-655.
- Tadayoni R, Svorenova I, Erginay A, Gaudric A, Massin P. Decreased retinal sensitivity after internal limiting membrane peeling for macular hole surgery. *Br J Ophthalmol*. 2012;96(12):1513-1516.
- Ito Y, Terasaki H, Takahashi A, Yamakoshi T, Kondo M, Nakamura M. Dissociated optic nerve fiber layer appearance after internal limiting membrane peeling for idiopathic macular holes. *Ophthalmology*. 2005;112(8):1415-1420.
- Sevim MS, Sanisoglu H. Analysis of retinal ganglion cell complex thickness after brilliant blue-assisted vitrectomy for idiopathic macular holes. *Curr Eye Res*. 2014;39(5):539-540.
- Sabater AL, Velázquez-Villoria Á, Zapata MA, et al. Evaluation of macular retinal ganglion cell-inner plexiform layer thickness after vitrectomy with internal limiting membrane peeling for idiopathic macular holes. *Biomed Res Int*. 2014;2014: 458631.
- Ishida M, Ichikawa Y, Higashida R, Tsutsumi Y, Ishikawa A, Imamura Y. Retinal displacement toward optic disc after internal limiting membrane peeling for idiopathic macular hole. *Am J Ophthalmol*. 2014;157(5):971-977.
- Kawano K, Ito Y, Kondo M, et al. Displacement of foveal area toward optic disc after macular hole surgery with internal limiting membrane peeling. *Eye (Lond)*. 2013;27(7):871-877.
- Duker JS, Kaiser PK, Binder S, et al. The International Vitreomacular Traction Study Group classification of vitreomacular adhesion, traction, and macular hole. *Ophthalmology*. 2013;120(12):2611-2619.
- Gass JDM. Müller cell cone, an overlooked part of the anatomy of the fovea centralis: hypotheses concerning its role in the pathogenesis of macular hole and foveomacular retinoschisis. *Arch Ophthalmol*. 1999;117(6):821-823.
- Uemoto R, Yamamoto S, Aoki T, Tsukahara I, Yamamoto T, Takeuchi S. Macular configuration determined by optical coherence tomography after idiopathic macular hole surgery with or without internal limiting membrane peeling. *Br J Ophthalmol*. 2002;86(11):1240-1242.
- Tadayoni R, Paques M, Massin P, Mouki-Benani S, Mikol J, Gaudric A. Dissociated optic nerve fiber layer appearance of the fundus after idiopathic epiretinal membrane removal. *Ophthalmology*. 2001;108(12):2279-2283.
- Baba T, Sato E, Oshitari T, Yamamoto S. Regional Reduction of Ganglion Cell Complex after Vitrectomy with Internal Limiting Membrane Peeling for Idiopathic Macular Hole. *J Ophthalmol*. 2014;2014:372589.
- Nukada K, Hangai M, Ooto S, Yoshikawa M, Yoshimura N. Tomographic features of macula after successful macular hole surgery. *Invest Ophthalmol Vis Sci*. 2013;54(4): 2417-2428.
- Ohta K, Sato A, Fukui E. Asymmetrical thickness of parafoveal retina around surgically closed macular hole. *Br J Ophthalmol*. 2010;94(11):1545-1546.
- Modi A, Giridhar A, Gopalakrishnan M. Gopalakrishnan m. Spectral domain optical coherence tomography-based microstructural analysis of retinal architecture post internal limiting membrane peeling for surgery of idiopathic macular hole repair. *Retina*. 2017;37(2):291-298.

19. Joe SG, Lee KS, Lee JY, Hwang J-U, Kim J-G, Yoon YH. Inner retinal layer thickness is the major determinant of visual acuity in patients with idiopathic epiretinal membrane. *Acta Ophthalmol.* 2013;91(3):e242-e243.
20. Cho KH, Park SJ, Cho JH, Woo SJ, Park KH. Inner-Retinal Irregularity Index Predicts Postoperative Visual Prognosis in Idiopathic Epiretinal Membrane. *Am J Ophthalmol.* 2016;168:139-149.
21. Kawano K, Ito Y, Kondo M, et al. Displacement of foveal area toward optic disc after macular hole surgery with internal limiting membrane peeling. *Eye (Lond).* 2013;27(7):871-877.

CHAPTER 3

Multifocal Electroretinography in Assessment of Macular Function after Internal Limiting Membrane Peeling in Macular Hole Surgery

Mun Faria, David Sousa, Sofia Mano, Raquel Marques, Nuno Ferreira, Ana Fonseca.

Journal of Ophthalmology, 2019 doi.org/10.1155/2019/1939523

In this chapter we studied macular function, by means of multifocal electroretinography, to determine the type of alterations after ILM peeling in a closed MH.

Aim: The purpose of this prospective study was to characterize macular function by means of multifocal electroretinography (mf ERG), before and after surgery. We try to relate integrity of inner and outer macular layers with functional results measured by mf ERG.

Methods:

Nonrandomized prospective study of 33 consecutive eyes of 33 patients with MH, who underwent vitrectomy with ILM peeling. BCVA and integrity of external layers were measured with OCT. RETIscan mf ERG, was used for mf ERG recording. Each component of multifocal electroretinography, N1 and P1 amplitude and latency, were measured. Mean follow-up time was at least 12 months after surgery.

Mun Faria contributed to Research Design, Data Interpretation, Manuscript Preparation Conceptualization and Investigation. David Sousa was involved in Methodology, Review, and Editing. Sofia Mano contributed in Resources, Raquel Marques contributed to Statistical Analysis, Nuno Ferreira was involved in Validation and Review, Ana Fonseca contributed to Manuscript Preparation, Review and Editing. All authors read and approved the final manuscript.

The results of this study allowed the following peer reviewed publication:

Paper 3- Multifocal Electroretinography in Assessment of Macular Function after Internal Limiting Membrane Peeling in Macular Hole Surgery. Journal of Ophthalmology, Volume 2019, Article ID 1939523, 7 pages <https://doi.org/10.1155/2019/1939523>

Research Article

Multifocal Electroretinography in Assessment of Macular Function after Internal Limiting Membrane Peeling in Macular Hole Surgery

M. Y. Faria ^{1,2}, D. C. Sousa,^{1,2} S. Mano,^{1,2} R. Marques,^{1,2} N. P. Ferreira ^{1,2}
and A. Fonseca^{1,2}

¹Ophthalmology University Clinic, Faculdade de Medicina Lisboa, Universidade de Lisboa, Lisbon, Portugal

²Ophthalmology Department, Hospital Santa Maria, Centro Hospitalar Universitário Lisboa Norte, Lisbon, Portugal

Correspondence should be addressed to M. Y. Faria; munfaria1@gmail.com

Received 24 December 2018; Accepted 7 March 2019; Published 27 March 2019

Guest Editor: Akihiro Ohira

Copyright © 2019 M. Y. Faria et al. This is an open access article distributed under the Creative Commons Attribution License, which permits unrestricted use, distribution, and reproduction in any medium, provided the original work is properly cited.

Purpose. Internal limiting membrane (ILM) peeling is important for macular hole (MH) surgery but may have secondary effects visible on spectral domain optical coherence tomography (OCT) and multifocal electroretinography (mfERG). We relate integrity of inner and outer macular layers with functional results with mfERG. **Methods.** Nonrandomized prospective study of 33 consecutive eyes of 33 patients with macular hole who underwent vitrectomy with ILM peeling. Best-corrected visual acuity was assessed, and integrity of external layers was measured using OCT. Each component of mfERG, N1 and P1 amplitude and latency, was also measured. **Results.** All eyes showed macular hole closure. Visual acuity improved from 20/400 to 20/40 in the Snellen visual acuity chart ($P < 0.001$), and OCT external lines were intact in 19 eyes and disrupted in 14 eyes. Postoperatively, N1 and P1 amplitudes in ring 1 increased compared to preoperative values ($P < 0.001$ for both). Latency remained delayed for both N1 and P1 wave. In the group of 19 eyes with integrity of outer retinal layers, N1 amplitude in ring 1 was superior to the group of 14 patients with disrupted outer retinal layers ($P = 0.042$). **Conclusions.** In macular hole surgery, structure analysis in OCT is one of the important outcomes for the retinal surgeon. Functional results are parallel with anatomic results, but visual gain is limited. The limited recovery in mfERG suggests an alteration of retinal physiology that could explain limited vision recover.

1. Introduction

Currently, macular hole is a common surgical feature, practiced in most vitreoretinal centers with high rate of closure [1]. Peeling of the internal limiting membrane (ILM) and inverted flap technique allows this high closure rate [2]. Indications for surgery and surgical technique to be used are based on structural images. Also, postoperative results are based on foveal anatomy. With ocular coherence tomography (OCT), it has become much easier to define and understand the retinal anatomy before and after macular hole surgery. In addition, it has also helped to explain poor visual acuity (VA) in cases where the retina appeared normal at biomicroscopic examination. Most efforts have focused on surgical technique to realign photoreceptors and improve

VA. However, exploring retinal function is another way of understanding the healing process of macular holes.

After successful hole closure, patients refer less metamorphopsia and an improved ability to read [3]. Nevertheless, even with hole closure, visual function improves but the gain in visual acuity is often limited. Visual function before and after macular hole surgery is usually assessed by visual acuity measurement [4]. However, the visual acuity level represents only a part of the visual function resulting from macular hole development, which includes metamorphopsia, scotoma, and blurred vision [5].

Because ILM is the basement membrane of Müller cells, the inner barrier of the neural retina and anatomically adjacent to the retinal nerve fiber layer (RNFL) and ganglion cell layer (GCL), ILM removal may alter the architecture of

the inner retinal layer and also alter the function of Müller cells, responsible for the generation of electroretinogram [6]. Nerve fibers are joined and fixed at the lamina crivosa, and after ILM peeling, a dissociated optic nerve layer has been referred by Tadayoni et al. [7]. Also, nasal displacement and contraction of this neural layer and ganglion cell axon allow the underlying macular tissue to react with the alteration of cytoarchitecture of external retinal layers [8]. All these structural alterations may have consequences on post-operative macular function. Moreover, the direct trauma of surgery to the nerve fiber layer, the gas tamponade, the stain used to visualize the transparent ILM, and the endoillumination light probe are all factors to consider as possible toxic effects to macular function.

Multifocal electroretinography (mfERG) is an objective clinical tool to assess visual function and selects the multiple retinal locations of the macular area to provide a topographic map of local central retinal electrophysiological activity [9]. The purpose of this prospective study was to characterize macular function by means of mfERG, before and after surgery.

2. Methods

2.1. Setting and Patients. In a nonrandomized prospective study, 33 consecutive eyes of 33 patients with MH underwent surgery between January 2015 and June 2017 at the Department of Ophthalmology of Santa Maria Hospital, Lisbon. Exclusion criteria were maculopathy other than MH, surgeries for MH recurrence, other retinal diseases, or an axial length greater than 26.0 mm. Mean follow-up time was at least 12 months after surgery. This study was approved by the Ethics Committee of Santa Maria Hospital. The tenets of the Declaration of Helsinki were followed. All subjects have given written informed consent to the surgical and the study procedures.

2.2. Collected Data. Preoperative data included age, gender, and complete ophthalmic examination. Best-corrected visual acuity (BCVA) was measured using a Snellen chart and converted to the logarithm of the minimum angle of resolution (logMAR) for statistical analysis. Hand motion was considered as logMAR 3 and counting fingers as logMAR 2.

2.3. Optical Coherence Tomography. All macular holes were staged based on recent OCT-based classification [10], and only full thickness macular hole, grade 2 to 4, was considered for the study. Retinal images were acquired using Spectralis SD-OCT (Heidelberg Engineering, Heidelberg®, Germany), using the eye-tracking feature with software posterior pole images centered on the fovea (61 acquisitions, 120 μ m interval).

The status of the foveal ellipsoid zone (EZ) and the external limiting membrane (ELM) were examined for each eye to test integrity: intact and disrupted. The intact eyes had a regular continuation of the hyperreflective line corresponding to the EZ or ELM. The disrupted eyes were characterized by hyporeflexive discontinuities in the EZ or ELM line (Figure 1). These classifications were assessed by agreement of two authors (MF and NF).

2.4. Multifocal Electroretinography. RETIscan Multifocal ERG (Version 6.12.5.12; Roland Consult) was used for mfERG recording. The recording procedures were the same as those described by the International Society for Clinical Electrophysiology of Vision [11]. The stimulus consisted of 61 hexagons that scale concentrically and covered the central 25 degrees of the fundus area. The viewing distance was 29 cm, which allowed a viewing angle of approximately 30 degrees. Each hexagon was modulated temporally between black (2 cd/m²) and white (200 cd/m²). Pupils were dilated with tropicamide and phenylephrine hydrochloride. After topical anesthesia, a contact lens jet electrode was placed, and signals were recorded. During the recordings, the patients' fixations were monitored. The signal was amplified (100,000) and bandpass filtered (10–300 Hz). Three-dimensional topography represents the retinal response density (amplitude per retinal area, nV/deg²).

The mean simultaneous response was recorded. The typical waveform of the basic mfERG response is a biphasic wave with an initial negative deflection followed by a positive peak. Implicit times (latencies) and the amplitude relative to their respective areas (nV/deg²) of the first negative peak (N1) and the first positive peak (P1) were measured using regional averages derived from 5 concentric rings (Figures 2 and 3). Three-dimensional topography (Figure 4) represents the retinal response density (amplitude per retinal area, nV/deg²). The studied field contained 61 hexagons in 5 rings within a field diameter of 25 degrees, 12.5 degrees radially centered on the fovea [12], and was analyzed with RETIscan software. Five rings correspond to 5 degree areas. Only ring 1 and ring 2 were considered, as they roughly parallel a 3 mm diameter ILM peel during surgery.

Multifocal ERG was recorded preoperatively and at 12 months after surgery. In the present study, we focused on amplitude and latency of N1 and P1, before and after surgery.

2.5. Surgical Procedure. A standard surgical procedure consisted of 23- or 25-gauge, three-port pars plana vitrectomy (PPV). Except in pseudophakic patients, every patient underwent combined cataract surgery, in order to avoid confounding results. Standard small-incision phacoemulsification and implantation of a standard foldable intraocular lens were associated with vitrectomy. In every eye, Brilliant Peel® Dual (Geuder, Germany) assisted ILM peeling was performed, in an area of approximately 3 mm, engaged with end-grip intraocular forceps. A flap is created, then peeled in a rosette way all around the hole, and trimmed until the border of the macula but leaving a flap big enough to invert and cover the hole. BSS was exchanged with 15% SF6 (sulfur hexafluoride) gas. The patients were instructed to maintain a face-down position for at least 5 days. All surgeries were performed by the same experienced surgeon (MF).

2.6. Postoperative Follow-Up. In postoperative observations, at day 1, month 3 and month 6, a thorough ophthalmic examination, including BCVA, mfERG, and OCT, whenever

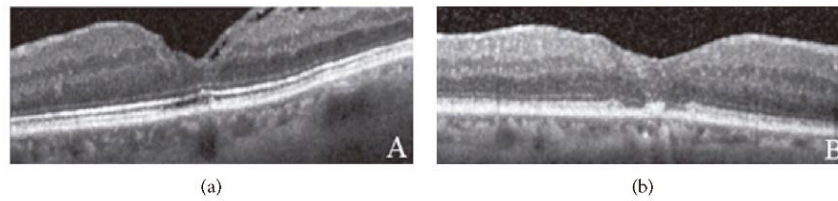


FIGURE 1: OCT with closed macular hole: integrity of ELM and EZ zone (a) and disrupt ELM and EZ (b).

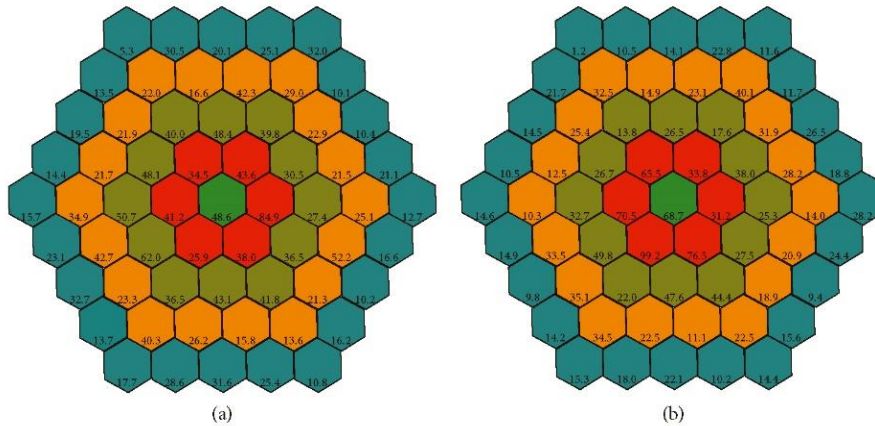


FIGURE 2: Amplitude of P1 nV/deg² in patient no. 4 in five rings centered in fovea, before surgery (a) and after surgery (b) Ring 1 (green) and ring 2 (red) are considered for study.

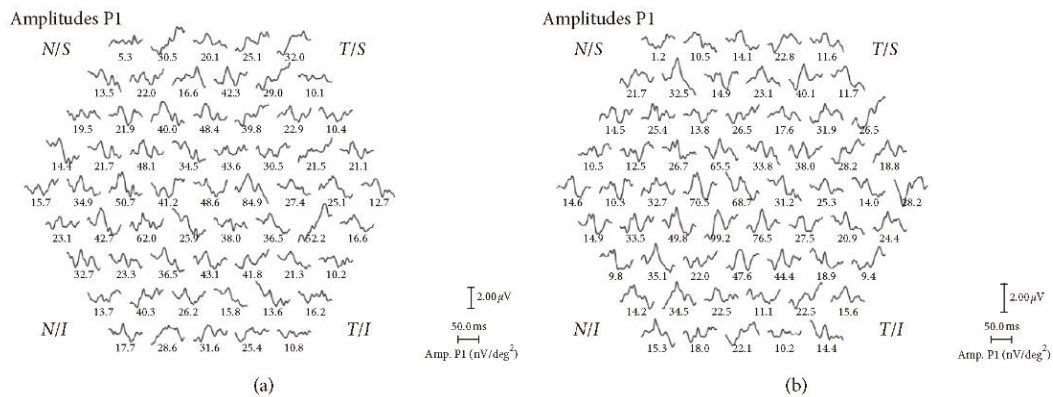


FIGURE 3: Amplitude of P1 in nV/deg² in patient no. 4 in topographic display around fovea, before (a) and after (b) surgery.

possible, and fundus revision were performed. Hole status, ELM, and EZ integrity at the fovea were measured in OCT. N1 and P1 waves of mfERG were measured for amplitude and implicit time.

2.7. Statistical Analysis. The results are expressed as medians (range). Only ring 1 and ring 2 of mfERG were considered as they correspond to the area of the ILM peel. Amplitude and latency of N1 and P1 of mfERG were compared before and after surgery. BCVA and amplitude of N1 and P1 of mfERG

were compared between the groups with intact or disrupted photoreceptor. For comparisons before and after surgery, the Wilcoxon signed-rank test was used. Between group analyses were performed with the Mann-Whitney *U* test. Correlations were tested using Spearman's ρ correlation coefficient. Statistical significance was established at $P < 0.05$.

3. Results

3.1. Demographic and Clinical Data. The median (range) age of the patients was 71 (21) years, and the study group

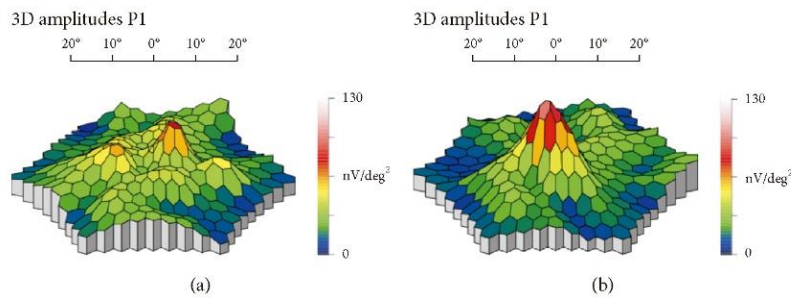


FIGURE 4: Three-dimensional topography of amplitude P1 of patient no. 4, before and after surgery for macular hole.

included 14 men and 19 women. Thirty-three eyes were studied, 26 patients underwent concomitant cataract surgery, and 7 were already pseudophakic. None of the patients required further treatment during the 12-month follow-up.

3.2. Amplitude of P1 and N1 and Respective Latency Times before and after Surgery. There was an increase in amplitude of P1 and N1 waves, in ring 1, after surgery ($P < 0.001$ for both). Ring 2 increase was only statistically significant for P1 wave ($P = 0.040$). Pre- and postoperative latency was not significant for neither waves (Table 1).

3.3. Visual Acuity and Amplitude of P1 and N1 by Photoreceptor Status before and after Surgery. The median (range) visual acuity, in logMAR, improved from 2.10 (2.90) to 0.70 (4.80), $P = 0.007$ and from 1.80 (1.60) to 1.10 (2.0), $P = 0.008$, from baseline to 12 months in the intact and disrupted photoreceptor groups, respectively. P1 and N1 in the first ring region of the retina increased both in the intact photoreceptor group and the disrupted photoreceptor group ($P < 0.001$ and $P = 0.001$, respectively), with no differences in the second-ring regions of the retina (Table 2).

3.4. Difference between Post- and Presurgery in BCVA, N1 Amplitude, and P1 Amplitude. Median (range) increase in visual acuity from pre to postsurgery was -0.80 (7.60) logMAR and -0.40 (1.40) logMAR, in the intact photoreceptor group and the disrupted photoreceptor group, respectively ($P = 0.114$). Increase in N1 ring 1 was 30.20 (75.20) nV/deg² and 10.25 (116.90) nV/deg², and increase in P1 ring 1 was 12.00 (99.10) nV/deg² and 20.95 (97.90) nV/deg² in the intact photoreceptor group and the disrupted photoreceptor group, respectively ($P = 0.042$ and $P = 0.418$, respectively), as assessed by the Mann-Whitney U test. There was no correlation between BCVA increase and N1 increase in any of the groups, intact or interrupted, as assessed by Spearman's ρ correlation coefficient.

4. Discussion

In macular hole surgery, removing the ILM may eliminate almost all traction, anterior-posterior and tangential, and lead to a higher probability of hole closure [13]. ILM peeling

was introduced as an additional maneuver to improve anatomical and functional outcomes [14], allowing 100% closure of idiopathic macular holes, especially with the inverted flap technique [2]. With the latest spectral domain OCT, with increased depth of resolution, it has become much easier to define and understand the retinal anatomy before and after macular hole surgery. In our study, peeling was performed in every surgery. However, the effects of ILM removal on retinal function remain unknown. Multifocal electroretinography is a noninvasive method that objectively measures visual function by selecting multiple retinal locations around macular area to provide a topographic map of electrophysiological activity in the central retina [9]. Based on the International Society for Clinical Electrophysiology of Vision (ISCEV), mfERG responses show greater amplitudes in the fovea where cone photoreceptors and bipolar cells are in greater number. It is believed that N1 is generated by photoreceptors in the outer retinal layer and P1 is generated by Müller and bipolar cells [15, 16].

If outer retinal layers are intact after surgery, photoreceptors will probably recover function, N1 will probably increase and influence internal layers, in recovering P1 functions. However, that is not always true, as peeling of ILM may negatively influence these internal layers.

Several previous studies with mfERG on eyes before and after MH surgery were published. Machida et al. [17] found no toxic effect of brilliant blue G, indocyanine green, or triamcinolone acetonide in macular hole surgery with ILM peel, as measured with focal macular electroretinograms. Scupola et al. [18] compared triamcinolone acetonide and infracyanine green in thirty eyes studied with focal electroretinogram and found late toxic effect with infracyanine green-assisted ILM peeling. Bellerive et al. [19] also compared toxicity of trypan blue and infracyanine green in macular hole surgery using mfERG before and after surgery and concluded that, at 12 months, there was improvement of P1 amplitude and implicit time, BCVA, and contrast sensitivity was not different between groups. Ferencz et al. [20] studied mfERG in 30 eyes with MH, found preoperative subnormal responses, and only at 20 months found significant improvement in both groups by probable toxicity with infracyanine green in surgery.

Studying macular hole before and after its closure is a unique situation where outer retinal cells do not exist at full thickness hole. After successful surgery, there is a closed hole with or without integrity of ELM, EZ, and retinal pigment

TABLE 1: Amplitude of P1 and N1 and respective latency times before and after surgery.

Parameter	Before surgery ($n = 33$)	After surgery ($n = 33$)	P value
P1 amplitude (nV/deg ²)			
Ring 1	36.00 (77.20)	59.20 (92.60)	<0.001
Ring 2	45.70 (62.30)	55.30 (97.30)	0.040
P1 latency (ms)			
Ring 1	33.30 (30.40)	34.30 (38.20)	0.806
Ring 2	33.30 (20.60)	34.30 (30.40)	0.955
N1 amplitude (nV/deg ²)			
Ring 1	28.30 (127.30)	46.30 (155.30)	<0.001
Ring 2	20.80 (85.80)	22.60 (47.40)	0.550
N1 latency (ms)			
Ring 1	17.60 (48.80)	18.60 (22.50)	0.330
Ring 2	17.60 (13.70)	17.60 (27.40)	0.977

Amplitude of P1 and N1 are expressed in nanovoltage (nV)/area degree² (deg²) and implicit time (latency) in milliseconds (ms). All values are expressed as median (range). P values are obtained from the Wilcoxon signed-rank test.

TABLE 2: Visual acuity and amplitude of P1 and N1 by photoreceptor status before and after surgery.

Parameter	Before surgery ($n = 33$)	After surgery ($n = 33$)	P value
Intact photoreceptor			
Visual acuity (logMAR)	2.10 (2.90)	0.70 (4.80)	0.007
P1 amplitude (nV/deg ²)			
Ring 1	37.70 (77.20)	59.00 (92.60)	<0.001
Ring 2	51.50 (39.70)	67.30 (97.30)	0.231
N1 amplitude (nV/deg ²)			
Ring 1	31.40 (120.80)	67.90 (117.80)	<0.001
Ring 2	20.30 (30.80)	24.80 (47.40)	0.571
Disrupted photoreceptor			
Visual acuity (logMAR)	1.80 (1.60)	1.10 (2.00)	0.008
P1 amplitude (nV/deg ²)			
Ring 1	35.65 (48.10)	60.80 (82.20)	0.001
Ring 2	35.15 (62.30)	45.85 (80.20)	0.084
N1 amplitude (nV/deg ²)			
Ring 1	23.35 (127.30)	31.65 (155.30)	0.001
Ring 2	21.30 (85.80)	21.50 (40.20)	0.861

Amplitude of P1 and N1 are expressed in nanovoltage (nV)/area degree² (deg²). All values are expressed as median (range). P values are obtained from the Wilcoxon signed-rank test.

epithelium. Also, there is a reduced thickness of internal macular layers after ILM peeling in macular hole surgery [8], especially ganglion cell layers and internal nuclear layers, measured at 3 mm diameter centered on fovea, roughly the degree reached by the second ring in mfERG.

In this macular hole study, mfERG recorded before surgery showed almost undetectable retinal response in foveal and parafoveal areas, in ring 1 and ring 2. After surgery, the improvement in the retinal response density of mfERG in the same ring seems to be consequent to closure of the macular hole with realignment of photoreceptor cells and glial cell activation. Resolution of the central scotoma seems to be attributed to anatomical repair and, in our study, we found a statistically significant increase in N1 and P1 in ring 1. Comparing ring 1 in N1 and P1 amplitude and outer retinal layer status, we found that P1 wave increased both in the intact and disrupted groups ($P < 0.001$ and $P = 0.001$, respectively), which is consistent with increase of P1 amplitude with closure of hole, whatever the outer layer status is. As to the N1 wave, the increase in the intact group was superior to the increase in the disrupted group

($P = 0.042$). All other results were not significant. Therefore, in our results, correct restoration with intact hyperreflective photoreceptor lines in OCT, ELM and EZ, results in improvement in outer retina response, as measured by the N1 wave. It has generally been thought that photoreceptor status by OCT is associated with visual recovery [21]. Although the N1 amplitude was reduced by the presence of MH, the increase in 66% of its amplitude after ILM peeling, hole closure, and realignment of photoreceptors agrees well with that the N1 amplitude was related to and generated from the outer retina.

The median BCVA of patients included in the study improved after surgery. The mechanism by which visual function improves after surgery is not clearly understood. However, the centripetal movement of the previously displaced photoreceptors to its original site as proven by OCT images may be the simplest explanation [4]. However, even with integrity in photoreceptor lines, vision improvement is limited.

BCVA increased in both the intact and disrupted groups ($P = 0.007$ and $P = 0.008$, respectively). Even though clinically the results are better in the intact group, there is a large

variability, which may have prevented a higher statistical significance in this group.

Besides the low recovery of P1, there was also a delay of implicit time. After ILM peeling and closure of the macular hole, implicit time of the P1 wave in ring 1 maintained delay of 33.96 (38.20) millisecond in this study compared to normative data [22]. The delay may be related to surgical aggression of ILM peeling, or even ischemia in the macular area [23]. Implicit time was delayed before surgery and never recovered, even after closure and visual recovery. Andréasson and Ghosh already referred [24] to a very slow cone function recovery even after successful anatomical healing.

Hood et al. [9] already suggested that the multifocal ERG value might affect numerous factors we could not detect and control. As to the N1 wave, the increase in the intact group was superior to the increase in the disrupted group ($P = 0.042$), and therefore, the P1 wave in the intact group was expected to increase superiorly than that in the disrupted group. However, P1 ring 1 increased both in the intact and disrupted groups, with no statistical differences, suggesting a loss of interaction with outer retinal layers.

Thus, we suspect that ILM peeling may damage inner retinal layers and Muller cell function which have some negative effect on the P1 wave of multifocal ERG and visual acuity.

In eyes with successful MH surgery, there is disappearance of central scotoma and improvement of visual acuity. This improvement is enhanced if there is realignment of photoreceptors and integrity of outer retinal layers. This results in NI increase in mfERG of 66% compared to 53% increase in the disrupt photoreceptor group.

P1 wave in mfERG also increases after surgery, 69% in intact and 109% in disrupted outer retinal layers, but below age-related normative data. This uneven increase of the P1 wave, whatever the outer retinal status is, may explain the functional impairment between inner and outer retinal layers. ILM is the end feet of glial cells, and an alteration of retinal physiology in inner retinal layers, where bipolar and glial cells interact with photoreceptors, may explain the limited improvement in BCVA.

The present study had several limitations. The number of patients included is small, which may limit the reliability of the statistical results. Also, only BCVA was measured, and no other visual functions were tested. We did not have a control group in which the ILM was not peeled in macular hole surgery. Performing the surgery without ILM peeling could lead to lower closure rates in grade 3 or 4 macular hole, and therefore, generating such a control group would be unethical. The peeled area of ILM is around 3 mm in diameter, but no film registration of each surgery was made in every patient to ensure the exact diameter of the peel.

Lastly, contrary to most diagnostic equipment in ophthalmology, normative data in mfERG may vary with each equipment, and laboratory and healthy fellow eyes were not used as control. Also, population-specific factors such as age, ethnicity, pupil size, axial length, and diurnal variation may influence normative data.

5. Conclusion

In eyes with successful MH surgery, there is disappearance of central scotoma and improvement of visual acuity. This improvement is enhanced if there is realignment of photoreceptors and integrity of outer retinal layers. However, functional results may not be parallel with anatomic results as visual gain is limited. ILM is the end feet of glial cells, and an alteration of retinal physiology in inner retinal layers, where bipolar and glial cells interact with photoreceptors, may explain the limited improvement in BCVA. The limited recovery in mfERG suggests an alteration of retinal physiology that could explain limited vision recover.

Data Availability

All data used to support the findings of this study are at Ophthalmology Department, Hospital Santa Maria, Centro Hospitalar Universitário Lisboa Norte, and available from the corresponding author upon request.

Conflicts of Interest

None of the authors has any conflicts of interest.

Acknowledgments

The authors thank the Orthoptic Department of Santa Maria Hospital, for coordinating and performing OCT and mfERG.

References

- [1] F. G. Ah-Fat, M. C. Sharma, M. A. Majid, J. N. McGalliard, and D. Wong, "Trends in vitreoretinal surgery at a tertiary referral centre: 1987 to 1996," *British Journal of Ophthalmology*, vol. 83, no. 4, pp. 396–398, 1999.
- [2] Z. Michalewska, J. Michalewski, R. A. Adelman, and J. Nawrocki, "Inverted internal limiting membrane flap technique for large macular holes," *Ophthalmology*, vol. 117, no. 10, pp. 2018–2025, 2010.
- [3] R. T. Wendel, A. C. Patel, N. E. Kelly, T. C. Salzano, J. W. Wells, and G. D. Novack, "Vitreous surgery for macular holes," *Ophthalmology*, vol. 100, no. 11, pp. 1671–1676, 1993.
- [4] R. N. Sjaarda, D. A. Frank, B. M. Glaser, J. T. Thompson, and R. P. Murphy, "Resolution of an absolute scotoma and improvement of relative scotomata after successful macular hole surgery," *American Journal of Ophthalmology*, vol. 116, no. 2, pp. 129–139, 1993.
- [5] F. Acosta, K. Lashkari, X. Reynaud, A. E. Jalkh, F. Van de Velde, and N. Chedid, "Characterization of functional changes in macular holes and cysts," *Ophthalmology*, vol. 98, no. 12, pp. 1820–1823, 1991.
- [6] H. Terasaki, Y. Miyake, R. Nomura et al., "Focal macular ERGs in eyes after removal of macular ILM during macular hole surgery," *Investigative Ophthalmology & Visual Science*, vol. 42, no. 1, pp. 229–234, 2001.
- [7] R. Tadayoni, M. Paques, P. Massin, S. Mouki-Benani, J. Mikol, and A. Gaudric, "Dissociated optic nerve fiber layer appearance of the fundus after idiopathic epiretinal membrane removal," *Ophthalmology*, vol. 108, no. 12, pp. 2279–2283, 2001.

- [8] M. Y. Faria, N. P. Ferreira, D. M. Cristóvão, S. Mano, D. C. Sousa, and M. Monteiro-Grillo, "Tomographic structural changes of retinal layers after internal limiting membrane peeling for macular hole surgery," *Ophthalmic Research*, vol. 59, no. 1, pp. 24–29, 2018.
- [9] D. C. Hood, W. Seiple, K. Holopigian, and V. Greenstein, "A comparison of the components of the multifocal and full-field ERGs," *Visual Neuroscience*, vol. 14, no. 3, pp. 533–544, 1997.
- [10] J. S. Duker, P. K. Kaiser, S. Binder et al., "The International Vitreomacular Traction Study Group classification of vitreomacular adhesion, traction, and macular hole," *Ophthalmology*, vol. 120, no. 12, pp. 2611–2619, 2013.
- [11] D. C. Hood, M. Bach, M. Brigell et al., "ISCEV standard for clinical multifocal electroretinography (mfERG) (2011 edition)," *Documenta Ophthalmologica*, vol. 124, no. 1, pp. 1–13, 2012.
- [12] J. W. Chan, "Electrophysiology of vision: clinical testing and applications," *Journal of Neuro-Ophthalmology*, vol. 26, no. 4, p. 301, 2006.
- [13] H. S. Yoo, H. L. Brooks Jr., A. Capone Jr., N. L. L'Hernault, and H. E. Grossniklaus, "Ultrastructural features of tissue removed during idiopathic macular hole surgery," *American Journal of Ophthalmology*, vol. 122, no. 1, pp. 67–75, 1996.
- [14] C. Eckardt, U. Eckardt, S. Groos, L. Luciano, and E. Reale, "Entfernung der membrana limitans interna bei makulalöchern," *Der Ophthalmologe*, vol. 94, no. 8, pp. 545–551, 1997.
- [15] S. L. Graham and A. Klistorner, "Electrophysiology: a review of signal origins and applications to investigating glaucoma," *Australian and New Zealand Journal of Ophthalmology*, vol. 26, no. 1, pp. 71–85, 1998.
- [16] D. C. Hood, J. G. Odel, C. S. Chen, and B. J. Winn, "The multifocal electroretinogram," *Journal of Neuro-Ophthalmology*, vol. 23, no. 3, pp. 225–235, 2003.
- [17] S. Machida, T. Nishimura, T. Ohzeki, K.-I. Murai, and D. Kurosaka, "Comparisons of focal macular electroretinograms after indocyanine green-, brilliant blue G-, or triamcinolone acetate-assisted macular hole surgery," *Graefes' Archive for Clinical and Experimental Ophthalmology*, vol. 255, no. 3, pp. 485–492, 2017.
- [18] A. Scupola, A. Mastrocola, P. Sasso et al., "Assessment of retinal function before and after idiopathic macular hole surgery," *American Journal of Ophthalmology*, vol. 156, no. 1, pp. 132.e1–139.e1, 2013.
- [19] C. Bellerive, B. Cinq-Mars, M. Louis et al., "Retinal function assessment of trypan blue versus indocyanine green assisted internal limiting membrane peeling during macular hole surgery," *Canadian Journal of Ophthalmology*, vol. 48, no. 2, pp. 104–109, 2013.
- [20] M. Ferencz, G. M. Somfai, Á. Farkas et al., "Functional assessment of the possible toxicity of indocyanine green dye in macular hole surgery," *American Journal of Ophthalmology*, vol. 142, no. 5, pp. 765.e1–770.e1, 2006.
- [21] C. I. Falkner-Radler, C. Glittenberg, S. Hagen, T. Benesch, and S. Binder, "Spectral-domain optical coherence tomography for monitoring epiretinal membrane surgery," *Ophthalmology*, vol. 117, no. 4, pp. 798–805, 2010.
- [22] R. Azad, U. Ghatak, Y. R. Sharma, and P. Chandra, "Multifocal electroretinogram in normal emmetropic subjects: correlation with optical coherence tomography," *Indian Journal of Ophthalmology*, vol. 60, no. 1, pp. 49–52, 2012.
- [23] C. Hvarfner, S. Andreasson, and J. Larsson, "Multifocal electroretinography and fluorescein angiography in retinal vein occlusion," *Retina*, vol. 26, no. 3, pp. 292–296, 2006.
- [24] S. Andréasson and F. Ghosh, "Cone implicit time as a predictor of visual outcome in macular hole surgery," *Graefes' Archive for Clinical and Experimental Ophthalmology*, vol. 252, no. 12, pp. 1903–1909, 2014.

CHAPTER 4

Inverted Internal Limiting Membrane Flap Techniques and Outer Retinal Layer Structures

Mun Faria, Helena Proença, Nuno Ferreira, David Sousa, Eliana Neto, Carlos Marques-Neves.

Retina, 2019, doi: 10.1097/IAE.0000000000002607.

ILM peeling and Inverted Flap MH surgery is a technique to treat large MH. Peeled ILM may be inverted until hole border and placed over the hole or placed into the hole. The two techniques differed mostly in how the peeled ILM flap is positioned over the hole and we relate that position with integrity of outer retina layers after MH closure.

Aim: To examine the influence of the position of peeled and inverted ILM in outer retinal layers of a surgically closed MH. Also, relation of integrity of each of the outer retinal layers, ELM and EZ and duration of symptoms before surgery.

Patients and Methods

Setting and patients

62 eyes of 58 patients with large MH, with hole diameter superior to 400 μ m, underwent surgery at the Department of Ophthalmology of Hospital de Santa Maria, Lisbon, Portugal. Only closed MH were included, with a minimum follow-up of 12 months. Twenty-four eyes had ILM inserted in macular hole (10 intentionally inserted and 14 due to misdirection of the ILM flap with fluid-air exchange) and thirty eight eyes had ILM covering MH. The two groups were compared with BCVA and OCT before and after surgery.

Optical coherence tomography

Retinal images were acquired using Spectralis SD-OCT (Heidelberg Engineering, Heidelberg®, Germany). The status of the foveal EZ and ELM were examined for each eye after successful surgery, to test their integrity, intact or disrupted.

Mun Faria contributed to Research Design, Data Interpretation, Manuscript Preparation Conceptualization and Investigation. David Sousa was involved in Methodology, Review, and Editing. Helena Proença contributed in Review and Editing. Eliana Neto was responsible for Investigation. Nuno Ferreira was involved in Validation, Review, and Editing. Carlos Marques Neves contributed with Editing and Review. All authors read and approved the final manuscript.

The results of this study allowed the following peer reviewed publication:

Paper 4 - Paper Inverted Internal Limiting Membrane Flap Techniques and Outer Retinal Layer Structures. Faria MY, Proença H, Ferreira NG, Sousa DC, Neto E, Marques-Neves C. Retina. 2019 Jun 21. doi: 10.1097/IAE.0000000000002607. [Epub ahead of print]
PMID: 31259810

INVERTED INTERNAL LIMITING MEMBRANE FLAP TECHNIQUES AND OUTER RETINAL LAYER STRUCTURES

MUN YUEH FARIA, MD,*† HELENA PROENÇA, MD,*† NUNO G. FERREIRA, MD,*†
DAVID CORDEIRO SOUSA, MD,*† ELIANA NETO, MD,*† CARLOS MARQUES-NEVES, PhD*†‡

Purpose: To examine the influence of the inverted flap (IF) internal limiting membrane (ILM) technique in macular hole (MH) closure on outer retinal layers after MH surgery.

Methods: Retrospective study. Postoperative position of ILM, recovery rate of external limiting membrane and ellipsoid zone, and best-corrected visual acuity were evaluated. The Inserted group, where the IF is placed inside the hole, was compared with the Cover group, where the IF completely covers the hole.

Results: Sixty-two eyes of 58 patients who underwent vitrectomy and ILM peeling with the IF technique for large MHs (>400 μm) with successful MH closure and a follow-up of 12 months were evaluated. In the 24 eyes of the Inserted group, there was no regeneration of external limiting membrane or ellipsoid zone after 12 months. In the 38 eyes of Cover group, external limiting membrane recovered in 55.3% of patients 1 month after surgery, and in 86.1% after 12 months. The ellipsoid zone layer was present in 58% of the patients.

Conclusion: Poorer anatomical and visual results were associated with the IF technique where ILM insertion occurs compared with ILM placed over the hole. These findings suggest that insertion of the ILM in the hole might prevent outer retinal layers realignment and visual recovery in MH surgery.

RETINA 00:1–7, 2019

Macular hole (MH) surgery has evolved from the initial studies of Wendel et al¹ and became a treatable disease with pars plana vitrectomy allowing for anatomical closure.

With the introduction of internal limiting membrane (ILM) peeling, tangential traction was reduced and a higher rate of closure was achieved, with less recurrence.² Park et al³ showed, in 58 eyes, that pars plana vitrectomy with ILM peeling was superior to vitrectomy alone in closing MHs. However, in large holes or myopic eyes, the failure rate was still high.^{4,5}

Since the introduction in 2010 of the inverted flap (IF) technique in MH surgery by Michalewska et al,⁶ the success of surgery in hole closure has increased in

large MH (>400 μm). The IF technique was also important in surgical repair of myopic MHs.⁷

The ILM flap techniques reported have differed mostly in how the ILM flap is positioned over the hole. Many of these differences are probably due to the difficulty in controlling the position of the flap during the fluid–air exchange. Therefore, the IF ILM technique is not unique nor exact showing some variations.⁸ Different techniques have been described in the literature for the ILM flap manipulation and positioning during the IF technique.⁸

Some surgeons intentionally insert the peeled ILM in the hole, after careful detachment around and up to the hole. Others choose to trim the excessive ILM using the vitrectomy probe, leaving one large ILM flap anchored on the border of the hole and inverted over the hole, with or without the help of perfluorocarbon⁹ or viscoelastic.^{10,11} If the inverted ILM stays in place, a small closed space over the MH allows for realignment of the external limiting membrane (ELM) and ellipsoid zone (EZ).¹² However, with fluid–air exchange, this flap may not stay in place, over the hole, but rather stuck inside the hole.¹³

From the *Ophthalmology University Clinic, Faculdade de Medicina Lisboa, Universidade de Lisboa, Lisbon, Portugal; †Ophthalmology Department, Hospital Santa Maria, Centro Hospitalar Universitário Lisboa Norte, Lisbon, Portugal; and ‡Centro de Estudos da Ciência e da Visão, University of Lisbon, Lisbon, Portugal.

None of the authors has any financial/conflicting interests to disclose.

Reprint requests: Mun Y. Faria, MD, Ophthalmology Department, Hospital de Santa Maria, Avenida Professor Egas Moniz, 1649-035 Lisbon, Portugal; e-mail: munfaria1@gmail.com

1

Copyright © by Ophthalmic Communications Society, Inc. Unauthorized reproduction of this article is prohibited.

After hole closure, the central scotoma gets less noticeable, and there is visual improvement.¹⁴ However, the functional improvement depends on the integrity of the outer retinal layers. External limiting membrane recovers first, and the EZ defects recover later.¹⁵ Both have defects that may decrease with time.¹⁵

In this study, we examined the influence of the IF ILM techniques in MH closure on the outer retinal layer structures after MH surgery.

Patients and Methods

Setting and Patients

This was a retrospective study of 62 eyes of 58 patients with large MH, who underwent surgery between January 2015 and June 2017 at the Department of Ophthalmology of Hospital de Santa Maria, Lisbon, Portugal. Only closed MHs with a minimum follow-up of 12 months were included in the study. Exclusion criteria were maculopathy other than MH, previous retinal surgeries, other retinal diseases, or an axial length greater than 26.0 mm. Mean follow-up time was at least 12 months after surgery. This study was approved by the Ethics Committee of Hospital de Santa Maria. The tenets of the Declaration of Helsinki were followed. All subjects have given written informed consent to the surgical and the study procedures.

Collected Data

Preoperative data included age, sex, and a complete ophthalmic examination. Best-corrected visual acuity was measured using Snellen visual acuity charts and converted to the logarithm of the minimum angle of resolution (logMAR) for statistical analysis. Hand motion was considered as logMAR 3.0 and counting fingers as logMAR 2.0.

Data Availability

All data used to support the findings of this study are at the Ophthalmology Department, Hospital Santa Maria, Centro Hospitalar Universitário Lisboa Norte and available from the corresponding author upon request.

Surgical Procedure

A standard surgical procedure consisted of 23- or 25-gauge, three-port pars plana vitrectomy. Except in pseudophakic patients, every patient underwent combined cataract surgery, to reduce confounding results. Standard small-incision phacoemulsification and implantation of a standard foldable intraocular lens were associated with vitrectomy. In every eye, Brilliant Peel

Dual (Geuder, Heidelberg, Germany) assisted ILM peeling was performed, in an area of approximately 3 mm, engaged with end grip intraocular forceps. With this technique, a flap is created and then peeled in a rosette way all around the hole and trimmed until the border of the macula, always leaving a flap large enough to invert and cover the hole, with or without the help of perfluorocarbon liquid or viscoelastic. In 10 of these eyes, the ILM was peeled around hole, and an attached flap is intentionally placed into the hole. Surgery was followed by fluid–air exchange and 15% SF₆ (sulfur–hexafluoride) gas. All patients were instructed to maintain a face-down position for at least 5 days. All surgeries were performed by the four experienced surgeons (M.Y.F., E.N., H.P., and C.M.-N.).

Optical Coherence Tomography

All MHs were staged according to recent optical coherence tomography (OCT)-based classification¹⁶ and only full-thickness MHs with hole diameter superior to 400 μm were considered for the study. Retinal images were acquired using Spectralis spectral domain-OCT (Heidelberg Engineering, Heidelberg, Germany), using the eye-tracking feature software with posterior pole images centered on the fovea (61 acquisitions, 120 μm interval). The status of the foveal EZ and ELM were examined for each eye to test their integrity, intact, or disrupted. The intact eyes had a regular and continuous hyperreflective line corresponding to the EZ or ELM—Figure 1. The disrupted eyes were characterized by hyporeflective discontinuities in the EZ or ELM line—Figures 2 and 3. These classifications were achieved by agreement of two authors (M.Y.F. and N.G.F.).

Postoperative Follow-up

In postoperative observations, at Day 1, Month 3, and Month 6, a thorough ophthalmic examination was performed, including best-corrected visual acuity and OCT. Hole status, macula diameters, and ELM and EZ

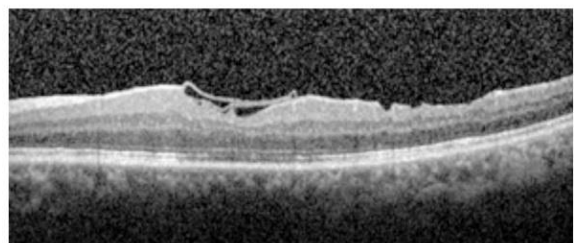


Fig. 1. Optical coherence tomography of closed MH, with ILM over the hole in Closure group.

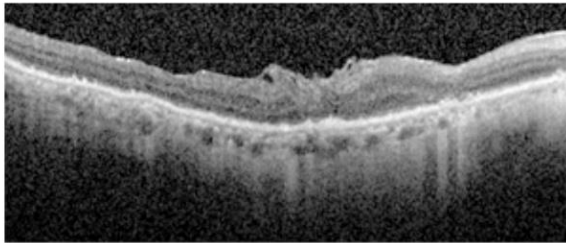


Fig. 2. Optical coherence tomography of closed MH, with ILM intentionally inserted in the hole, without integrity of ELM or EZ.

integrity at the fovea were measured by spectral OCT at 1 and 12 months after surgery.

Statistical Analysis

Results are expressed as medians (interquartile range) or n (%). Two groups were compared: Inserted group and Cover group. Within the Cover group, evolution time of the MH was also compared. Best-corrected visual acuity was compared before and after surgery. Between-group analyses were performed with the Mann-Whitney *U* test for continuous variables and the χ^2 test for discrete variables. For comparisons before and after surgery, the Wilcoxon signed-rank test was used. Statistical significance was established at $P < 0.05$.

Results

Baseline Characteristics

Sixty-two eyes were submitted to surgery and four patients had bilateral MH. Twenty-four eyes resulted in inserted ILM (10 intentionally inserted and 14 due to misdirection of the ILM flap with fluid-air exchange), and 38 eyes resulted in hole cover by the ILM. Age, sex, eye and hole dimension did not differ significantly between the Inserted and Cover groups—Table 1. There were no differences in age or hole dimension between intact or disrupted layers. Within the Inserted group, there was also no difference in age or hole dimension between intentionally inserted or inadvertently inserted ILM.

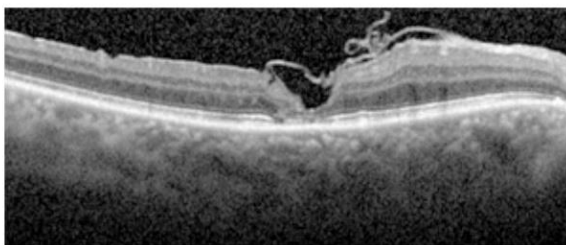


Fig. 3. Optical coherence tomography with ILM intentionally inserted in the hole but with early post operative dislocation over the hole. Integrity of ELM or EZ not achieved.

Table 1. Baseline Characteristics According to Two Groups: Inserted and Cover

	Inserted (n = 24)	Cover (n = 38)	<i>P</i>
Age, years	74 (13)	68 (11)	0.05
Female gender, n (%)	8 (38.1%)	19 (55.9%)	0.27
Right Eye, n (%)	13 (54.2%)	13 (34.2%)	0.19
Hole dimension, micron	579.0 (191.0)	597.5 (280.0)	0.44

Age and hole dimension: median (IQR). *P* values obtained from the Mann-Whitney test or the χ^2 test, as appropriate. IQR, interquartile range.

Best-Corrected Visual Acuity Before and After Surgery

All analyzed groups showed an increased postsurgery best-corrected visual acuity—Table 2. There was disappearance of central scotoma in all groups.

External Retinal Layers (External Limiting Membrane + Ellipsoid Zone) Alignment 12 Months After Surgery

When comparing the Inserted group with the Cover group considering both external retinal layers (ELM + EZ), disrupted or intact at 12 months, the Inserted group showed 100.0% disrupted layers and the Cover group 71.1% intact layers—Figure 4.

External Limiting Membrane and Ellipsoid Zone Alignment at 1 and 12 Months After Surgery

All eyes in the Inserted group showed interrupted ELM and EZ at 1 and 12 months after surgery with foveal hyperreflective lesions in the inner retina as assessed by OCT. The Cover group showed an increase in realignment of ELM from Month 1 to 12 (55% to 86%), with 0% realignment of EZ at Month 1, which increased to 57.9% at Month 12—Figure 5. Reconstruction of the ELM preceded restoration of the foveal EZ in all cover technique cases.

Evolution Time of the Macular Hole Before Surgery

In the Inserted group, both ELM and EZ were 100% interrupted at both 1 and 12 months, regardless of the evolution time of the MH before surgery. In the Cover group, realignment of ELM was superior when the evolution time was <6 months compared with >12 months at both 1-month and 12-month assessments—Figure 6A—while there were no differences regarding EZ realignment—Figure 6B.

Table 2. Best-Corrected Visual Acuity Before and After Surgery

	Pre-op Snellen	Pre-op logMAR	Post-op Snellen	Post-op logMAR	P
Cover	20/200	1.00 (1.60)	20/63	0.50 (0.40)	<0.001
Cover and intact layers	20/200	1.00 (1.30)	20/50	0.40 (0.50)	<0.001
Cover and disrupted layers	20/2000	2.00 (1.00)	20/100	0.70 (0.60)	0.005
Inserted	20/250	1.10 (1.30)	20/200	1.00 (1.60)	<0.001

Best-corrected visual acuity in Snellen and logMAR. Values expressed as median (IQR). P values obtained from the Wilcoxon signed-rank test.

IQR, interquartile range.

Complications

No complications in the form of retinal detachment or glaucoma occurred during this study.

Discussion

The technique of inverted ILM flap was described by Michalewska et al,⁶ which was shown to provide superior anatomical and functional outcomes in cases of large MHs. This involves preserving a flap of the ILM connected to the border of the MH and then inverting this to cover the MH. According to the OCT images in the original study by Michalewska et al, the inverted ILM flap covering of the MH was important for hole closure.^{6,11,17}

Even with the best surgical technique, the inverted ILM may 1) flip back during fluid–air exchange, even if it is in the proper position, which will result in surgical failure; 2) dip into the hole and become in contact with the inner lining of the hole, or 3) stay over the hole on the intended position.

The first situation can happen, even with all the care taken during surgery, slow fluid–air exchange after inverting the flap over the hole, or even using a viscoelastic cap to fold and secure the ILM into the MH before air exchange.¹⁸

The second case may be intentional to avoid flip back, or occur after surgery in postoperative face-down position, and it cannot be prevented. In fact, some surgeons

intentionally gently tuck the flap into the MH to secure the free end under the hole edge during fluid–air exchange.^{8,13} This insert or tuck in technique was also described by other authors, such as Rizzo et al,¹³ who also found, in a retrospective study on 620 eyes of 570 patients, that vitrectomy, ILM peeling, and IF technique are more effective than the standard ILM peeling technique. These authors peeled the ILM around the hole and detached it from the retina up to the edge of the hole. Excessive ILM was trimmed using the vitrectomy probe, and the ILM flap anchored on the edge of the hole was inverted and inserted into the hole. Although the hole will close if the flap is inserted into the hole, either intentionally or not, the outer retinal layers will not realign, at least during the first 12 months after surgery, as shown by our results.

The third situation, when the inverted ILM stays over the hole on the intended position, is apparently the ideal achievement because the hole will close, with better visual outcomes and outer retinal layers realignment, as shown by our results, and supported by the results obtained by Shin et al.⁹ These authors avoided packing the MH with the folded ILM, resulting in a multilayered membrane, as observed in OCT, and used perfluorocarbon to guarantee a single-layered ILM to provide a more regular structure for glial proliferation and aid in regeneration of outer retinal layers in closing the MH. Park et al¹⁹ also compared the ILM insertion technique with the IF technique and concluded that both techniques were effective in closing large MHs, although the IF was superior in recovery of photoreceptors layers and better postoperative visual acuity.

In our study, we peeled about 3 mm of the ILM around the hole, trimmed until the border with care taken to leave one piece of ILM inverted over the hole. This attached and inverted ILM was left free and maintained in position in fluid–air exchange, with or without perfluorocarbon liquid or viscoelastic to maintain the flap in position. Even with these precautions taken, 14 eyes resulted in ILM tuck into the hole, preventing the realignment of photoreceptors. The eyes with IF and one layer of ILM completely covering the hole achieved a closed space and ELM and EZ restored after 12 months.

Based on these results, it seems that ILM anchored in the hole prevents centripetal movement of photoreceptors,

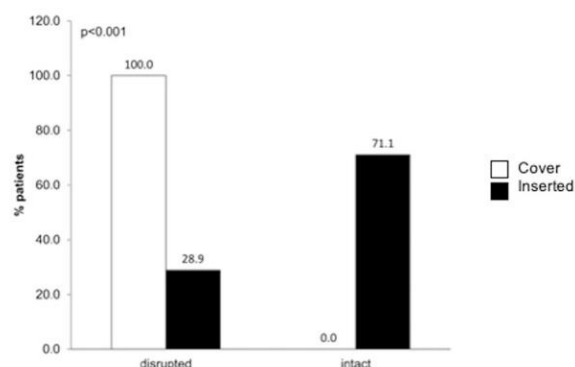
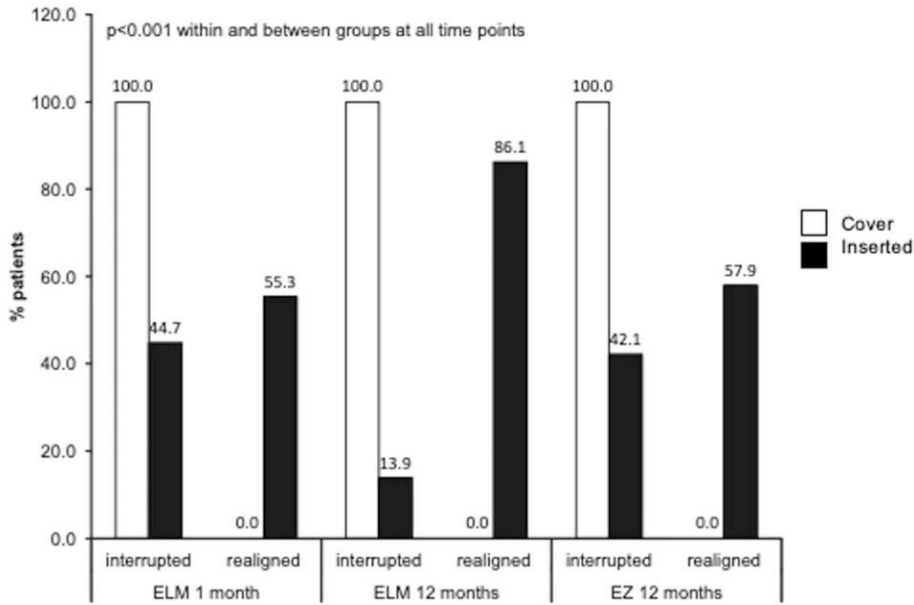


Fig. 4. External retinal layers (ELM + EZ) alignment 12 months after surgery in the Inserted and Cover groups.



therefore inhibiting realignment of MLE and EZ, either by obstruction or excessive gliosis.¹² Hu et al¹² reported that OCT after the inverted ILM flap technique revealed foveal hyperreflective lesions suggestive of excessive gliosis in the fovea. In this study, foveal hyperreflective lesions are apparent after ILM inserted in the hole, and the ELM and EZ at this site are disrupted. Should it result in scar formation, this may limit the recovery of ELM and the EZ.

In the report of Wakabayashi et al,²⁰ a hyperreflective lesion replacing all intraretinal layers at the fovea was found in all cases that showed disruption of the ELM line. By contrast, when the ELM line was restored, the reflective lesion was at the inner retina above the ELM line or was absent. In our study, we found hyperreflective material within the MH in all cases of the fill in group.

When the hole is covered with the ILM flap, there may be glial activation with Muller cell gliosis associated with bridging the gap between the edges of the retinal hole,²¹ and glial and retinal pigment epithelium cells might play an important role.²² Humoral factors such as angiogenic factors may incite realignment of photoreceptors and ELM and EZ and closing of the hole. Shioda et al²³ studies of idiopathic MH have found that the migration and gliosis of Muller cells are induced in environments where ILM acts as a scaffold surrounded by a dried environment rather than being surrounded by vitreous fluid, that may result in nonclosure of MH, even if ILM is in position. Other authors, such as Boninska et al,²⁴ refer that in cases where only a thin ILM flap was noted over the MH after the surgery, regeneration of retinal

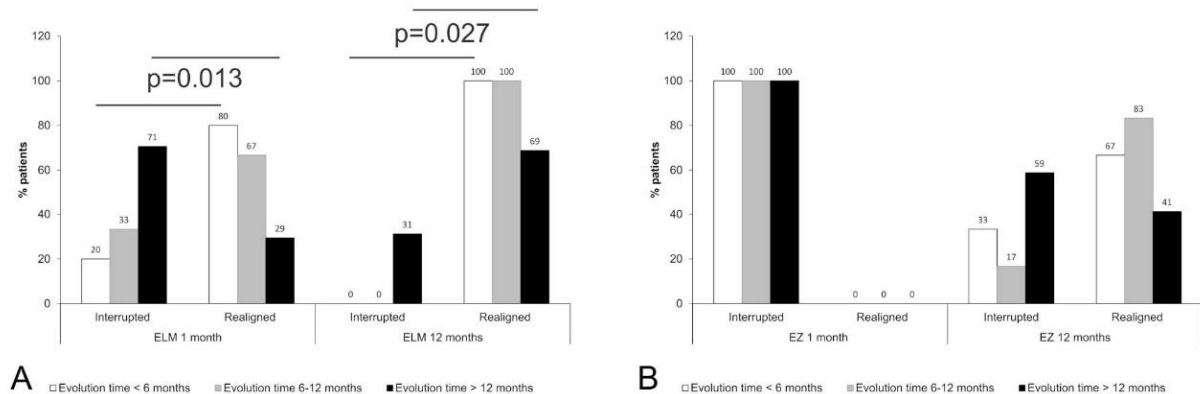


Fig. 6. Evolution time of the MH before surgery in the inserted and cover groups. **A.** External limiting membrane realignment; **(B)** EZ realignment. White: evolution time < 6 months; grey: evolution time 6–12 months; black: evolution time > 12 months.

tissue starting from the ELM was followed by restoration of the EZ layer.

Finally, the evolution time of the MH before surgery seems to have a role in the realignment of ELM in the Cover group, as shown by our results, since realignment of ELM was superior when the evolution time was <6 months compared with >12 months at both 1-month and 12-month assessment. However, evolution time of the hole does not seem to be a factor neither for the realignment of EZ in Cover group nor for the realignment of both ELM and EZ in Inserted group because in this last case, 100% of the eyes were interrupted at both 1 and 12 months.

In conclusion, our results show that the ELM and the EZ recovery rates after ILM flap with flap closure were higher than those obtained using the ILM peeled and inserted in the hole. Every effort should be made to maintain an IF on top of the retina, covering the hole, because this may facilitate the reconstruction of the outer retinal layer structures after MH surgery. Nevertheless, even in surgeries where the ILM is carefully placed over the hole, after the IF technique, ILM flap position may be difficult to control, due to fluid–air exchange, intraocular gas, and the patient maintaining the recommended face-down position. Placing viscoelastic over the ILM flap after fluid–air exchange may prevent slippage of the flap.

The evolution time of the MH seems to have a role in the realignment of ELM when there is flap closure, with no effect on outcomes in the case of fill in. Nevertheless, these results suggest that these patients should undergo surgery as soon as possible, to achieve the best possible outcomes.

This study had some limitations such as the low number of surgeries, especially the low number of surgeries with ILM inserted in the hole. Ethically, we could not continue inserting the ILM in the hole as the results were much better with ILM over the hole. Also, there were four different surgeons performing surgeries which increases the variability.

Key words: internal limiting membrane, macular hole, outer retinal layers.

References

- Wendel RT, Patel AC, Kelly NE, et al. Vitreous surgery for macular holes. *Ophthalmology* 1993;100:1671–1676.
- Yoshida M, Kishi S. Pathogenesis of macular hole recurrence and its prevention by internal limiting membrane peeling. *Retina* 2007;27:169–173.
- Park DW, Sipperley JO, Sneed SR, et al. Macular hole surgery with internal-limiting membrane peeling and intravitreal air. *Ophthalmology* 1999;106:1392–1397; discussion 1397–1398.
- Mahalingam P, Sambhav K. Surgical outcomes of inverted internal limiting membrane flap technique for large macular hole. *Indian J Ophthalmol* 2013;61:601–603.
- Wu TT, Kung YH. Comparison of anatomical and visual outcomes of macular hole surgery in patients with high myopia vs. non-high myopia: a case-control study using optical coherence tomography. *Graefes Arch Clin Exp Ophthalmol* 2012;250:327–331.
- Michalewska Z, Michalewski J, Adelman RA, Nawrocki J. Inverted internal limiting membrane flap technique for large macular holes. *Ophthalmology* 2010;117:2018–2025.
- Michalewska Z, Michalewski J, Dulczewska-Cichecka K, Nawrocki J. Inverted internal limiting membrane flap technique for surgical repair of myopic macular holes. *Retina* 2014;34:664–669.
- Casini G, Mura M, Figus M, et al. Inverted internal limiting membrane flap technique for macular hole surgery without extra manipulation of the flap. *Retina* 2017;37:2138–2144.
- Shin MK, Park KH, Park SW, et al. Perfluoro-n-octane-assisted single-layered inverted internal limiting membrane flap technique for macular hole surgery. *Retina* 2014;34:1905–1910.
- Morizane Y, Shiraga F, Kimura S, et al. Autologous transplantation of the internal limiting membrane for refractory macular holes. *Am J Ophthalmol* 2014;157:861–869 e1.
- Iwasaki M, Kinoshita T, Miyamoto H, Imaizumi H. Influence of inverted internal limiting membrane flap technique on the outer retinal layer structures after a large macular hole surgery. *Retina* 2018.
- Hu XT, Pan QT, Zheng JW, Zhang ZD. Foveal microstructure and visual outcomes of myopic macular hole surgery with or without the inverted internal limiting membrane flap technique. *Br J Ophthalmol* 2018;pii: bjophthalmol-2018-313311.
- Rizzo S, Tartaro R, Barca F, et al. Internal limiting membrane peeling versus inverted flap technique for treatment of full-thickness macular holes: a comparative study in a large series of patients. *Retina* 2018;38:S73–S78.
- Hikichi T, Ishiko S, Takamiya A, et al. Scanning laser ophthalmoscope correlations with biomicroscopic findings and foveal function after macular hole closure. *Arch Ophthalmol* 2000;118:193–197.
- Chang YC, Lin WN, Chen KJ, et al. Correlation between the dynamic postoperative visual outcome and the restoration of foveal microstructures after macular hole surgery. *Am J Ophthalmol* 2015;160:100–106 e101.
- Duker JS, Kaiser PK, Binder S, et al. The International Vitreomacular Traction Study Group classification of vitreomacular adhesion, traction, and macular hole. *Ophthalmology* 2013;120:2611–2619.
- Kuriyama S, Hayashi H, Jingami Y, et al. Efficacy of inverted internal limiting membrane flap technique for the treatment of macular hole in high myopia. *Am J Ophthalmol* 2013;156:125–e1.
- Andrew N, Chan WO, Tan M, et al. Modification of the inverted internal limiting membrane flap technique for the treatment of chronic and large macular holes. *Retina* 2016;36:834–837.
- Park JH, Lee SM, Park SW, et al. Comparative analysis of large macular hole surgery using an internal limiting membrane insertion versus inverted flap technique. *Br J Ophthalmol* 2019;103:245–250.
- Wakabayashi T, Oshima Y. Restoration of ELM reflection line crucial for visual recovery in surgically closed MH. *Retina Today* 2010:48–51.

21. Frangieh GT, Green WR, Engel HM. A histopathologic study of macular cysts and holes. *Retina* 2005;25:311–336.
22. Yamana T, Kita M, Ozaki S, et al. The process of closure of experimental retinal holes in rabbit eyes. *Graefes Arch Clin Exp Ophthalmol* 2000;238:81–87.
23. Shiode Y, Morizane Y, Matoba R, et al. The role of inverted internal limiting membrane flap in macular hole closure. *Invest Ophthalmol Vis Sci* 2017;58:4847–4855.
24. Boninska K, Nawrocki J, Michalewska Z. Mechanism of “flap closure” after the inverted internal limiting membrane flap technique. *Retina* 2018;38:2184–2189.

CHAPTER 5

Morphology of Internal Limiting Membrane Peeled on Macular Hole Surgery

Mun Faria, David Sousa, Bruna Almeida, Andreia Pinto, Nuno Ferreira

Journal of Ophthalmology, 2019, doi.org/10.1155/2019/1345683

In this chapter we tried to study the Morphology of ILM Peeled on MH Surgery, in ILM pieces collected during surgery and studied by OM and TEM.

Aim: This work aims to describe ultrastructure and behavior of ILM peeled in macular hole (MH) surgery.

Patients and Methods:

Seven patients with stage four MH were submitted to a standard surgical procedure. The surgery consisted of a 23-gauge, three-port PPV and ILM peeling. ILM is peeled in a rosette way around macula, trimmed until the border of hole, but one large flap is left, big enough to invert over the MH. Two other samples of ILM, per patient, were also collected, elsewhere in macular area, and harvested for laboratory analysis.

Laboratory Analysis

Of the two samples of ILM per patient that were harvested, one was immediately fixed and submitted to Optic Microscopy (OM) and Transmission Electron Microscopy (TEM) analysis, and another sample was incubated in enriched medium 199 (Gibco) for 20 minutes at room temperature, after which it was also fixed and submitted to OM and TEM analysis. The Electron Microscopy protocol for ILM, are:

- 1 If the samples were incubated in enriched medium upon harvest, let them rest at room temperature for 30-40min, then, remove the medium and replace it with EM fixative. [If the samples need to be immediately fixed go directly to step 2]
- 2 Fix samples for at least 1h in 2% formaldehyde and 0,2% glutaraldehyde in 0,1M phosphate buffer (0,1M PB) balanced with 8% sucrose at 4°C;
- 3 Wash 2 x 5min in 0,1M PB (8% sucrose) buffer at 4°C;
- 4 Embed fragments in 1% agarose in PBS; once the agarose is set, slice a small cube around your sample. [this step reduces sample lost along the protocol]
- 5 Wash 2 x 5min in 0,1M PB (8% sucrose) buffer at 4°C;
- 6 Post-fix in Osmium tetroxide 1% in 0,1M PB (8% sucrose) buffer, 1h with agitation on ice;
- 7 Wash 3 x 5min in distilled water, with agitation, room temperature (R.T.) (if necessary leave O.N);

8 Post-fix and counter-stain with Uranyl Acetate 1% in distilled water, 30min, protect from light, with agitation, R.T;

9 Wash 2x5min in distilled water, agitation, R.T;

10 Dehydrate 2x5min in 50% EtOH, agitation, R.T;

11 Dehydrate 2x5min in 70% EtOH, agitation, R.T;

12 Dehydrate 2x5min in 96% EtOH, agitation, R.T;

13 Dehydrate 2x10min in 100% dry EtOH, agitation, R.T;

14 Prepare the samples with 2 changes of Propylene Oxide for 15min each, with agitation, R.T.;

15 Pre-impregnate with a mixture of 1:1 propylene oxide and EPON Resin (hard) 1h at R.T with agitation

16 Impregnation with EPON resin (hard) O.N. at 4°C with agitation;

17 Inclusion in silicon moulds, 48h at 60°C.

Mun Faria contributed to Research Design, Data interpretation and Manuscript preparation. David Sousa was involved in Methodology, Review, and Editing. Bruna Almeida contributed to Resources. Andreia Pinto was responsible for Histology and ILM samples Preparations, Selections and Interpretation. Nuno Ferreira was involved in Validation, Review, and Editing. All authors read and approved the final manuscript.

The results of this study allowed the following peer reviewed publication:

Paper 5- Morphology of Internal Limiting Membrane Peeled on Macular Hole Surgery.

Journal of Ophthalmology, Volume 2019, Article ID 1345683, 6 pages

<https://doi.org/10.1155/2019/1345683>

Clinical Study

Morphology of Peeled Internal Limiting Membrane in Macular Hole Surgery

Mun Y. Faria ^{1,2}, David C. Sousa,^{1,2} Bruna C. Almeida,³ Andreia L. Pinto,³
and Nuno P. Ferreira ^{1,2}

¹Ophthalmology University Clinic, Faculdade de Medicina Lisboa, Universidade de Lisboa, 1649-028 Lisboa, Portugal

²Ophthalmology Department, Hospital Santa Maria, Centro Hospitalar Universitário Lisboa Norte, 1649-035 Lisboa, Portugal

³Histology and Comparative Pathology Laboratory, Instituto de Medicina Molecular, Lisboa, Portugal

Correspondence should be addressed to Mun Y. Faria; munfaria1@gmail.com

Received 26 December 2018; Revised 22 February 2019; Accepted 28 March 2019; Published 2 May 2019

Guest Editor: Akihiro Ohira

Copyright © 2019 Mun Y. Faria et al. This is an open access article distributed under the Creative Commons Attribution License, which permits unrestricted use, distribution, and reproduction in any medium, provided the original work is properly cited.

Purpose. The aim of this work was to describe the ultrastructure and behavior of peeled internal limiting membrane (ILM) in macular hole (MH) surgery. **Methods.** Seven patients with MH were included, and vitrectomy with ILM peeling was performed in all patients. The ILM inverted flap technique was used. Two other flaps of ILM of the same patient were collected and studied using light and transmission electron microscopy (TEM). ILM cell type, distribution, and morphology were analyzed, and the proliferation or fusion potential of the ILM interface was evaluated. **Results.** ILM vitreous sides in apposition showed signs of proliferative fibrotic activity, producing a basal membrane that merges ILM sides. **Conclusions.** Epiretinal cells in ILM show proliferative capacity, with formation of microfibrils between adjacent sides of the ILM, which may explain adherence of ILM flaps to the hole border, contributing to closure of the hole in MH surgery. This trial is registered with NCT03799575.

1. Introduction

Full thickness macular hole (MH) is an anatomic opening in the fovea, the central area of the retina, and affects mostly women after the 5th decade. As the fovea is responsible for central vision, the loss of vision caused by a MH is very severe. MH was considered untreatable until Kelly and Wendel reported closing a macular hole after pars plana vitrectomy, which removed all anteroposterior (AP) traction [1].

Besides the importance of AP vitreoretinal traction in MH formation, tangential traction seems to have a significant role in progression and recurrence of MHs [2]. Activated glial cells, especially Muller cells and astrocytes, may proliferate and migrate from the retinal side to the vitreous side and form epiretinal cells causing tangential traction [3]. Also, hyalocytes from the vitreous cavity may induce cellular proliferation at the internal limiting membrane (ILM) [4]. These hyalocytes are found on the vitreous cortex, in close contact with the ILM at the posterior retina, and may have macrophagic-like activity [2].

ILM peeling is widely accepted as a safe surgical technique, showing a high success rate in MH closure [5]. The recent inverted flap technique introduced by Michalewska and Nawrocki for large macular holes allows for an even higher closure rate [6]. Instead of removing one piece of ILM, with this technique, the ILM is peeled until the hole border and one larger piece is left free and inverted over the hole and kept secure with intraocular gas, allowing for a large macular hole to close (Figure 1). The inverted flap to cover a large macular hole may be a temporal or superior flap of partially peeled ILM [7].

Herein, we describe novel findings concerning the morphological features of peeled ILM during IMH surgery that may help to explain the mechanisms of hole closure after MH surgery.

2. Patients and Methods

2.1. Surgical Procedure. Seven patients with MH larger than 400 μm , according to OCT-based classification [8] were

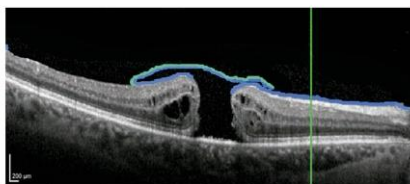


FIGURE 1: Schematic representation of the position of peeled ILM in macular hole surgery. Inverted flap with vitreous side adherent to vitreous side of ILM of the other border, not inverted.

submitted to a standard surgical procedure. The surgery was performed by the same surgeon (MF) and consisted of a 23-gauge, three-port pars plana vitrectomy and ILM peeling. Balanced salt solution (BSS; Alcon, Fort Worth, TX) was used as an irrigation solution. Posterior vitreous detachment was completed when needed and assisted with triamcinolone acetamide. A single-use macular contact lens (Grieshaber®, Alcon, TX) was used in ILM peeling. Brilliant Blue® Dual (Geuder, Germany) assisted ILM identification, which was then engaged with an end-grip intraocular forceps. ILM was peeled in a rosette way around the macula and trimmed until the border of the hole, but one large flap was left, large enough to invert over the macular hole. Two other samples of ILM, per patient, were also collected, elsewhere in the macular area, and harvested for laboratory analysis.

The tenets of the Declaration of Helsinki were followed. All patients provided written informed consent to the surgical and study procedures. Approval was obtained from the Ethics Committee of Hospital Santa Maria.

2.2. Laboratory Analysis. Of the two samples of ILM per patient that were harvested, one was immediately fixed and submitted to optic microscopy (OM) and transmission electron microscopy (TEM) analysis and the other sample was incubated in enriched medium 199 (Gibco) for 20 minutes at room temperature, after which it was also fixed and submitted to OM and TEM analysis. Analysis of all samples followed the protocol available at <https://doi.org/10.17504/protocols.io.qjiduke>.

2.3. Image Acquisition. Six electron micrographs were acquired for each fragment, using a Hitachi H-7000 electron microscope equipped with a megaview III digital camera. Fields of interest were randomly selected, and 15,000x magnification images were acquired.

2.4. Quantitative Analysis. Collagen areas were measured using the iTEM software (Olympus®) measurement tool. For each micrograph, collagen areas were manually assessed in relation to the total amount of sample present, and average values for each patient and fragment were calculated. A collagen fraction (%) for each fragment was also calculated (values in μm^2).

3. Results

3.1. Macular Hole Closure. The macular hole was closed and vision improved in all seven patients. In postoperative OCT, each macular hole was covered with ILM and bridging of external limiting membrane (Figure 2).

3.2. Histology and Immunohistochemistry. ILM samples were stained with anti-GFAP antibody (antiglial fibrillary acidic protein), and the majority of cells found were positive for anti-GFAP. GFAP is the hallmark protein in astrocytes [9], a main type of glial cells in the central nervous system (Figure 3).

3.3. Light Microscopic Features. Microscopy analysis of semithin sections of both samples showed a continuous folded and wrinkled ILM strand. The vitreous side of the ILM was smooth and continuous while the retinal side was characterized by irregular undulations (Figure 4).

3.4. Transmission Electron Microscopy. The morphological features of both the vitreous and the retinal sides of the ILM were evaluated in terms of cell distribution. The retinal side had scarce cells, while the vitreous side had some epiretinal cells.

The same structures on both sides of the ILM were identified: the fragment that was immediately fixed was wrinkled with both the vitreous and retinal sides showing no evidence of merging activity nor fibrotic material between the two sides of the juxtaposed ILM (Figure 5).

On the contrary, in the ILM sample that was kept in enriched medium for 20 minutes, the two vitreous sides of the folded piece of ILM came in contact and proliferative fibrotic material was present in the areas where adhesion occurred. In terms of morphology and structure, these fibers resemble collagen microfibrils/fibers (Figures 6 and 7).

Table 1 describes the percentage area of collagen in each observed sample, fixed immediately upon collection and after 20 min incubation with enriched medium.

4. Discussion

ILM peeling has been the standard procedure in MH surgery allowing closure rates of nearly 100% [10]. However, large macular holes, over 400 μm diameter, have an increased risk of failure, and 44% do not close at first surgery, with 19% having been reported to stay flat and open [6]. Macular hole surgery has improved the rate of closure after the introduction of the inverted flap technique, especially in long-standing and large macular holes and in holes seen in high myopia [11]. Also, in cases of refractory macular holes, the autologous transplantation of ILM allowed for an improved anatomical outcome of these macular holes [12].

In these difficult macular holes, after releasing all anteroposterior and tangential tractions, the surgical technique of sealing the macular hole with inverted ILM consists in closing the hole with ILM peeled to the hole border, inverted over, and then attached to the borders of

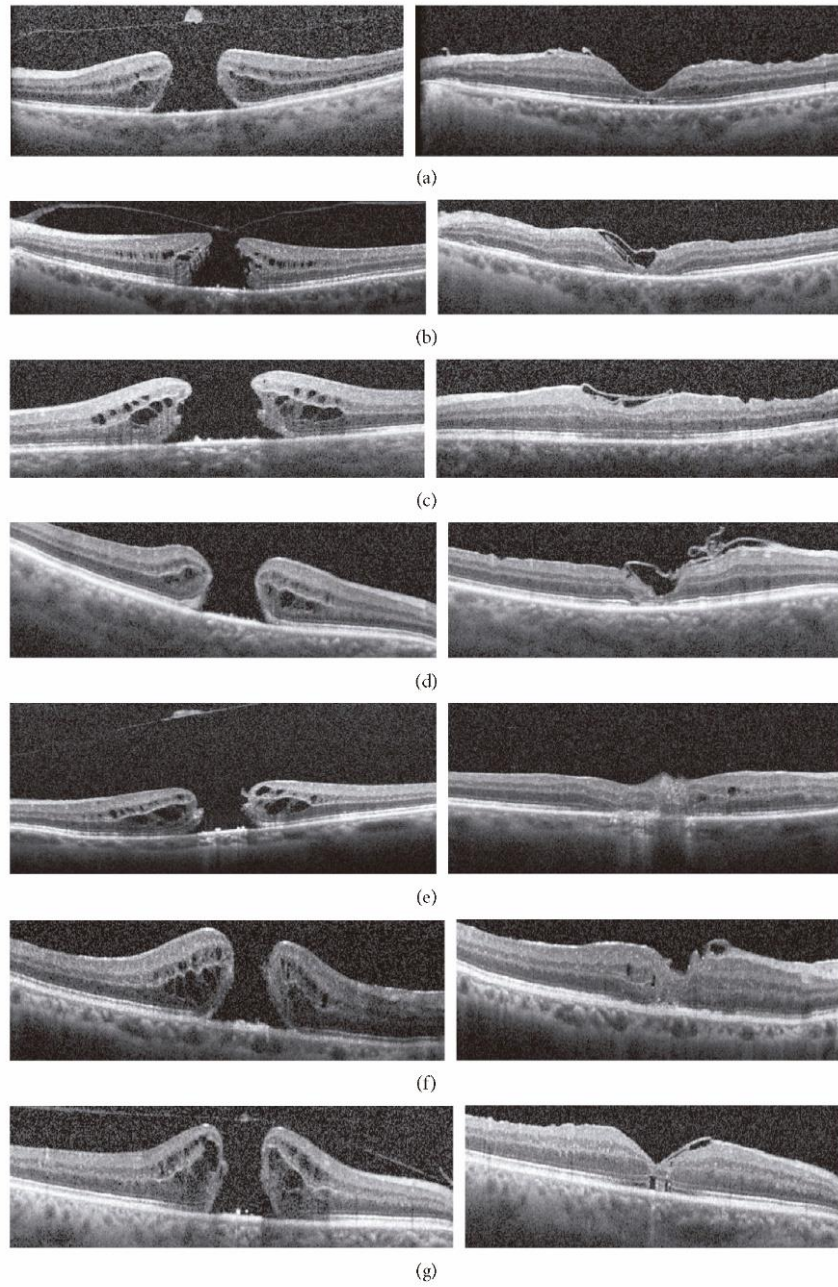


FIGURE 2: Preoperative (left) and postoperative (right) OCT of every patient. (a) Patient A. (b) Patient B. (c) Patient C. (d) Patient D. (e) Patient E. (f) Patient F. (g) Patient G.



FIGURE 3: Internal limiting membrane (blue). Glial cells protein A coupled to 15 nm gold particle (gold), marked with black arrows and magnified.

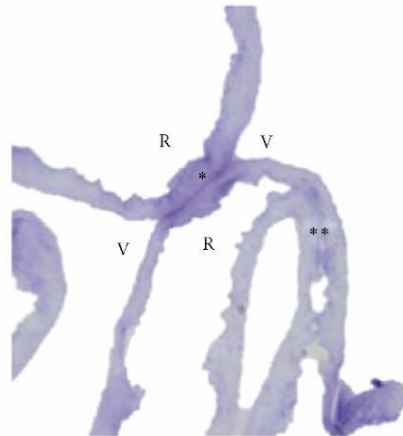


FIGURE 4: Optic light microscopy of ILM. V: vitreous side; R: retinal side. *Vitreous side contact; **retinal side contact.

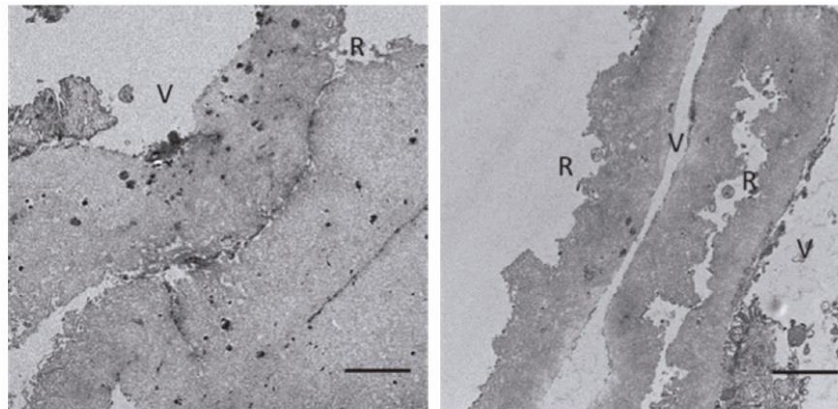


FIGURE 5: Juxtaposed sides of ILM with no apparent interaction between the vitreous side (V) and the retinal side (R). Bar: 2 μ m.

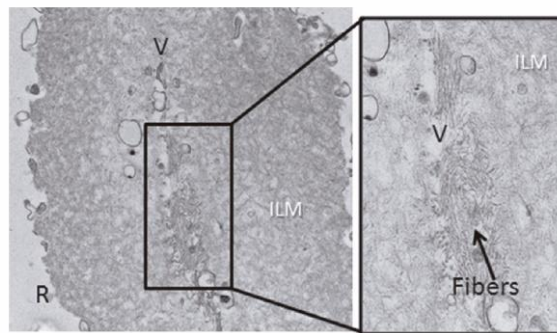


FIGURE 6: Representative electron micrographs of ILM of patient A, showing both vitreous sides (V) of the same membrane merged, and, in the center, the existence of fibers. Bar: 500 nm.

the hole, instead of completely peeling all ILMs around the hole. In case of autologous transplant, there is no more ILM near the hole to peel. A piece of ILM is peeled elsewhere in the retina of the same eye and is carefully placed on top of the hole, with the help of perfluorocarbon liquid, secured with air and gas. The peeled ILM,

transplanted or inverted, contains Muller cells fragments that can induce gliosis on the retina and on the surface of the ILM. The macular hole closes, eventually due to the merging of the ILM with structures at the hole borders, and we speculate that the creation of this closed space may activate growth factors that induce cell realignment. In an

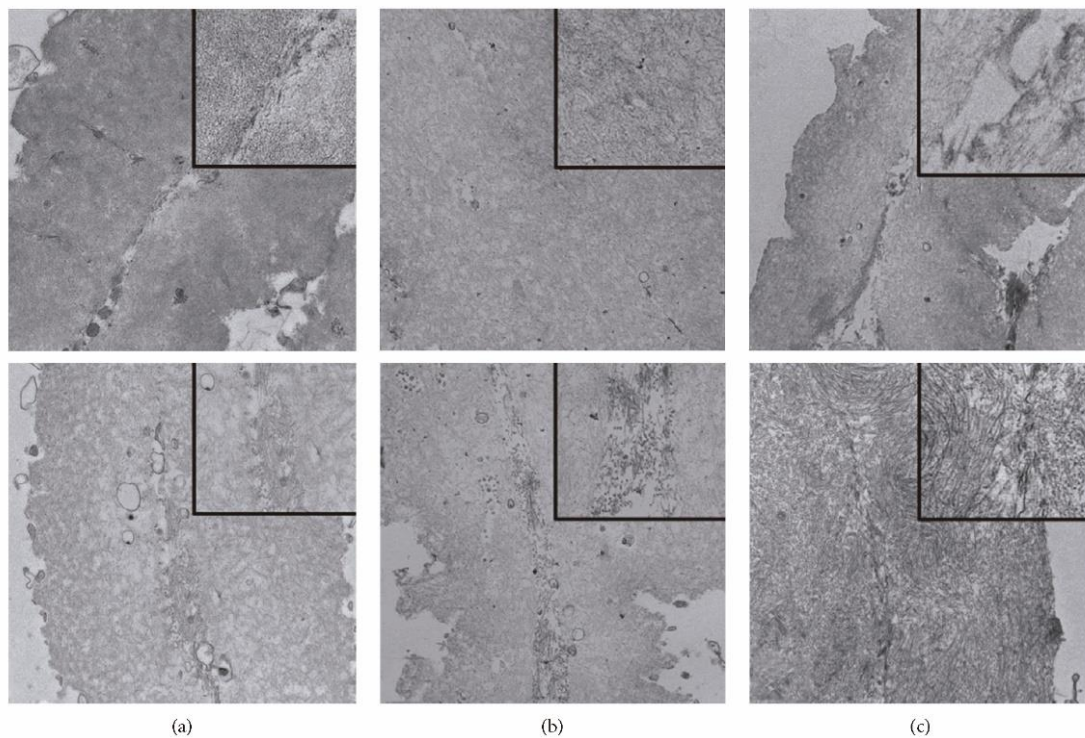


FIGURE 7: Transmission electron microscopy details of two internal limiting membrane (ILM) fragments from patients A, B, and C, with and without enriched medium. (a1–c1) Fragments of ILM from each patient which were immediately fixed. (a2–c2) A second ILM fragment of the same patient after 20-minute incubation in the enriched medium. Percentage area of collagen.

TABLE 1: Area of collagen in percentage (%) on samples fixed upon collection and after 20 min incubation with enriched medium.

	Collagen area fraction (%)	
	Fixed upon collection	Fixed after medium enrichment
Patient A	0.00	19.50
Patient B	0.00	6.68
Patient C	0.00	50.23
Patient D	5.77	17.78
Patient E	0.00	17.78
Patient F	0.00	0.00
Patient G	2.87	7.46

Values in % μm^2 .

experimental animal model, Shiode et al. tried to identify the components of the ILM that were important for the proliferation of Muller cells and collagen and fibronectin were found to enhance their migration [13]. Yokota et al. described newly synthesized collagen fibers in an ultrastructure study of peeled ILM after vitrectomy for myopic traction maculopathy [14]. Schumann et al. reported newly formed collagen at the vitreous side of the ILM removed from failed macular hole surgery [15]. In our study, we found a merging tendency of ILM pieces when kept in enriched media, in six of seven patients, accompanied by collagen fibers and fibrosis, as observed by TEM analysis. Considering our results and the results reported by

Schumann et al. associated with the novel inverted flap, we speculate that this fibrosis may actually happen in the ILM vitreous side of our patients' eyes, allowing for hole closure, either because the vitreous side of the ILM has epiretinal cells or because of the presence of collagen fibers from the vitreous cavity.

In a clinical situation, surgery with vitrectomy and ILM peeling relieves anteroposterior and tangential mechanical forces. Gas tamponade creates prolonged contact of ILM tissue fragment with each other or with the underlying retinal tissue, which seems to be fundamental for hole closure. In our study, we found that when the two vitreous sides of ILM were in contact, epiretinal cells present in the ILM vitreous side form microfibrils that may contribute to the sealing process of MH surgery.

The limitations of this study include the small number of studied cases, with the possible consequence of randomness in the obtained findings. The identification of specific immunohistochemical markers for better cell characterization will also be a future added value. Also, the type of collagen, old and newly synthesized, has not been characterized.

Data Availability

All data used to support the findings of this study are available from the corresponding author upon request.

Conflicts of Interest

The authors declare that they have no conflicts of interest.

Authors' Contributions

Mun Faria contributed to conceptualization and investigation. David Sousa was involved in methodology, review, and editing. Bruna Almeida contributed resources. Andreia Pinto was responsible for investigation. Nuno Ferreira was involved in validation, review, and editing.

References

- [1] R. T. Wendel, A. C. Patel, N. E. Kelly, T. C. Salzano, J. W. Wells, and G. D. Novack, "Vitreous surgery for macular holes," *Ophthalmology*, vol. 100, no. 11, pp. 1671-1676, 1993.
- [2] J. Sebag, "Anomalous posterior vitreous detachment: a unifying concept in vitreo-retinal disease," *Graefe's Archive for Clinical and Experimental Ophthalmology*, vol. 242, no. 8, pp. 690-698, 2004.
- [3] R. G. Schumann, K. H. Eibl, F. Zhao et al., "Immunocytochemical and ultrastructural evidence of glial cells and hyalocytes in internal limiting membrane specimens of idiopathic macular holes," *Investigative Ophthalmology & Visual Science*, vol. 52, no. 11, pp. 7822-7834, 2011.
- [4] E. A. Balazs, L. Z. J. Toth, E. A. Eckl, and A. P. Mitchell, "Studies on the structure of the vitreous body," *Experimental Eye Research*, vol. 3, no. 1, pp. 57-71, 1964.
- [5] N. Lois, J. Burr, J. Norrie et al., "Internal limiting membrane peeling versus no peeling for idiopathic full-thickness macular hole: a pragmatic randomized controlled trial," *Investigative Ophthalmology & Visual Science*, vol. 52, no. 3, pp. 1586-1592, 2011.
- [6] Z. Michalewska, J. Michalewski, K. Dulciewska-Cichecka, R. A. Adelman, and J. Nawrocki, "Temporal inverted internal limiting membrane flap technique versus classic inverted internal limiting membrane flap technique," *Retina*, vol. 35, no. 9, pp. 1844-1850, 2015.
- [7] Y. Takai, M. Tanito, K. Sugihara, T. Kodama, and A. Ohira, "Temporal inverted internal limiting membrane flap technique for a macular hole patient unable to maintain post-operative prone positioning," *Retinal Cases & Brief Reports*, vol. 10, no. 4, pp. 323-326, 2016.
- [8] J. S. Duker, P. K. Kaiser, S. Binder et al., "The International Vitreomacular Traction Study Group classification of vitreomacular adhesion, traction, and macular hole," *Ophthalmology*, vol. 120, no. 12, pp. 2611-2619, 2013.
- [9] E. M. Hol and M. Pekny, "Glial fibrillary acidic protein (GFAP) and the astrocyte intermediate filament system in diseases of the central nervous system," *Current Opinion in Cell Biology*, vol. 32, pp. 121-130, 2015.
- [10] K. Spiteri Cornish, N. Lois, N. W. Scott et al., "Vitreotomy with internal limiting membrane peeling versus no peeling for idiopathic full-thickness macular hole," *Ophthalmology*, vol. 121, no. 3, pp. 649-655, 2014.
- [11] S. Kuriyama, H. Hayashi, Y. Jingami, N. Kuramoto, J. Akita, and M. Matsumoto, "Efficacy of inverted internal limiting membrane flap technique for the treatment of macular hole in high myopia," *American Journal of Ophthalmology*, vol. 156, no. 1, pp. 125-131, 2013.
- [12] Y. Morizane, F. Shiraga, S. Kimura et al., "Autologous transplantation of the internal limiting membrane for refractory macular holes," *American Journal of Ophthalmology*, vol. 157, no. 4, pp. 861-869, 2014.
- [13] Y. Shiode, Y. Morizane, R. Matoba et al., "The role of inverted internal limiting membrane flap in macular hole closure," *Investigative Ophthalmology & Visual Science*, vol. 58, no. 11, pp. 4847-4855, 2017.
- [14] R. Yokota, A. Hirakata, N. Hayashi et al., "Ultrastructural analyses of internal limiting membrane excised from highly myopic eyes with myopic traction maculopathy," *Japanese Journal of Ophthalmology*, vol. 62, no. 1, pp. 84-91, 2018.
- [15] R. G. Schumann, M. Rohleder, M. M. Schaumberger, C. Haritoglou, A. Kampik, and A. Gandorfer, "Idiopathic macular holes," *Retina*, vol. 28, no. 2, pp. 340-349, 2008.

CHAPTER 6

Global Discussion and Concluding Remarks

1. Global Discussion

Since the introduction of PPV for closure of FTMH by Kelly and Wendel in 1991, there have been several refinements in this surgical technique, aimed at improving anatomical and functional outcomes after surgery (3)(13). One of these was the use ILM peeling, first described by Eckardt (14), and has been reported to significantly improve the rate of anatomical closure (18). ILM peeling releases the tangential traction of the residual prefoveal vitreous after PVD and removes the traction of the epiretinal cellular constituents adjacent to the MH. These two factors should alter the mobility of the MH edge (40) and allow better closure. Also, ILM peeling is a major trauma that tears the footplates of Muller cells. This incites the contraction of glial cells that proliferate following the MH surgery with ILM peeling. The balance between glial cell proliferation and centripetal displacements of the photoreceptors determines the successful restoration of foveal integrity (112)(113)(114).

In the last 10 years, ILM peeling during surgery for an MH has become a routine step and is performed by most surgeons. However, removing the ILM during surgery might have adverse consequences, due to loss of its structural role or secondary collateral nerve fiber layer loss during removal, and thus may be detrimental to the retina (8).

In paper 1 and 2 we concluded that at 6 months after MH surgery with ILM peeling, analysis of macular layers' thickness revealed thinning of RNFL-GCL-IPL complex, in both the nasal and temporal side of the macula. This complex consists of three layers, RNFL, made of axons of ganglion cells, GCL, containing the bodies of ganglion cells, and IPL, made of dendrites of ganglion cells. All these three layers appear decreased in this study, both nasal and temporal to fovea, and this seems to be an indicator of ganglion cell damage, as these cells are concentrated at the macula and are most sensitive to ischemic changes (115)(116).

In this work, Outer Retinal thickening was found on both nasal and temporal sides of the fovea. The outer retina consists of ELM, ellipsoid zone, and RPE. ELM is the first membrane to restore continuity after MH closure (117). Only afterwards, displacement and restoration of the outer portion of photoreceptors begins, with determination of continuity in the ellipsoid zone, which seems to explain the ORL thickening we found in this

study(84). Hasimoto et al (118) also came to same conclusion, that the thickening of ORL may be related to progressively restoration of outermost retinal layers, ELM and EZ. This ORL thickening may be one explanation for ELM realignment and photoreceptor restoration as part of MH closure and vision restoration.

Also, in our study, we found an asymmetric parafoveal retinal thickness in eyes with closed MH, with increased total nasal and decreased total temporal thickness, associated to nasal displacement of the fovea. It seems that after removal of rigid preoperative ILM, there are biomechanical retinal forces that displace the fovea, resulting in stretching and thinning of retinal parenchyma in the temporal subfield, as seen by other authors (119)(120), and thickening of the nasal macula.

In the present study, we found that increased nasal thickness was dependent on the medial part of IRL. This layer includes deeper regions of IPL, INL, OPL, and inner segments of photoreceptors. Although Modi et al (120) only refers to increased thickness of INL, in our study, both INL and OPL layers seem to be thickened after ILM peeling. INL contains mainly horizontal, bipolar, and glial cells, which seem to be the most altered and thickened, because of stretching. The OPL is the area in which photoreceptors communicate with the horizontal cells and bipolar cells, and we speculate that this is of major importance in the recovery of disrupted photoreceptors.

In other vitreomacular traction syndromes, such as epiretinal membrane (121)(122), the middle part of the inner retinal layer structure is important for visual recovery and metamorphopsia improvement and we propose that in MH surgery with ILM peeling, thickening of middle part of IRL should be important in macular closure, eventually inducing glial proliferation and anatomical restructuring of photoreceptor outer segment.

Thickening of the middle part of IRL after closure of MH may also be associated to fovea displacement. In cases of spontaneous closure of MH there is no foveal displacement (123), so we can infer that ILM peeling is the cause of macular displacement. The ILM is attached to the optic disc and after peeling there is a rebalance of tractional forces and nasal shift of the closed MH. The reason for displacement of the denuded and elastic retinal tissue after the removal of rigid preoperative ILM is yet to be established. Ishida et al (119) suggested neural contraction excited by ILM peeling. Thickening of the nasal

medial part of IRL, especially INL and OPL, may be a cause or a consequence of this nasal shift.

Temporal macula thinning was also reported by several authors. RNFL is thinner at the temporal area than at the nasal area and exposure to Brilliant Blue dye may be a factor to take into consideration. Traumatic temporal grasping could also be an explanation. Nukada et al (124) and Ohta et al (110) also reported deeper retinal structural damage more frequently in the temporal macula, resulting in marked atrophy in MH surgery.

The purpose of the third study was to characterize macular function by means of multifocal ERG, before and after MH surgery.

Each component of mf ERG, N1 and P1 amplitude and latency, were measured, before and after surgery. Also, we tried to relate each of the studied components with ILM peeling, MH closure and integrity of outer nuclear layers.

Multifocal electroretinography (mf ERG) assesses visual function providing a topographic map of local retinal electrophysiological activity in central retina (125). after MH closure. Our results revealed a reduced thickness of internal macular layers, especially GCL (126), measured at 3 mm diameter centered on the fovea, roughly the degree reached by the second ring in mf ERG.

It has generally been thought that outer retina integrity after MH surgery is associated to visual recovery (127). Although the N1 amplitude was reduced in the presence of MH, the 66% increase of its amplitude after ILM peeling, hole closure and realignment of photoreceptors, confirms that the N1 amplitude was related to and generated from the outer retina.

In this study, we showed that the visual acuity of patients improved after MH surgery. The mechanism by which visual function improves after surgery is not clearly understood. The centripetal movement of the previously displaced photoreceptors to its original site as proven by OCT images may be the simplest explanation (128). However, even with integrity in photoreceptor lines, vision improvement is limited. BCVA increased in both the intact and disrupted groups. Even though clinically the results are better in the intact group, there is a large variability, which may have prevented a higher statistical significance in this group.

Besides the low recovery of P1, there was also a delay of implicit time. After ILM peeling and closure of MH, implicit time of P1 wave in ring 1 maintained a delay compared to normative data (129). The delay may be related to surgical aggression of ILM peeling, or even ischemia in the macular area (130). Implicit time was delayed before surgery and never recovered, even after closure and visual recovery (131). Andréasson and Ghosh(132) already referred to a very slow cone function recovery even after successful anatomical healing.

Hood et al (125) have suggested that multifocal ERG value might be affected by numerous factors that cannot be detected and controlled. In our study, P1 in ring 1 increased both in the intact and disrupted groups, with no statistical differences, suggesting a loss of interaction with ORL. Thus, we suspect that ILM peeling may damage inner retinal layers and Muller cell function which, and might have some negative effect on P1 wave of multifocal ERG and visual acuity.

In the fourth paper, we tried to relate final position of peeled ILM over the MH and the integrity of outer nuclear layers. Large MH are difficult to close and the flap technique reported by Michalewska et al (20) allowed good rate of hole closure. According to OCT images by this author and other authors such as Kuriyama et al in 2013 (133) and Iwasaki et al in 2018 (134), the inverted ILM flap covering of the MH was important for hole closure. A difficulty in this technique was that the ILM flap could detach during fluid-air exchange. The intentional anchoring of ILM flap to hole border to avoid flip back, or even spontaneous relocation of ILM flap deep in MH after surgery, in post-operative face down position, results in MH closure. In fact, some surgeons intentionally gently tuck the flap into the MH to secure the free end under the hole edge during fluid-air exchange, like Casini in 2017 (135). This insert or tuck in technique was also described by other authors, such as Rizzo et al in 2018 (100), who also found, in a retrospective study on 620 eyes of 570 patients, that vitrectomy, ILM peeling and inverted flap technique are more effective than the standard ILM peeling technique. These authors peeled the ILM and anchored the ILM flap into the hole. However, in these situations, ILM flap reach the bottom of the hole, the hole closes, but the flap may become an obstacle to natural MH closure and/or functional recovery of outer retina.

If the flap is placed over the hole, even with the best surgical technique, the inverted ILM may 1) flip back during fluid-air exchange, even if initially in proper position, which may result in surgical failure; 2) dip into the hole and become in contact with the inner lining of the hole or 3) stay over the hole on the intended position.

If the inverted ILM stays over the hole on the intended position, it allows a dry closed hole provided by fluid air exchange, allowing realignment of retinal layers, as shown by our results, and supported by the results obtained by Shin et al in 2014 (136). These authors avoided packing the MH with the folded ILM, resulting in a multilayered membrane, as observed in OCT, and used perfluorocarbon to guarantee a single layered ILM to provide a more regular structure for glial proliferation and aid in regeneration of ORL in closing the MH. Park et al in 2019 (137), also compared the ILM insertion technique with the inverted flap technique and concluded that both techniques were effective in closing large MH, although the inverted flap was superior in recovery of photoreceptors layers and better postoperative visual acuity.

In our study, we peeled about 3mm of the ILM around the hole, trimmed until the border with care taken to leave one piece of ILM inverted over the hole. One of the surgeons intentionally placed the ILM flap into the hole. All others tried to place the inverted ILM free, and maintained an inverted position in MH surgery. Even with all the precautions, 14 eyes of this over the hole technique, resulted in ILM tuck into the hole, preventing the realignment of photoreceptors in a closed MH. The eyes with inverted flap and one layer of ILM completely covering the hole achieved a closed space and ELM and EZ restored after 12 months. Based on these results, it seems that ILM anchored in the hole allows hole closure but prevents centripetal movement of photoreceptors, therefore inhibiting realignment of MLE and EZ, either by obstruction or excessive gliosis. Hu et al in 2018 (138) reported that OCT after the inverted ILM flap technique revealed foveal hyper-reflective lesions suggestive of excessive gliosis in the fovea. In our study, foveal hyper-reflective lesions were also apparent after ILM inserted in the hole, and the ELM and EZ at this site were disrupted. Should it result in scar formation, this may limit the recovery of ELM and the ellipsoid zone.

When the hole is covered with the ILM flap, there may be glial activation with Muller cell gliosis associated to bridging the gap between the edges of the retinal hole, confirmed

with studies by Frangieh in 2005 (139) and Yamana in 2000 (140). Shiode et al in 2017 (141), in the studies of idiopathic MH, have found that the migration and gliosis of Muller cells are induced in environments where ILM acts as a scaffold surrounded by a dried environment rather than being surrounded by vitreous fluid, that may result in non-closure of MH, even if ILM is in position. Other authors, such as Boninska et al in 2018 (142), refer that in cases where only a thin ILM-flap was noted over the MH after surgery, regeneration of retinal tissue starting from the external limiting membrane was followed by restoration of the EZ layer.

In conclusion, our results show that the ELM and the EZ recovery rates after ILM flap with ILM covering MH were higher than those obtained using the ILM peeled and inserted in the hole. Also, in this paper, we found that the duration of symptoms of MH seems to have a role in the realignment of ELM in the Cover group, with no effect on outcomes in the case of inserted cases, as shown by our results. These results are consistent with Preferred Practice Pattern (PPP) of Idiopathic MH by American Academy of Ophthalmology, (edition 2017) in which patients with duration of symptoms fewer than 6 months may achieve better closure rates. Also, these results are consistent with a recent systematic review and large meta-analysis of 5480 eyes, by Rahimy and McCannell who concluded that ILM peeling at the time of surgery significantly reduces the likelihood of the hole reopening (143) and a recent Idiopathic MH Preferred Practice Pattern (144) published in September 2019, in which approximately 90% of recent MH that are <400 μm diameter can be closed with vitrectomy surgery.

Besides studying anatomical and functional changes, in the fifth paper, we also analyzed peeled ILM in seven patients, using light and transmission electron microscopy.

During surgery, after ILM peeling around the hole and trimming of excess tissue, a piece of ILM big enough to cover the hole is placed inverted over the hole. Two other samples of ILM, per patient, were also collected, elsewhere in macular area, and harvested for laboratory analysis.

Some ILM samples were stained with anti-Glial Fibrillary Acidic Protein (anti-GFAP) antibody and the majority of cells found were positive for this protein. GFAP is the hallmark protein in astrocytes (145), a main type of glial cells in the central nervous

system. We also analyzed the area of collagen in percentage (values in % μm^2) on ILM samples fixed upon collection or after culture for 20 min in enriched medium. This culture period led to a significant increase in collagen in ILM.

ILM peeling and flap is widely accepted as a safe surgical technique with high success rates, in large MH closure. Also, in cases of refractory MH, the autologous transplantation of ILM allowed for an improved anatomical outcome of these MH (146). The peeled ILM, transplanted or inverted, contains Muller cell fragments that can induce gliosis on the retina and on the surface of ILM. The MH closes, eventually because ILM merges with structures at the hole borders, and we speculate that the creation of this closed space may activate growth factors that induce cell realignment. In our study we found a merging tendency of ILM pieces when kept in enriched media, in six of seven patients, accompanied by collagen fibers and fibrosis, as observed by TEM analysis. Yokota et al (147) described newly synthesized collagen fibers in an ultrastructure study of peeled ILM after vitrectomy for myopic traction maculopathy. Schumann also found newly formed collagen at vitreal side of the removed ILM from failure MH surgery in 2008 (36). We suggest that this fibrosis may actually happen in the ILM vitreous side of our ILM sample, with the flap technique, allowing hole closure, either because the vitreous side of the ILM has epiretinal cells, or because of the presence of collagen fibers from the vitreous cavity.

In summary, we suggest in this paper that the epiretinal cells present in the ILM vitreous side may be important in the sealing process of MH surgery. Results of this study are suggestive of the fibrotic activity between the two sealed ILM sides creating a closed space which restricts the diffusion of various cell growth factors, allowing high local concentrations of these factors, which facilitates restructuring of the MH. However, this can only occur once the mechanical forces, antero-posterior and tangential, have been relieved by surgery.

2. Concluding Remarks

The purpose of the present thesis was to examine anatomical and functional effects of ILM peeling in MH surgery.

We conducted a clinical study and 12 months of follow-up to examine morphological and functional outcomes after MH surgery with ILM peeling, intraocular gas and face down position. Morphologic and functional outcomes were assessed after surgery. ILM samples obtained during surgery were analyzed.

The hypotheses which established the rationale for conducting the study were verified through the following findings:

1-Surgery for MH with ILM peeling was found to induce nasal thickening and temporal thinning of internal macular layers. Nasal thickening was mainly due to middle part of internal retinal layer. ORL increased in every side, nasal and temporal, of closed MH.

2- Surgery for MH with ILM peeling not only induced nasal and temporal, RNFL-GCL-IPL complex thinning, but also nasal displacement of the closed hole.

3- After macular closure, ORL, ELM and EZ were intact or disrupted. The improvement of mean visual acuity and electrophysiological parameters were dependent on integrity of photoreceptor layers. N1 wave increase in intact photoreceptor was superior than in disrupted photoreceptor group,

4- Final visual outcome after closure of MH was highly correlated to foveal photoreceptor layer Integrity. We found that this integrity was dependent on how ILM flap was placed over the hole. If ILM covered the hole during all post-operative time, there could be some integrity of the foveal photoreceptor layer. In cases where ILM flap were inserted in the hole, there seem to be an obstacle to realignment and discontinuity of the foveal photoreceptor layer was present in every patient.

5-The duration of symptoms of MH before surgery seems to have a role in the realignment of ELM in the Cover group, with realignment of ELM being superior when the evolution time was less than 6 months.

6- Results of light and transmission electron microscopy of ILM samples showed formation of microfibrils between adjacent sides of ILM. This finding may explain adherence of ILM flaps to the hole border, allowing better closure of the hole in this type of MH surgery. Also, ILM samples were stained with anti-GFAP antibody (anti-glia fibrillary acidic protein) and the cells found in peeled ILM were positive for this protein.

Taken together, our results showed that MH surgery with ILM peeling is associated to important anatomical and functional consequences.

In eyes with successful MH surgery there is disappearance of central scotoma and improvement of visual acuity. Morphological studies of closed MH with OCT, detected thickness effects on postoperative macular structure. The thinning of Internal layers did not seem to interfere with BCVA, and the thickening of external layers could be related to reconstruction of the foveal ELM.

Integrity and changes of the central photoreceptor layer matrix, ELM, EZ and RPE, 12 months after surgical closure may predict the likelihood of an eye regaining reading vision after 12 months, shown in electrophysiological studies. The limited recovery in mf ERG suggests an alteration of retinal physiology that could explain limited vision recovery. There is improvement in vision recovery if there is realignment of photoreceptors, integrity of ORL.

In addition, we found that pos-operative integrity of foveal photoreceptor layer, ELM and EZ was also dependent on how a peeled ILM is placed over the hole or into the hole during surgery. The more intact this structure was on OCT 12 months after, the better the visual acuity. Every effort should be made in order to maintain an inverted flap on top of the retina, covering the hole, since this may facilitate the reconstruction of the ORL structures after MH surgery. Nevertheless, even in surgeries where the ILM is carefully placed over the hole, after the inverted flap technique, fluid-air exchange, intraocular gas and facedown position, the flap position may be difficult to control and may be driven into the hole.

Also, the realignment of ELM was superior when the duration of symptoms were less than 6 months compared with over 12 months at both one month and 12 months assessment.

These results suggest that these patients should undergo surgery as soon as possible, in order to achieve the best possible outcomes.

ILM is very thin and transparent. But we managed to dye, peel, invert over the MH, and also peel two other pieces big enough for analysis. The ultrastructure studies of these ILM pieces in Electron Microscopy allowed us to identify cells and also, in certain conditions, collagen microfibrils in adjacent vitreal faces in contact.

Few studies have provided evidence of collagen microfibrils between ILM vitreal faces in contact. In this thesis, electron microscopic analysis provided significant images of collagen that could contribute to understand the fusion potential between two ILM faces in contact and closure of MH.

Further studies are needed on the effects of ILM peeling in eyes particularly susceptible to mechanical and metabolic damage. Eyes suffering from glaucoma, diabetes, macular degeneration, high myopia, and so on, might be more susceptible to trauma from ILM peeling. These eyes could suffer additional injury from macular surgery that could impair the planned visual recovery. Also, there are still disputes regarding the safety of vital dyes used to allow visualization of ILM and further studies are necessary to validate their use in MH surgery.

Therefore, a more accurate analysis using retinal imaging methods and functional tests might help us to understand and distinguish in which cases ILM peeling can be useful and in which cases it can be dangerous. It would be desirable to develop increasingly precise and minimally traumatic techniques to permit removal of the ILM with the least impact possible on Muller cells. Surgeons should be aware that it is necessary to limit ILM peeling in eyes with concurrent diseases and to learn to limit the extent of this maneuver, especially in retinal areas more prone to mechanical trauma such as the temporal side of the macula.

An interesting concept currently being studied is the possible role of intraoperative OCT in ILM dissection, which would suggest performing ILM peeling only when ILM pathological thickening is present, especially if associated with the presence of an epiretinal membrane (148). Also, timing of surgery, and position of peeled ILM during surgery affects photoreceptor integrity and, ultimately, BCVA, and should be carefully considered prior to surgery.

Lastly, research with the newly introduced OCT angiography (OCTA) (149)(150), a relatively new, dye-less, depth-resolved technique that allows the visualization of retinal microvasculature by detecting intravascular blood flow, could be used to noninvasively investigate retinal capillary networks and foveal avascular zone changes in patients who underwent macular surgery.

References

1. Gass JDM. Idiopathic Senile Macular Hole. *Arch Ophthalmol*. 1988 May 1;106(5):629.
2. Ali FS, Stein JD, Blachley TS, Ackley S, Stewart JM. Incidence of and Risk Factors for Developing Idiopathic Macular Hole Among a Diverse Group of Patients Throughout the United States. *JAMA Ophthalmol*. 2017;135(4):299–305.
3. Johnson RN, Gass JD. Idiopathic macular holes. Observations, stages of formation, and implications for surgical intervention. *Ophthalmology*. 1988 Jul;95(7):917–24.
4. Gaudric A, Haouchine B, Massin P, Paques M, Blain P, Erginay A. Macular hole formation: new data provided by optical coherence tomography. *Arch Ophthalmol (Chicago, Ill 1960)*. 1999 Jun;117(6):744–51.
5. Bainbridge J, Herbert E, Gregor Z. Macular holes: vitreoretinal relationships and surgical approaches. *Eye (Lond)*. 2008 Oct;22(10):1301–9.
6. Smiddy WE, Flynn HW. Pathogenesis of macular holes and therapeutic implications. *Am J Ophthalmol*. 2004 Mar;137(3):525–37.
7. Tanner V, Chauhan DS, Jackson TL, Williamson TH. Optical coherence tomography of the vitreoretinal interface in macular hole formation. *Br J Ophthalmol*. 2001 Sep 1;85(9):1092–7.
8. Christensen UC. Value of internal limiting membrane peeling in surgery for idiopathic macular hole and the correlation between function and retinal morphology. *Acta Ophthalmol*. 2009 Dec;87 Thesis:1–23.
9. Spaide RF, Wong D, Fisher Y, Goldbaum M. Correlation of vitreous attachment and foveal deformation in early macular hole. *Am J*. 2002 Feb;133(2):226–9.
10. Takano M, Kishi S. Foveal retinoschisis and retinal detachment in severely myopic eyes with posterior staphyloma. *Am J Ophthalmol*. 1999 Oct 128(4):472–6.

11. Kelly NE, Wendel RT. Vitreous Surgery for Idiopathic Macular Holes. *Arch Ophthalmol*. 1991 May 1;109(5):654.
12. Johnson RN, Gass JD. Idiopathic macular holes. Observations, stages of formation, and implications for surgical intervention. *Ophthalmology*. 1988 Jul;95(7):917–24.
13. Wendel RT, Patel AC, Kelly NE, Salzano TC, Wells JW, Novack GD, et al. Vitreous surgery for macular holes. *Ophthalmology*. 1993 Nov;100(11):1671–6.
14. Eckardt C, Eckardt U, Groos S, Luciano L, Reale E. Removal of the internal limiting membrane in macular holes. Clinical and morphological findings. *Ophthalmologie*. 1997 Aug 94(8):545–51.
15. Lois N, Burr J, Norrie J, Vale L, Cook J, McDonald A, et al. Clinical and cost-effectiveness of internal limiting membrane peeling for patients with idiopathic full thickness macular hole. Protocol for a Randomised Controlled Trial: FILMS (Full-thickness macular hole and Internal Limiting Membrane peeling Study). *Trials*. 2008 Dec 3;9(1):61.
16. Ternent L, Vale L, Boachie C, Burr JM, Lois N, Full-Thickness Macular Hole and Internal Limiting Membrane Peeling Study (FILMS) Group. Cost-effectiveness of internal limiting membrane peeling versus no peeling for patients with an idiopathic full-thickness macular hole: results from a randomised controlled trial. *Br J Ophthalmol*. 2012 Mar;96(3):438–43.
17. Jackson TL, Donachie PHJ, Sparrow JM, Johnston RL. United Kingdom National Ophthalmology Database Study of Vitreoretinal Surgery: Report 2, Macular Hole. *Ophthalmology*. 2013 Mar 120(3):629–34.
18. Spiteri Cornish K, Lois N, Scott NW, Burr J, Cook J, Boachie C, et al. Vitrectomy with internal limiting membrane peeling versus no peeling for idiopathic full-thickness macular hole. *Ophthalmology*. 2014 Mar 121(3):649–55
19. Kwok a KH, Lai TYY, Yip WWK. Vitrectomy and gas tamponade without internal limiting membrane peeling for myopic foveoschisis. *Br J Ophthalmol*. 2005;89(9):1180–3.

20. Michalewska Z, Michalewski J, Adelman RA, Nawrocki J. Inverted Internal Limiting Membrane Flap Technique for Large Macular Holes. *Ophthalmology*. 2010 Oct;117(10):2018–25.
21. Kadonosono K, Itoh N, Uchio E, Nakamura S, Ohno S. Staining of internal limiting membrane in macular hole surgery. *Arch Ophthalmol (Chicago, Ill 1960)*.2000 Aug;118(8):1116–8.
22. Lois N, Burr J, Norrie J, Vale L, Cook J, McDonald A, et al. Internal limiting membrane peeling versus no peeling for idiopathic full-thickness macular hole: a pragmatic randomized controlled trial. *Invest Ophthalmol Vis Sci*. 2011 Mar;52(3):1586–92.
23. Tadayoni R, Svorenova I, Erginay A, Gaudric A, Massin P. Decreased retinal sensitivity after internal limiting membrane peeling for macular hole surgery. *Br J Ophthalmol*. 2012 Dec;96(12):1513–6.
24. Rubinstein A, Bates R, Benjamin L, Shaikh A. Iatrogenic eccentric full thickness macular holes following vitrectomy with ILM peeling for idiopathic macular holes. *Eye (Lond)*.2005 Dec 12;19(12):1333–5.
25. Mason JO, Feist RM, Albert MA. Eccentric macular holes after vitrectomy with peeling of epimacular proliferation. *Retina*. 2007 Jan;27(1):45–8.
26. Clark A, Balducci N, Pichi F, Veronese C, Morara M, Torrazza C, et al. Swelling of the arcuate nerve fiber layer after internal limiting membrane peeling. *Retina*. 2012 Sep;32(8):1608–13.
27. Tadayoni R, Paques M, Massin P, Mouki-Benani S, Mikol J, Gaudric A. Dissociated optic nerve fiber layer appearance of the fundus after idiopathic epiretinal membrane removal. *Ophthalmology*. 2001 Dec;108(12):2279–83.
28. Ito Y, Terasaki H, Takahashi A, Yamakoshi T, Kondo M, Nakamura M. Dissociated optic nerve fiber layer appearance after internal limiting membrane peeling for idiopathic macular holes. *Ophthalmology*. 2005 Aug 1;112(8):1415–20.
29. Terasaki H, Miyake Y, Nomura R, Piao CH, Hori K, Niwa T, et al. Focal macular ERGs in eyes after removal of macular ILM during macular hole surgery. *Invest Ophthalmol Vis Sci*. 2001 Jan;42(1):229–34.

30. Kumagai K, Hangai M, Ogino N. Progressive Thinning of Regional Macular Thickness After Epiretinal Membrane Surgery. *Invest Ophthalmol Vis Sci*. 2015 Nov 1;56(12):7236–42.
31. Keenan TDL, Clark SJ, Unwin RD, Ridge LA, Day AJ, Bishop PN. Mapping the differential distribution of proteoglycan core proteins in the adult human retina, choroid, and sclera. *Invest Ophthalmol Vis Sci*. 2012 Nov 7;53(12):7528–38.
32. Candiello J, Balasubramani M, Schreiber EM, Cole GJ, Mayer U, Halfter W, et al. Biomechanical properties of native basement membranes. *FEBS J*. 2007 Jun;274(11):2897–908.
33. Henrich P, Monnier C, Halfer W, Haritoglou C, Strauss R, Lim R, Loparic M. Nanoscale topographic and biomechanical studies of the human internal limiting membrane. - *Invest Ophthalmol Vis Sci*, 53 (6), 2561-70, 2012 Jun
34. Wollensak G, Spoerl E, Grosse G, Wirbelauer C. Biomechanical significance of the human internal limiting lamina. *Retina*. 2006 Oct;26(8):965–8.
35. Ohta K, Sato A, Fukui E. Asymmetrical thickness of parafoveal retina around surgically closed macular hole. *Br J Ophthalmol*. 2010 Nov 1;94(11):1545–6.
36. Schumann RG, Rohleder M, Schaumberger MM, Haritoglou C, Kampik A, Gandorfer A. Idiopathic macular holes: Ultrastructural aspects of surgical failure. *Retina*. 2008 Feb;28(2):340–9.
37. Toft-Kehler AK, Skytt DM, Kolko M. A Perspective on the Müller Cell-Neuron Metabolic Partnership in the Inner Retina. *Mol Neurobiol*. 2018 Jun 19;55(6):5353–61.
38. Reichenbach A, Bringmann A. New functions of Müller cells. *Glia*. 2013 May;61(5):651–78.
39. Yamada E. Some structural features of the fovea centralis in the human retina. *Arch Ophthalmol (Chicago, Ill 1960)*. 1969 Aug;82(2):151–9.
40. Gass JDM. Müller Cell Cone, an Overlooked Part of the Anatomy of the Fovea Centralis. *Arch Ophthalmol*. 1999 Jun 1 117(6):821.

41. Hee MR, Puliafito CA, Wong C, Duker JS, Reichel E, Schuman JS, et al. Optical coherence tomography of macular holes. *Ophthalmology*. 1995 May;102(5):748–56.
42. Kishi S, Kamei Y, Shimizu K. Tractional elevation of Henle’s fiber layer in idiopathic macular holes. *Am J Ophthalmol*. 1995 Oct;120(4):486–96.
43. Puliafito CA, Hee MR, Lin CP, Reichel E, Schuman JS, Duker JS, et al. Imaging of macular diseases with optical coherence tomography. *Ophthalmology*. 1995 Feb 102(2):217–29
44. Oh J, Smiddy WE, Flynn HW, Gregori G, Lujan B. Photoreceptor inner/outer segment defect imaging by spectral domain OCT and visual prognosis after macular hole surgery. *Invest Ophthalmol Vis Sci*. 2010 Mar 1;51(3):1651–8.
45. Spaide RF, Koizumi H, Pozonni MC, Pozonni MC. Enhanced Depth Imaging Spectral-Domain Optical Coherence Tomography. *Am J Ophthalmol*. 2008 Oct;146(4):496–500.
46. Davis RP, Smiddy WE, Flynn HW, Puliafito CA. Surgical Management of Vitreofoveal Traction Syndrome: Optical Coherence Tomographic Evaluation and Clinical Outcomes. *Ophthalmic Surgery, Lasers, and Imaging* 2010 Mar 1;41(2):150–6.
47. Yamashita T, Yamashita T, Kawano H, Sonoda Y, Yamakiri K, Sakamoto T. Early imaging of macular hole closure: A diagnostic technique and its quality for gas-filled eyes with spectral domain optical coherence tomography. *Ophthalmologica*. 2012 Dec;229(1):43–9.
48. Hirano M, Morizane Y, Kimura S, Hosokawa M, Shiode Y, Doi S, et al. Assessment of Lamellar Macular Hole and Macular Pseudohole With a Combination of En Face and Radial B-scan Optical Coherence Tomography Imaging. *Am J Ophthalmol*. 2018 Apr 1;188:29–40.
49. Borrelli E, Palmieri M, Aharrh-Gnama A, Ciciarelli V, Mastropasqua R, Carpineto P. Intraoperative optical coherence tomography in the full-thickness macular hole surgery with internal limiting membrane inverted flap placement. *Int Ophthalmol*. 2019 Apr 15;39(4):929–34.

50. Wykoff CC, Berrocal AM, Scheffler AC, Uhlhorn SR, Ruggeri M, Hess D. Intraoperative OCT of a full-thickness macular hole before and after internal limiting membrane peeling. *Ophthalmic Surg Lasers Imaging*. 2010 Jan;41(1):7–11.
51. Taku Wakabayashi; Yusuke Oshima. Retina Today - Restoration of ELM Reflection Line Crucial for Visual Recovery in Surgically Closed MH. *Retina Today*. 2010, Sept, p. 48–51.
52. Bottoni F, De Angelis S, Luccarelli S, Cigada M, Staurenghi G, A G, et al. The Dynamic Healing Process of Idiopathic Macular Holes after Surgical Repair: A Spectral-Domain Optical Coherence Tomography Study. *Investig Ophthalmology Vis Sci*. 2011 Jun 22;52(7):4439.
53. Ezra E. Idiopathic full thickness macular hole: natural history and pathogenesis. *Br J Ophthalmol*. 2001 Jan;85(1):102–8.
54. la Cour M, Friis J. Macular holes: Classification, epidemiology, natural history and treatment. *Acta Ophthalmol Scand*. 2002;80(6):579–87.
55. McCannel CA, Ensminger JL, Diehl NN, Hodge DN. Population-based Incidence of Macular Holes. *Ophthalmology*. 2009 Jul;116(7):1366–9.
56. Xu L, You QS, Wang YX, Liang QF, Cui TT, Yang XH, et al. Prevalence of macular holes as cause for visual impairment. The Beijing Eye Public Healthcare Project. *Acta Ophthalmol*. 2013 Mar 1 91(2):e157–8.
57. Ezra E, Wells JA, Gray RH, Kinsella FMP, Orr GM, Grego J, et al. Incidence of idiopathic full-thickness macular holes in fellow eyes: A 5-year prospective natural history study. *Ophthalmology*. 1998 Feb 1;105(2):353–9.
58. Kumagai K, Ogino N, Hangai M, Larson E. Percentage of fellow eyes that develop full-thickness macular hole in patients with unilateral macular hole. *Arch Ophthalmol (Chicago, Ill 1960)*. 2012 Mar 1;130(3):393–4.
59. Evans JR, Schwartz SD, McHugh JDA, Thamby-Rajah Y, Hodgson SA, Wormald RPL, et al. Systemic risk factors for idiopathic macular holes: A case-control study. *Eye*. 1998 Mar;12(2):256–9.

60. Darian-Smith E, Howie AR, Allen PL, Vote BJ. Tasmanian macular hole study: whole population-based incidence of full thickness macular hole. *Clin Exp Ophthalmol*. 2016 Dec 1;44(9):812–6.
61. Smith RL, Sivaprasad S, Chong V. Retinal biochemistry, physiology and cell biology. *Dev Ophthalmol*. 2015;55:18–27.
62. Sebag J. Structure, function, and age-related changes of the human vitreous. *Bull Soc Belge Ophthalmol*. 1987 223 Pt 1:37–57.
63. Sebag J. Anomalous posterior vitreous detachment: a unifying concept in vitreo-retinal disease. *Graefes Arch Clin Exp Ophthalmol*. 2004 Aug 10;42(8):690–8.
64. Jackson TL, Nicod E, Simpson A, Angelis A, Grimaccia F, Kanavos P. Symptomatic vitreomacular adhesion. *Retina*. 2013 Sep;33(8):1503–11.
65. Johnson MW. Posterior Vitreous Detachment: Evolution and Complications of Its Early Stages. *Am J Ophthalmol* 2010 Mar 1 149(3):371-382.e1.
66. Sebag J. Anatomy and pathology of the vitreo-retinal interface. *Eye (Lond)*. 1992 Nov;6(6):541–52.
67. Steel DHW, Lotery AJ. Idiopathic vitreomacular traction and macular hole: a comprehensive review of pathophysiology, diagnosis, and treatment. *Eye (Lond)* 2013 Oct;27 Suppl 1:S1-21.
68. Sebag J, Gupta P, Rosen RR, Garcia P, Sadun AA. Macular holes and macular pucker: the role of vitreoschisis as imaged by optical coherence tomography/scanning laser ophthalmoscopy. *Trans Am Ophthalmol Soc*. 2007 Jan;105:121–9; discussion 129-31.
69. Byer NE. Natural history of posterior vitreous detachment with early management as the premier line of defense against retinal detachment. *Ophthalmology*. 1994 Sep;101(9):1503–13; discussion 1513-4.
70. Mori K, Kanno J, Gehlbach PL, Yoneya S. Montage images of spectral-domain optical coherence tomography in eyes with idiopathic macular holes. *Ophthalmology*. 2012 Dec;119(12):2600–8.
71. Haouchine B, Massin P, Gaudric A. Foveal pseudocyst as the first step in macular hole formation. *Ophthalmology* 2001 Jan;108(1):15–22.

72. Duker JS, Kaiser PK, Binder S, de Smet MD, Gaudric A, Reichel E, et al. The International Vitreomacular Traction Study Group Classification of Vitreomacular Adhesion, Traction, and Macular Hole. *Ophthalmology*. 2013 Dec;120(12):2611–9.
73. Le Goff MM, Bishop PN. Adult vitreous structure and postnatal changes. In: *Eye*. Nature Publishing Group; 2008. p. 1214–22.
74. Govetto A, Virgili G, Rodriguez FJ, Figueroa MS, Sarraf D, Hubschman JP. Functional and anatomical significance of the ectopic inner foveal layers in eyes with idiopathic epiretinal membranes: Surgical Results at 12 Months. *Retina*. 2019 Feb 1;39(2):347–57.
75. Hasebe H, Matsuoka N, Terashima H, Sasaki R, Ueda E, Fukuchi T. Restoration of the Ellipsoid Zone and Visual Prognosis at 1 Year after Surgical Macular Hole Closure. *J Ophthalmol*. 2016;2016.
76. Ch'ng SW, Patton N, Ahmed M, Ivanova T, Baumann C, Charles S, et al. The Manchester Large Macular Hole Study: Is it Time to Reclassify Large Macular Holes? *Am J Ophthalmol*. 2018 Nov;195:36–42.
77. Machemer R. The development of pars plana vitrectomy: a personal account. *Graefes Arch Clin Exp Ophthalmol*. 1995 Aug 233(8):453–68.
78. O'Malley C, Heintz RM. Vitrectomy with an alternative instrument system. *Ann Ophthalmol*. 1975 Apr;7(4):585–8, 591–4.
79. Wang CC, Charles S. Microsurgical instrumentation for vitrectomy: Part II. *J Clin Eng* 9(1):63–71.
80. Wendel RT, Patel AC, Kelly NE, Salzano TC, Wells JW, Novack GD. Vitreous surgery for macular holes. *Ophthalmology*. 1993 Nov;100(11):1671–6.
81. Mireskandari K, Garnham L, Sheard R, Ezra E, Gregor ZJ, Sloper JJ. A prospective study of the effect of a unilateral macular hole on sensory and motor binocular function and recovery following successful surgery. *Br J Ophthalmol*. 2004 Oct;88(10):1320.
82. Kuhn F, Morris R, Mester V, Witherspoon CD. Internal limiting membrane removal for traumatic macular holes. *Ophthalmic Surg Lasers*.;32(4):308–15.

83. Tognetto D, Grandin R, Sanguinetti G, Minutola D, Di Nicola M, Di Mascio R, et al. Internal limiting membrane removal during macular hole surgery: results of a multicenter retrospective study. *Ophthalmology*. 2006 Aug 113(8):1401–10.
84. Wakabayashi T, Fujiwara M, Sakaguchi H, Kusaka S. Foveal Microstructure and Visual Acuity in Surgically Closed Macular Holes: Spectral- Domain Optical Coherence Tomographic Analysis. *OPHTHA*. 2010;117:1815–24.
85. Villate N, Lee JE, Venkatraman A, Smiddy WE. Photoreceptor layer features in eyes with closed macular holes: optical coherence tomography findings and correlation with visual outcomes. *Am J Ophthalmol*. 2005 Feb 139(2):280–9.
86. Smiddy WE, Feuer W, Cordahi G. Internal limiting membrane peeling in macular hole surgery. *Ophthalmology*. 2001;108(8):1471–6.
87. Al-Abdulla NA, Thompson JT, Sjaarda RN. Results of Macular Hole Surgery with and without Epiretinal Dissection or Internal Limiting Membrane Removal. *Ophthalmology*. 2004;111(1):142–9.
88. Christensen UC, Kroyer K, Thomadsen J, Jorgensen TM, La Cour M, Sander B. Normative data of outer photoreceptor layer thickness obtained by software image enhancing based on Stratus optical coherence tomography images. *Br J Ophthalmol*. 2008 Jun;92(6):800–5.
89. Haritoglou C, Gass CA, Schaumberger M, Ehrt O, Gandorfer A, Kampik A, et al. Macular changes after peeling of the internal limiting membrane in macular hole surgery. *Am J Ophthalmol*. 2001 Sep 1 ;132(3):363–8.
90. Yooh HS, Brooks HL, Capone A, L'Hernault NL, Grossniklaus HE. Ultrastructural features of tissue removed during idiopathic macular hole surgery. *Am J Ophthalmol* 1996 Jul;122(1):67–75.
91. Park DW, Sipperley JO, Sneed SR, Dugel PU, Jacobsen J. Macular hole surgery with internal-limiting membrane peeling and intravitreal air. *Ophthalmology*. 1999 Jul;106(7):1392–7; discussion 1397-8.
92. Schaal KB, Bartz-Schmidt KU, Dithmar S. Current strategies for macular hole surgery in Germany, Austria and Switzerland. *Ophthalmologie*. 2006 Nov;103(11):922–6.

93. Mester V, Kuhn F. Internal limiting membrane removal in the management of full-thickness macular holes. *Am J Ophthalmol*. 2000 Jun;129(6):769–77.
94. Brooks HL. Macular hole surgery with and without internal limiting membrane peeling. *Ophthalmology* 2000 Oct 107(10):1939–48; discussion 1948-9.
95. Castro Navarro J, González-Castaño C. Macular hole surgery with and without internal limiting membrane peeling. Vol. 78, *Archivos de la Sociedad Española de Oftalmología*. 2003. p. 159–64.
96. Haritoglou C, Gass CA, Schaumberger M, Gandorfer A, Ulbig MW, Kampik A. Long-term follow-up after macular hole surgery with internal limiting membrane peeling. *Am J Ophthalmol*. 2002 Nov 1;134(5):661–6.
97. Engelbrecht NE, Freeman J, Sternberg P, Aaberg TM, Aaberg TM, Martin DF, et al. Retinal pigment epithelial changes after macular hole surgery with indocyanine green-assisted internal limiting membrane peeling. *Am J Ophthalmol*. 2002;133(1):89–94.
98. Remy M, Thaler S, Schumann RG, May CA, Fiedorowicz M, Schuettauf F, et al. An in vivo evaluation of Brilliant Blue G in animals and humans. *Br J Ophthalmol*. 2008 Aug;92(8):1142–7.
99. Andrew N, Chan WO, Tan M, Ebnetter A, Gilhotra JS. Modification of the Inverted Internal Limiting Membrane Flap Technique for the Treatment of Chronic and Large Macular Holes. *Retina* 2016 Apr;36(4):834–7.
100. Rizzo S, Tartaro R, Barca F, Caporossi T, Bacherini D, Giansanti F. Internal limiting membrane peeling versus inverted flap technique for treatment of full-thickness macular holes: a comparative study in a large series of patients. *Retina*. 2018 Sep;38 Suppl 1:S73–8.
101. Kannan NB, Kohli P, Parida H, Adenuga OO, Ramasamy K. Comparative study of inverted internal limiting membrane (ILM) flap and ILM peeling technique in large macular holes: a randomized-control trial. *BMC Ophthalmol*. 2018 Dec 20 18(1):177.

102. Wong D, Steel DHW. Free ILM patch transplantation for recalcitrant macular holes; should we save some internal limiting membrane for later? *Graefes Arch Clin Exp Ophthalmol*. 2016 Nov 10;254(11):2093–4.
103. Tornambe, Paul E.; Poliner LS. Definition of Macular Hole Surgery End Points: Elevated/Open. *RETINA*. Retina. 1998. p. Volume 18-Issue 3-ppg 286.
104. Simcock PR, Scalia S. Phacovitrectomy without prone posture for full thickness macular holes. *Br J Ophthalmol*. 2001;85(11):1316–9.
105. Hecht I, Mimouni M, Blumenthal EZ, Barak Y, Charles S. Sulfur Hexafluoride (SF₆) versus Perfluoropropane (C₃F₈) in the Intraoperative Management of Macular Holes: A Systematic Review and Meta-Analysis. Vol. 2019, *Journal of Ophthalmology*. Hindawi Limited; 2019.
106. Clark A, Balducci N, Pichi F, Veronese C, Morara M, Torrazza C, et al. Swelling of the arcuate nerve fiber layer after internal limiting membrane peeling. *Retina*. 2012 Sep;32(8):1608–13.
107. Mitamura Y, Suzuki T, Kinoshita T, Miyano N, Tashimo A, Ohtsuka K. Optical coherence tomographic findings of dissociated optic nerve fiber layer appearance. *Am J Ophthalmol*. 2004 Jun;137(6):1155–6.
108. Spaide RF. “Dissociated optic nerve fiber layer appearance” after internal limiting membrane removal is inner retinal dimpling. *Retina*. 2012 Oct 32(9):1719–26.
109. Ohta K, Sato A, Fukui E. Retinal thickness in eyes with idiopathic macular hole after vitrectomy with internal limiting membrane peeling. *Graefe’s Arch Clin Exp Ophthalmol*. 2013;251(5):1273–9.
110. Ohta K, Sato A, Fukui E. Asymmetrical thickness of parafoveal retina around surgically closed macular hole. *Br J Ophthalmol*. 2010 Nov 1;94(11):1545–6.
111. Haritoglou C, Schumann R, Reiniger I, Rohleder M, Priglinger SG, Kampik A, et al. Evaluation of the internal limiting membrane after conventional peeling during macular hole surgery. *Retina*. 2006 Jan;26(1):21–4.
112. Uemoto R, Yamamoto S, Aoki T, Tsukahara I, Yamamoto T, Takeuchi S. Macular configuration determined by optical coherence tomography after idiopathic macular

- hole surgery with or without internal limiting membrane peeling. *Br J Ophthalmol*. 2002 Nov;86(11):1240–2.
113. Wakabayashi T, Fujiwara M, Sakaguchi H, Kusaka S, Oshima Y. Foveal microstructure and visual acuity in surgically closed macular holes: Spectral-domain optical coherence tomographic analysis. *Ophthalmology*. 2010 Sep;117(9):1815–24.
 114. Hasebe H, Matsuoka N, Terashima H, Sasaki R, Ueda E, Fukuchi T. Restoration of the Ellipsoid Zone and Visual Prognosis at 1 Year after Surgical Macular Hole Closure. 2016 [cited 2019 Oct 20];
 115. Quigley HA, Dunkelberger GR, Green WR. Retinal ganglion cell atrophy correlated with automated perimetry in human eyes with glaucoma. *Am J Ophthalmol*. 1989 May 15 107(5):453–64.
 116. Sellés-Navarro I, Villegas-Pérez MP, Salvador-Silva M, Ruiz-Gómez JM, Vidal-Sanz M. Retinal ganglion cell death after different transient periods of pressure-induced ischemia and survival intervals. A quantitative in vivo study. *Invest Ophthalmol Vis Sci* 1996 Sep;37(10):2002–14.
 117. Inoue M, Watanabe Y, Arakawa A, Sato S, Kobayashi S, Kadonosono K. Spectral-domain optical coherence tomography images of inner/outer segment junctions and macular hole surgery outcomes. *Graefe's Arch Clin Exp Ophthalmol*. 2009 Mar 19;247(3):325–30.
 118. Hashimoto Y, Saito W, Fujiya A, Yoshizawa C, Hirooka K, Mori S, et al. Changes in Inner and Outer Retinal Layer Thicknesses after Vitrectomy for Idiopathic Macular Hole: Implications for Visual Prognosis. Abe T, editor. *PLoS One*. 2015 Aug 20;10(8):e0135925.
 119. Ishida M, Ichikawa Y, Higashida R, Tsutsumi Y, Ishikawa A, Imamura Y. Retinal Displacement Toward Optic Disc After Internal Limiting Membrane Peeling for Idiopathic Macular Hole. *Am J Ophthalmol*. 2014 May;157(5):971–7.
 120. Modi A, Giridhar A, Gopalakrishnan M. Spectral domain optical coherence tomography-based microstructural analysis of retinal architecture post internal limiting membrane peeling for surgery of idiopathic macular hole repair. *Retina*. 2017 Feb;37(2):291–8.

121. Joe SG, Lee KS, Lee JY, Hwang J-U, Kim J-G, Yoon YH. Inner retinal layer thickness is the major determinant of visual acuity in patients with idiopathic epiretinal membrane. *Acta Ophthalmol.* 2013 May;91(3):e242-3.
122. Cho KH, Park SJ, Cho JH, Woo SJ, Park KH. Inner-Retinal Irregularity Index Predicts Postoperative Visual Prognosis in Idiopathic Epiretinal Membrane. *Am J Ophthalmol.* 2016 Aug;168:139–49.
123. Kawano K, Ito Y, Kondo M, Ishikawa K, Kachi S, Ueno S, et al. Displacement of foveal area toward optic disc after macular hole surgery with internal limiting membrane peeling. *Eye (Lond).* 2013 Jul 27(7):871–7.
124. Nukada K, Hangai M, Ooto S, Yoshikawa M, Yoshimura N. Tomographic features of macula after successful macular hole surgery. *Invest Ophthalmol Vis Sci.* 2013 Apr 1;54(4):2417–28.
125. Hood DC, Seiple W, Holopigian K, Greenstein V. A comparison of the components of the multifocal and full-field ERGs. Vol. 14, *Visual Neuroscience.* 1997. p. 533–44.
126. Faria MY, Ferreira NP, Cristóvão DM, Mano S, Sousa DC, Monteiro-Grillo M. Tomographic Structural Changes of Retinal Layers after Internal Limiting Membrane Peeling for Macular Hole Surgery. *Ophthalmic Res* 2018 59(1):24–9.
127. Machida S, Nishimura T, Ohzeki T, Murai K-I, Kurosaka D. Comparisons of focal macular electroretinograms after indocyanine green-, brilliant blue G-, or triamcinolone acetate-assisted macular hole surgery. *Graefes Arch Clin Exp Ophthalmol.* 2017 Mar 7;255(3):485–92.
128. Sjaarda RN, Frank DA, Glaser BM, Thompson JT, Murphy RP. Resolution of an absolute scotoma and improvement of relative scotomata after successful macular hole surgery. *Am J Ophthalmol.* 1993 Aug 15 116(2):129–39.
129. Scupola A, Mastrocola A, Sasso P, Fasciani R, Montrone L, Falsini B, et al. Assessment of Retinal Function Before and After Idiopathic Macular Hole Surgery. *Am J Ophthalmol.* 2013 Jul;156(1):132-139.e1.
130. Bellerive C, Cinq-Mars B, Louis M, Tardif Y, Giasson M, Francis K, et al. Retinal function assessment of trypan blue versus indocyanine green assisted internal

- limiting membrane peeling during macular hole surgery. *Can J Ophthalmol* 2013 Apr;48(2):104–9.
131. Ferencz M, Somfai GM, Farkas A, Kovács I, Lesch B, Récsán Z, et al. Functional assessment of the possible toxicity of indocyanine green dye in macular hole surgery. *Am J Ophthalmol* 2006 Nov;142(5):765–70.
 132. Andréasson S, Ghosh F. Cone implicit time as a predictor of visual outcome in macular hole surgery. *Graefes Arch Clin Exp Ophthalmol*. 2014 Dec 2 252(12):1903–9.
 133. Kuriyama S, Hayashi H, Jingami Y, Kuramoto N, Akita J, Matsumoto M. Efficacy of Inverted Internal Limiting Membrane Flap Technique for the Treatment of Macular Hole in High Myopia. *Am J Ophthalmol*. 2013 Jul 156(1):125-131.e1.
 134. Iwasaki M, Kinoshita T, Miyamoto H, Imaizumi H. Influence of inverted internal limiting membrane flap technique on the outer retinal layer structures after a large macular hole surgery. *Retina*. 2019 Aug;39(8):1470–7.
 135. Casini G, Mura M, Figus M, Loiudice P, Peiretti E, De Cillà S, et al. Inverted internal limiting membrane flap technique for macular hole surgery without extra manipulation of the flap. *Retina*. 2017 Nov;37(11):2138–44.
 136. Shin MK, Park KH, Park SW, Byon IS, Lee JE. Perfluoro-n-Octane–Assisted Single-Layered Inverted Internal Limiting Membrane Flap Technique for Macular Hole Surgery. *Retina* 2014 Sep;34(9):1905–10.
 137. Park JH, Lee SM, Park SW, Lee JE, Byon IS. Comparative analysis of large macular hole surgery using an internal limiting membrane insertion versus inverted flap technique. *Br J Ophthalmol* 2019 Feb;103(2):245–50.
 138. Hu X-T, Pan Q-T, Zheng J-W, Zhang Z-D. Foveal microstructure and visual outcomes of myopic macular hole surgery with or without the inverted internal limiting membrane flap technique. *Br J Ophthalmol*. 2018 Nov 23;bjophthalmol-2018-313311.
 139. Frangieh GT, Green WR, Engel HM. A histopathologic study of macular cysts and holes. 1981. *Retina*.;25(5 Suppl):311–36.

140. Yamana T, Kita M, Ozaki S, Negi A, Honda Y. The process of closure of experimental retinal holes in rabbit eyes. *Graefes Arch Clin Exp Ophthalmol*. 2000 Jan 238(1):81–7.
141. Shiode Y, Morizane Y, Matoba R, Hirano M, Doi S, Toshima S, et al. The Role of Inverted Internal Limiting Membrane Flap in Macular Hole Closure. *Invest Ophthalmol Vis Sci* 2017 Sep 1;58(11):4847–55.
142. Bonińska K, Nawrocki J, Michalewska Z. Mechanism of “flap closure” after the inverted internal limiting membrane flap technique. *Retina*. 2018 Nov;38(11):2184–9.
143. Rahimy E, McCannel CA. Impact of internal limiting membrane peeling on macular hole reopening: A Systematic Review and Meta-Analysis. *Retina*. 2015 Oct 5
144. Flaxel CJ, Adelman RA, Bailey ST, Fawzi A, Lim JI, Vemulakonda GA, et al. Idiopathic Macular Hole Preferred Practice Pattern®. *Ophthalmology*. 2019 Sep 25
145. Hol EM, Pekny M. Glial fibrillary acidic protein (GFAP) and the astrocyte intermediate filament system in diseases of the central nervous system. *Curr Opin Cell Biol*. 2015 Feb;32:121–30.
146. Morizane Y, Shiraga F, Kimura S, Hosokawa M, Shiode Y, Kawata T, et al. Autologous Transplantation of the Internal Limiting Membrane for Refractory Macular Holes. *Am J Ophthalmol*. 2014 Apr 157(4):861-869.e1.
147. Yokota R, Hirakata A, Hayashi N, Hirota K, Rii T, Itoh Y, et al. Ultrastructural analyses of internal limiting membrane excised from highly myopic eyes with myopic traction maculopathy. *Jpn J Ophthalmol*. 2018 Jan 25;62(1):84–91.
148. Ehlers JP, Dupps WJ, Kaiser PK, Goshe J, Singh RP, Petkovsek D, et al. The prospective intraoperative and perioperative ophthalmic imaging with optical CoherEncE TomogRaphy (PIONEER) study: 2-year results. *Am J Ophthalmol*. 2014 Nov 1;158(5):999-1007.e1.
149. Akahori T, Iwase T, Yamamoto K, Ra E, Kawano K, Ito Y, et al. Macular Displacement After Vitrectomy in Eyes With Idiopathic Macular Hole Determined by Optical Coherence Tomography Angiography. *Am J Ophthalmol*. 2018 May 1;189:111–21.

150. Cho JH, Yi HC, Bae SH, Kim H. Foveal microvasculature features of surgically closed macular hole using optical coherence tomography angiography. *BMC Ophthalmol.* 2017 Nov 28;17(1).